# Miniature Masterminds

Neurobiology of brain scaling in the parasitic wasp *Nasonia vitripennis*

Miniature Masterminds

Jitte Groothuis

2018

Jitte Groothuis

Propositions

1. Genetic tools like the UAS/GAL4 system are desperately needed for the study of Nasonia neurobiology.
   (this thesis)

2. "Invisible isometry" is probably far more common than expected.
   (this thesis)

3. The size of an invasive species does not correlate with its ability to upset local ecosystems.

4. "Research parasites" are as essential a part of the scientific world as regular parasites are in the natural world.

5. Every able person should spend time cleaning up after others in order to learn how to clean up after themselves.

6. The practice of proposing reviewers for a submitted manuscript is, at best, detrimental to scientific objectivity and, at worst, enabling publication fraud by fake peer review.

Propositions belonging to the PhD thesis entitled

"Miniature Masterminds:
Neurobiology of brain scaling in the parasitic wasp *Nasonia vitripennis*"

Jitte Groothuis
Wageningen University & Research
April 3 , 2018

Miniature Masterminds

**Neurobiology of brain scaling in
the parasitic wasp *Nasonia vitripennis***

Jitte Groothuis

Miniature Masterminds

Neurobiology of brain scaling in the parasitic wasp *Nasonia vitripennis*

Jitte Groothuis

Thesis
submitted in fulfilment of the requirements for the degree of doctor
at Wageningen University
by the authority of the Rector Magnificus,
Prof. Dr A.P.J. Mol,
in the presence of the
Thesis Committee appointed by the Academic Board
to be defended in public
on Tuesday 3 April 2018
at 11 a.m. in the Aula.

Table of contents

Nasonia vitripennis

Chapter 1

General introduction

Miniature Masterminds

Animals on Earth take all shapes and sizes that astonish naturalists, philosophers, and other scientists from centuries past, and centuries to come. Though the animal kingdom is tremendously varied, we share a common *Bauplan*—or blueprint—with the largest, as well as the smallest animals that share our world. Tiny insects may appear outwardly alien, but even here we can find homologies. Perhaps most peculiar in all these animals is their nervous system. Despite being much smaller than humans, or even the smallest mammal, insects such as bees have large repertoires of complex behaviors that are hard to even understand for us humans (Chittka and Niven, 2009). Even the tiniest parasitic wasps show remarkable characteristics such as the ability to hitchhike on larger insects (Huigens et al., 2009). Truly, these miniature masterminds must have complex, or perhaps very efficient, brains.

How even the smallest insects are able to scale their brain to match their body size is a vexing puzzle, and one I hope to add pieces to in this thesis.

Haller's rule

The scaling of body parts with overall body size is most often described by power laws, i.e. [Trait size] = a × [Body size]^b. In such a power law, the scaling coefficient 'b' is most important in describing to what extent trait size is influenced by body size. Scaling of the brain with body size is governed by a process described as **Haller's rule** (Rensch, 1948), originally described by Albrecht von Haller (1762). Haller's rule states that this brain scaling always has a scaling coefficient that is smaller than 1: negative allometry. This means that a smaller animal will have a relatively larger brain than a large animal. Allometry is best visualized (and analyzed) on a logarithmic scale, as the power law is then transformed to a linear relationship: Log([Trait size]) = Log(a) + b × Log([Body size]). Log-transformed, the scaling coefficient 'b' is the slope of this function.

There are several possible reasons that, alone or combined, explain how an increase in body size may lead to a decrease in relative brain size. One reason pertains to the innervation of the body, which is concentrated on its inner and outer surfaces. Though a body may be larger or smaller in terms of volume (i.e. by the cube), its innervation changes by area (i.e. by the square). As such, the nervous system would not require equal scaling of its volume when body size is scaled (Rensch, 1956). Another point of note is the cognitive requirements for different animals. Though the impressive behavioral array of small insects

is without question (Chittka and Niven, 2009), having a smaller brain (or, fewer neurons) is likely to cause some functional loss. For smaller animals to minimize such an effect and maintain cognitive capabilities, their brain should scale down less than their body (compared to larger animals), resulting in relatively larger brains for small animals. Furthermore, an important determinant for brain scaling is the energetic cost of neural tissues (Aiello and Wheeler, 1995). Their high metabolic requirements make increases in volume beyond what is strictly necessary highly unlikely. What is "necessary" may be a combination of the aforementioned reasons: requirements for cognition and innervation. Together, these factors are balanced in Haller's rule: negative allometric scaling of the brain.

Other traits may not scale differently at all (isometry, b ≈ 1), such as the mammalian heart (Prothero, 1979), or may even scale positively with body size (positive allometry, b > 1), such as the horn of rhinoceros beetles or mandibles of stag beetles that become relatively larger with increasing body size (Huxley, 1931; Kawano, 1995).

An interesting feature of Haller's rule is that it applies to brains throughout the animal kingdom (Rensch, 1948; 1956); though originally conceived for vertebrates, it holds true for arthropods as well (Rensch, 1948; Seid et al., 2011). Moreover, it functions equally well when comparing *within* species (intraspecific variation, or **static allometry**), as it does when comparing *between* species, or groups of species (interspecific variation, or **evolutionary allometry**). In general, static allometry is often stronger (= a lower 'b' value, or a shallower relationship) than evolutionary allometry (Pagel and Harvey, 1988).

What is brain size?

"Brain size" is a peculiar metric. Though brain volume or brain mass are typical measurements, they do not provide a complete picture. Some important factors that are not part of most brain scaling analyses are specific adaptation in the structure of the brain, as well as neuronal number and density. These factors go unnoticed in traditional studies of allometric and isometric scaling that typically deal with (total) volumes.

Structural effects, for example, includes gyrification of the vertebrate cortex (increasing surface area by formation of folds in the brain surface). As the brain surface contains the neurons, a larger surface area greatly increases the "amount
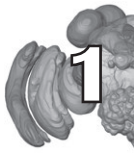
of brain" in a given volume (our human brains being a prime example). The relationship between [Brain surface area] and [Body size] would thus show quite a different relationship than that for [Total brain volume]. A comparison based on volume alone hides this information about the surface, and is therefore uninformative.

Another example can be found in the compartmentalization of brain regions, which can also be described as brain mosaicism (Barton and Harvey, 2000). Brains can be divided in distinct regions such as the cerebrum and cerebellum in the human brain, or, as one analyzes in more detail, the neocortex within the cerebrum and the visual cortex within the neocortex. Similar to gyrification, mosaic development of brains may hide differences unseen in analyses of total volume/mass. Elephants, for example, devote a larger relative proportion of the total brain to the cerebellum than humans. Large effects in brain mosaicism may occur when anatomy and associated function of areas evolve together, irrespective of other structures (Barton and Harvey, 2000; Montgomery et al., 2016).

Similar to the structural effects, one may consider neuronal number and density when comparing brains (Herculano-Houzel and Lent, 2005; Herculano-Houzel et al., 2007). Cellular scaling rules may vary, especially when the comparison concerns animals of different taxonomic orders or families (Herculano-Houzel et al., 2006; Herculano-Houzel et al., 2007). When brain size increases, some animals may invest in larger neurons, more (smaller) neurons, or change the neuron/glia ratio.

Returning to the previous elephant example, we find that its brain weighs roughly three times as much as a human brain (about 4.6 kg to 1.2-1.4 kg), and contains about three times as many neurons (257 billion neurons to 86 billion). Its cerebrum, however, contains only about a third of the neurons in the human cerebral cortex, despite weighing twice as much (Herculano-Houzel et al., 2014a). So, in addition to the volumetric mosaicism mentioned above, the cellular scaling rules for this animal are different as well.

The insect brain

After getting over the fact that arthropods do in fact *have* brains, it may be easy to see parallels between a vertebrate brain (Figure 1A) and an insect brain (Figure 1B). Both show bilateral symmetry, both have an outer layer of "stuff", and an inner layer of differently colored "stuff".
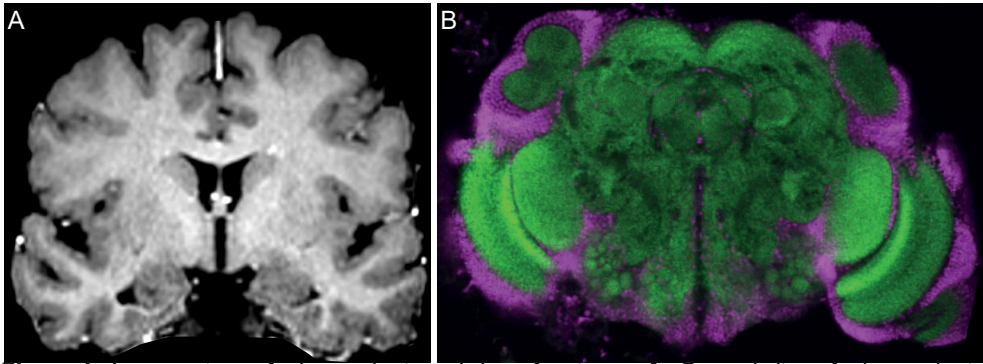
Figure 1. A comparison of a human brain and that of an insect. **A.** Coronal slice of a human brain (Y. van Dongen) obtained by T1 weighted magnetic resonance imaging. Reproduced with permission. Contrast increased in ImageJ. **B.** Coronal slice of a parasitic wasp brain (*Nasonia vitripennis*), obtained by immunofluorescent labeling and confocal laser scanning microscopy.

Regrettably, this superficial comparison is false (apart from the symmetry): in vertebrates the outer layer is what is known as the "grey matter", the inner layer the "white matter". Residing in the grey matter, the cortex, are the neurons and the connections between them. Through the center of the brain, the white matter, these neurons extend towards the spinal cord with long axons enveloped with fatty myelin (the reason for the name *white* matter). There are no connections between axons in the white matter.

In insects (and other invertebrates) the outer layer of the brain does contain neurons, but only their cell bodies. All connections are made in the inner layer, where the neurons both receive incoming signals, as well as send signals of their own.

Areas of nervous tissue where connections are made are called "**neuropil**". In vertebrate brains this neuropil is part of the cellular tissue of the grey matter, but as outlined above this is not the case for insects. In insects the entire central part of the brain is composed of neuropil and tracts of fibers with destinations within that neuropil. As such, we can refer to this central part simply as "neuropil", or a collection of "neuropils", as we can identify specific regions or components within it.

Brain components

Some components of the brain, or neuropils, are easily recognizable because they lie (partly) separate from the rest of the brain and are surrounded by the outer layer of cell bodies, or **cell body rind**. Here I will introduce several of these neuropils. Examples of easily recognizable neuropils are the **optic lobes**,

11
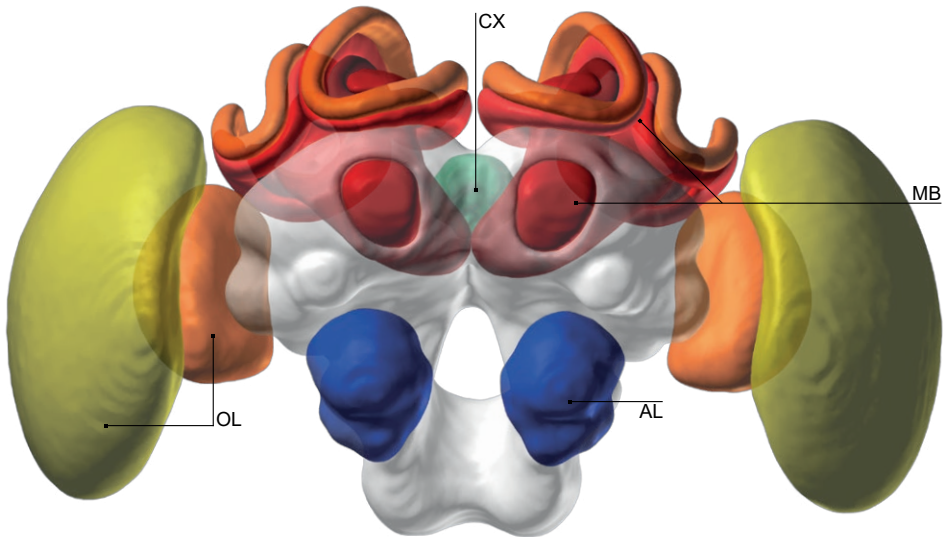
Figure 2. A three-dimensional schematic model of the honey bee brain. Obtained from the Insect Brain Database (insectbraindb.org) based on data from Brandt et al. (2005). Abbreviations: AL, antennal lobe; CX, central complex; MB, mushroom body; OL, optic lobes.

located at the lateral sides of the brain (Figures 1B, 2), closest to the compound eyes. The optic lobes are, as the name hints at, the primary visual neuropils where signals from the retina enter the brain.

Equally recognizable are the **antennal lobes**, bulbous neuropil structures at the front side of the brain that, like the optic lobes, lie separate of the main mass of the brain. The antennal lobes are the primary olfactory neuropil; here, signals evoked by the antennae are grouped (based on similarity) in areas of the antennal lobe known as **glomeruli**.

Other neuropils that can be recognized may lie (partly) inside the central brain mass, but are encapsulated in a sheath of glial processes that forms a boundary with the neighboring neuropil. The **mushroom bodies** and the **central complex**, for example, can be recognized this way. The mushroom bodies are named for their distinctive shape: a cup-like **calyx** is the mushroom cap, the mushroom stalk is formed by the **pedunculus** and the **medial and vertical lobes**. The mushroom body is a multi-modal integrative center, receiving secondary olfactory and visual information, as well as reinforcing or modulating signals (about the value of a stimulus, for example). Functional studies have shown that the mushroom body is critical for associative memory (Heisenberg, 1998).

The central complex is a group of neuropils in the middle of the brain that, despite their relatively small size in the brain, are involved in many processes from locomotion to orientation (Pfeiffer and Homberg, 2014).
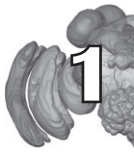
Scaling of brain components

As with the brain mosaicism mentioned above, insects can vary in the (relative) size of the neuropils.

Between species, the relative size of a neuropil can be correlated with the behavior or sensory ecology of a species: a nocturnal moth relies less on visual information than a diurnal butterfly, and thus the optic lobes of a moth are relatively smaller than those of the butterfly (Rospars, 1983). The same is true for ants that are mainly subterranean or are visual hunters (Gronenberg and Hölldobler, 1999) and nocturnal and diurnal dung beetles (Immonen et al., 2017). Such differences are not merely reflected in the primary sensory neuropils, but at secondary levels as well (Gronenberg and Hölldobler, 1999; Stöckl et al., 2016). Rather than representing an ability to perceive, this may represent the relative importance of certain cues: moths that differ in the ratio between visual and olfactory neuropils can learn (and respond to) either cue, but when forced to choose between conflicting cues will mainly respond to the cue corresponding with the largest neuropils (Stöckl et al., 2016).

Within species, relative neuropil size may differ due to age- and experience-dependent plasticity. Mushroom body size, for example, increases with age in *Camponotus floridanus* ants (Gronenberg et al., 1996), but social interactions are required for this (Seid and Junge, 2016). Similar forms of mushroom body size plasticity have also been recorded for bees as well (e.g. a sweat bee: Smith et al. (2010) and honey bee: Maleszka et al. (2009)), as well as for the internal structure of the honey bee mushroom body (e.g. Fahrbach and Van Nest (2016)).

Genetic differences (within a species) may also determine neuropil size (and potential consequences thereof). It has been shown in *Pieris* butterflies that they can differ consistently in relative mushroom body size, and that butterflies with larger mushroom bodies perform better in learned tasks (Snell-Rood et al., 2009).

Social insects may show further differentiation of neuropil volume based on caste (Muscedere and Traniello, 2012; O'Donnell et al., 2014) or task specialization (Amador-Vargas et al., 2015).
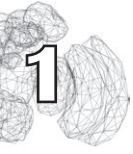
Finally, scaling of neuropils can be related to total brain size of the insect. In honey bees, for example, most neuropils have the same relative volume regardless of brain size, but the central complex is relatively smaller in larger brains (Gronenberg and Couvillon, 2010). In *Drosophila melanogaster* fruit flies, smaller brains (caused by nutrient deprivation during development) are correlated with relatively smaller mushroom body calyces and optic lobes (Heisenberg et al., 1995; Lanet et al., 2013). On the other hand, smaller *Trichogramma evanescens* individuals have relatively smaller (but equal numbers of) antennal lobe glomeruli (van der Woude and Smid, 2016).

Brain scaling in the smallest animals

Having established the existence and make-up of insect brains, I will now discuss the brain-body size relationship in arthropods. As mentioned above, the allometric function known as Haller's rule states that smaller animals have relatively larger brains. It has long been known that this is true in insects when comparing different species (**evolutionary allometry**) (Rensch, 1948). In recent years this has been confirmed with newer and more detailed methodologies for various spiders (Eberhard and Wcislo, 2011), ants (Seid et al., 2011; Bulova et al., 2016), and social wasps (O'Donnell and Bulova, 2017). Even in a comparison of several species of the tiniest parasitic wasps, Haller's rule was shown to apply (Polilov, 2016). One of the smallest wasps, *Megaphragma mymaripenne*, is thought to scale its brain to such a tiny size by lysing the nuclei of many of its neurons, leaving more space for neuropil in its head capsule (Polilov, 2012).

Comparisons of individuals within a species (**static allometry**) may reveal a different picture. Haller's rule holds true for static allometry in ants: a study on the highly polymorphic ant *Atta colombica* revealed negative allometry for the intraspecific relationship (Seid et al., 2011). However, the authors describe a novel kind of allometry that is not expected from Haller's rule: **diphasic allometry**. Large *A. colombica* scale their brain with a low allometric coefficient, but smaller conspecifics show much steeper brain scaling with a coefficient twice as high. Smaller ants thus have smaller brains than what would be expected if *A. colombica* had only one allometric "phase". Still, the smallest of these ants (weighing 410 µg) have brains constituting 8% of their body weight; an impressive feat of body size miniaturization, considering the cost of brain tissue (Aiello and Wheeler, 1995).

Is this steeper allometry at smaller body sizes indicative of a limit for the validity of Haller's rule? An answer to this question came from the much smaller egg parasitoid *T. evanescens* (van der Woude et al., 2013). The large variation in body mass of this wasp (2.5 to 18 μg) allowed for an intraspecific study of its brain-body size relationship, which revealed that *T. evanescens* breaks Haller's rule. This study found a scaling coefficient of 1, indicating **isometric** brain scaling. The authors hypothesize that the reason why the smallest *T. evanescens* do not have a relatively larger brain is found in the metabolic cost of their neural tissue: at the smallest body sizes there might simply not be not enough energy to maintain (relatively) larger brains.

Haller's rule can be broken. From the results obtained in *A. colombica* and *T. evanescens* it appears that the increase of the scaling coefficient is paired with a decrease in body size. Yet, questions remain:

- Is an increase in the brain scaling coefficient really linked to body size?
- Is isometry perhaps a unique adaptation to miniaturization in *T. evanescens*, like the loss of nuclei might be in *M. mymaripenne*?
- Is isometric brain scaling unique to the Hymenoptera?
- How did miniaturization evolve and what is the role of brain scaling therein?
- Are "brains smaller than expected" adapted to be small? Are there sacrifices that allow this scaling?

Answering these questions requires more intraspecific studies in animals of various orders in similar size ranges. Moreover, these animals need to vary in body size in order to be able to study brain scaling. Tiny ants such as *Brachymyrmex* or *Monomorium* would provide a good comparison, but they are monomorphic and do not show much variation in size.

Nasonia vitripennis

With these questions and limitations we come to the jewel wasp *Nasonia vitripennis*, a parasitoid of fly pupae. Like *T. evanescens* and *A. colombica*, this wasp has the potential for large phenotypic variation in body size, making it suitable for an analysis of brain scaling. This variation covers a range of 40 to 440 μg, which not only is a tremendous level of developmental plasticity, it also squarely fits in the body size gap left between the *T. evanescens* and *A. colombica* studies. In addition, as a hymenopteran model species it has been studied extensively,
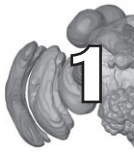
a sequenced genome is available, and genetic tools are being developed, which allows findings on brain scaling to be placed into a broader context and may open avenues for further research.

Objective and hypotheses

The aim of this thesis is twofold. First, to gain further understanding on insect brain scaling at the limits of miniaturization. Second, to provide the research community with much needed fundamental knowledge on, and tools for the study of, the brain of *N. vitripennis*.

Specifically, I sought to answer the following questions:

1. What is the general morphology of the *N. vitripennis* brain, and how does it relate to the brain of other insects?

As *N. vitripennis* is not an extremely miniaturized insect, I hypothesize that its brain shares much similarity with larger Hymenoptera such as the honey bee. The behavioral ecology of *N. vitripennis* may be reflected in in the relative volumes of its neuropils.

2. How does the brain of *Nasonia vitripennis* scale over its large body size range, and are there specific adaptations to accommodate this range?

I assume that the occurrence of isometric brain scaling in *T. evanescens* is caused by its minute size. Therefore I hypothesize that the *N. vitripennis* (a slightly larger wasp species) adhere to Haller's rule and show allometric brain scaling. Due to the large variation in size I expect to find adaptations in the modular layout of its brain, which will be most obvious in the neuropils of least or most ecological relevance.

3. Are there cell type-specific adaptations in brains of different sizes, and does this relate to behavior?

Based on a comparison between *N. vitripennis* and other insects I aim to identify cellular clusters using the neuromodulator dopamine. I hypothesize that smaller brains have fewer neurons overall, and fewer in particular in dopaminergic clusters corresponding to those involved in appetitive memory formation in other species.

4. Is relative brain size a trait that can be selected for, and what are the effects of such a selection?

Answering this question may help resolve our understanding of the evolution of brain scaling. I hypothesize that it is possible to select for varying levels of brain scaling, resulting in different relative brain sizes, and that the difference in brain size will be accompanied with neuropil adaptations similar to those found in brains with large phenotypic size variation.
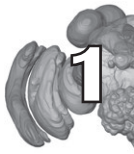
Thesis outline

In **Chapter 2**, I focus on a gap in the current neurobiological knowledge of *Nasonia*. To my knowledge, the last description of the *Nasonia* nervous system stems from 1922, where the general morphology of the *N. vitripennis* brain was described in the context of embryology and metamorphosis. This was only followed in 2014, when a description of the octopaminergic system, but not overall morphology, was published for *N. vitripennis* and *Nasonia giraulti* (Haverkamp and Smid, 2014).

Here, I describe the morphology of 14 regions of interest in the female *N. vitripennis* brain, and compare it to brains of other model species such as the honey bee *Apis mellifera* and the fruit fly *Drosophila melanogaster*. This will serve as an anatomical basis for the rest of my dissertation. First and foremost, however, this chapter presents the first version of the Jewel Wasp Standard Brain (JWSB). The JWSB will serve as a reference framework for future studies on *Nasonia* neurobiology and can be used as a tool to integrate multidisciplinary results. The JWSB is based on morphological data obtained by means of immunohistochemistry, confocal laser scanning microscopy, and volumetric analysis in three-dimensional modelling software. Iterative shape averaging was used to generate the final average standard brain.

Chapter 3 concerns the astounding plasticity in body size found in *N. vitripennis*. Using an isogenic line, I studied the effects of brain-body size scaling independent of genetic variation. I first set out to study the intraspecific validity of Haller's rule in this species. By experimentally manipulating the number of wasp larvae developing in a fly host, I generated varying levels of scramble competition. I measured the resulting variation in relative brain size, using a novel approach to measure head volume by bleaching and confocal laser scanning microscopy.

Second, I addressed the question of whether the large differences in absolute brain size are reflected in changes in its modular layout. Using immunohistochemistry, confocal laser scanning microscopy, and a volumetric analysis I compared the relative volume of 14 distinct neuropils in brains of the smallest and largest
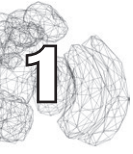
N. vitripennis wasps. This reveals how the complexity of brains is impacted by large differences in absolute volume, as well as the remarkable potential for developmental plasticity contained in a single genome.

Parallel lines of research have revealed significant size-dependent differences in the memory dynamics of *N. vitripennis*, as well as distinctive differences between *N. vitripennis* and its sister-species *Nasonia giraulti*. From studies in various other insects, the modulatory neurotransmitters octopamine and dopamine are known to be involved in memory formation. Prior research found no difference in the octopaminergic network for *N. vitripennis* and *N. giraulti*. So, to further elucidate the dissimilarity in the memory dynamics of these species, **Chapter 4** describes the clusters of dopaminergic neurons in the brains of these wasps by using immunohistochemistry, confocal laser scanning microscopy, and counting of cells with the help of three-dimensional modelling software. A comparison was made between the two species, but also between large and small *N. vitripennis*. Paired with a comparison to the fruit fly and honey bee, the number of cells per cluster in each analyzed group is discussed in the context of their potential role in the behavior they modulate.

In contrast to previous chapters, **Chapter 5** discusses differences in brain scaling caused by genetic factors. Instead of large absolute and phenotypic size effects, I performed artificial selection on an outbred population of *N. vitripennis* to create lines with large or small relative brains. A relatively large brain may improve the cognitive abilities of these wasps, but may also impose a larger energetic cost. In this chapter the effects of relative brain size are studied in the context of olfactory learning, absolute brain size, scaling of brain compartments, and one life history trait: longevity.

Finally, **Chapter 6** consolidates the previous chapters and focuses on the integration of the knowledge obtained therein to answer the main questions and hypotheses outlined above. The findings are discussed from an evolutionary perspective and consider a larger context of how neuroanatomical differences influence arthropod ecology. Furthermore, I discuss future perspectives and speculate on the broader future for neurobiological research in the *Nasonia* field.

Acknowledgements

References

Aiello LC, Wheeler P. 1995. The expensive-tissue hypothesis - the brain and the digestive-dystem in human and primate evolution. Curr Anthropol 36(2):199-221.

Amador-Vargas S, Gronenberg W, Wcislo WT, Mueller U. 2015. Specialization and group size: brain and behavioural correlates of colony size in ants lacking morphological castes. Proc R Soc B 282(1801).

Barton RA, Harvey PH. 2000. Mosaic evolution of brain structure in mammals. Nature 405(6790):1055-1058.

Brandt R, Rohlfing T, Rybak J, Krofczik S, Maye A, Westerhoff M, Hege HC, Menzel R. 2005. Three-dimensional average-shape atlas of the honeybee brain and its applications. J Comp Neurol 492(1):1-19.

Bulova S, Purce K, Khodak P, Sulger E, O'Donnell S. 2016. Into the black and back: the ecology of brain investment in Neotropical army ants (Formicidae: Dorylinae). Sci Nat 103(3):1-11.

Chittka L, Niven J. 2009. Are bigger brains better? Curr Biol 19(21):R995-R1008.

Eberhard WG, Wcislo WT. 2011. Grade changes in brain-body allometry: morphological and behavioural correlates of brain size in miniature spiders, insects and other invertebrates. In: Casas J, ed. Advances in Insect Physiology. Vol 40: Elsevier Limited. p 155-214.

Fahrbach SE, Van Nest BN. 2016. Synapsin-based approaches to brain plasticity in adult social insects. Curr Opin Insect Sci 18:27-34.

Gronenberg W, Couvillon MJ. 2010. Brain composition and olfactory learning in honey bees. Neurobiol Learn Mem 93(3):435-443.

Gronenberg W, Heeren S, Hölldobler B. 1996. Age-dependent and task-related morphological changes in the brain and the mushroom bodies of the ant *Camponotus floridanus*. J Exp Biol 199(9):2011-2019.

Gronenberg W, Hölldobler B. 1999. Morphologic representation of visual and antennal information in the ant brain. J Comp Neurol 412(2):229-240.

Haller A. 1762. Elementa physiologiae corporis humani: IV cerebrum, nervi, musculi. Lausanne: Grasset.

Haverkamp A, Smid HM. 2014. Octopamine-like immunoreactive neurons in the brain and subesophageal ganglion of the parasitic wasps *Nasonia vitripennis* and *N. giraulti*. Cell Tissue Res 358(2):313-329.

Heisenberg M. 1998. What do the mushroom bodies do for the insect brain? An introduction. Learning & memory 5(1-2):1-10.

Heisenberg M, Heusipp M, Wanke C. 1995. Structural plasticity in the *Drosophila* brain. J Neurosci 15(3):1951.

Herculano-Houzel S, Avelino-de-Souza K, Neves K, Porfirio J, Messeder D, Mattos Feijo L, Maldonado J, Manger PR. 2014a. The elephant brain in numbers. Front Neuroanat 8:46.

Herculano-Houzel S, Collins CE, Wong P, Kaas JH. 2007. Cellular scaling rules for primate brains. Proc Natl Acad Sci U S A 104(9):3562-3567.

Herculano-Houzel S, Lent R. 2005. Isotropic fractionator: A simple, rapid method for the quantification of total cell and neuron numbers in the brain. J Neurosci 25(10):2518-2521.

Herculano-Houzel S, Mota B, Lent R. 2006. Cellular scaling rules for rodent brains. Proc Natl Acad Sci U S A 103(32):12138-12143.

Huigens ME, Pashalidou FG, Qian MH, Bukovinszky T, Smid HM, van Loon JJA, Dicke M, Fatouros NE. 2009. Hitch-hiking parasitic wasp learns to exploit butterfly antiaphrodisiac. Proc Natl Acad Sci U S A 106(3):820-825.

Huxley JS. 1931. Relative growth of mandibles in stag-beetles (Lucanidae). Journal of the
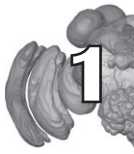
Linnean Society of London, Zoology 37(255):675-703.

Immonen EV, Dacke M, Heinze S, El Jundi B. 2017. Anatomical organization of the brain of a diurnal and a nocturnal dung beetle. J Comp Neurol 525(8):1879-1908.

Kawano K. 1995. Horn and wing allometry and male dimorphism in giant rhinoceros beetles (Coleoptera, Scarabaeidae) of tropical Asia and America. Ann Entomol Soc Am 88(1):92-99.

Lanet E, Gould AP, Maurange C. 2013. Protection of neuronal diversity at the expense of neuronal numbers during nutrient restriction in the Drosophila visual system. Cell Rep 3(3):587-594.

Maleszka J, Barron AB, Helliwell PG, Maleszka R. 2009. Effect of age, behaviour and social environment on honey bee brain plasticity. J Comp Physiol A 195(8):733-740.

Montgomery SH, Mundy NI, Barton RA. 2016. Brain evolution and development: adaptation, allometry and constraint. Proc R Soc B 283(1838).

Muscedere ML, Traniello JF. 2012. Division of labor in the hyperdiverse ant genus *Pheidole* is associated with distinct subcaste- and age-related patterns of worker brain organization. PLoS One 7(2):e31618.

O'Donnell S, Bulova S. 2017. Development and evolution of brain allometry in wasps (Vespidae): size, ecology and sociality. Curr Opin Insect Sci 22:54-61.

O'Donnell S, Clifford MR, Bulova SJ, DeLeon S, Papa C, Zahedi N. 2014. A test of neuroecological predictions using paperwasp caste differences in brain structure (Hymenoptera: Vespidae). Behav Ecol Sociobiol 68(4):529-536.

Pagel MD, Harvey PH. 1988. The taxon-level problem in the evolution of mammalian brain size - facts and artifacts. Am Nat 132(3):344-359.

Pfeiffer K, Homberg U. 2014. Organization and functional roles of the central complex in the insect brain. Annu Rev Entomol 59:165-184.

Polilov AA. 2012. The smallest insects evolve anucleate neurons. Arthropod Struct Dev 41(1):29-34.

Polilov AA. 2016. At the size limit: Effects of miniaturization in insects: Springer.

Prothero J. 1979. Heart-weight as a function of body-weight in mammals. Growth 43(3):139-150.

Rensch B. 1948. Histological changes correlated with evolutionary changes of body size. Evolution 2(3):218-230.

Rensch B. 1956. Increase of learning capability with increase of brain-size. Am Nat 90(851):81-95.

Rospars JP. 1983. Invariance and sex-specific variations of the glomerular organization in the antennal lobes of a moth, *Mamestra brassicae*, and a butterfly, *Pieris brassicae*. J Comp Neurol 220(1):80-96.

Seid MA, Castillo A, Wcislo WT. 2011. The allometry of brain miniaturization in ants. Brain Behav Evol 77(1):5-13.

Seid MA, Junge E. 2016. Social isolation and brain development in the ant *Camponotus floridanus*. Sci Nat 103(5):1-6.

Smith AR, Seid MA, Jimenez LC, Wcislo WT. 2010. Socially induced brain development in a facultatively eusocial sweat bee *Megalopta genalis* (Halictidae). Proc R Soc B 277(1691):2157-2163.

Snell-Rood EC, Papaj DR, Gronenberg W. 2009. Brain size: a global or induced cost of learning? Brain Behav Evol 73(2):111-128.

Stöckl A, Heinze S, Charalabidis A, el Jundi B, Warrant E, Kelber A. 2016. Differential investment in visual and olfactory brain areas reflects behavioural choices in hawk moths.

Sci Rep 6:26041.

van der Woude E, Smid HM. 2016. How to escape from Haller's rule: olfactory system complexity in small and large *Trichogramma evanescens* parasitic wasps. J Comp Neurol 524(9):1876-1891.

van der Woude E, Smid HM, Chittka L, Huigens ME. 2013. Breaking Haller's rule: brain-body size isometry in a minute parasitic wasp. Brain Behav Evol 81(2):86-92.
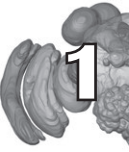
Nasonia vitripennis

Chapter 2

The Jewel Wasp Standard Brain:

Average shape atlas and morphology of the female *Nasonia vitripennis* brain

Jitte Groothuis,
Keram Pfeiffer,
Hans M. Smid

Submitted

Abstract

Use of the jewel wasp *Nasonia vitripennis* as a hymenopteran model species has increased in recent years. Though genetic tools are being developed and the genome of *N. vitripennis* has been published, knowledge on its nervous system is lacking until now. Here, we present a morphological description of several landmark neuropils in the female *N. vitripennis* brain, based on immunofluorescence of the morphological marker NC82. These landmark neuropils include the optic lobes (lobula, medulla, and lamina), the anterior optic tubercle, the antennal lobes, the lateral horn, the mushroom body (calyx, pedunculus, medial-, and vertical lobe), and the central complex (fan-shaped body, ellipsoid body, noduli, and protocerebral bridge). We discuss a volumetric analysis of these neuropils in the context of brains of other insect species.

Furthermore, we present an average standard brain of ten recently eclosed naïve female wasps obtained by the iterative shape averaging method. This standard brain, which we name the Jewel Wasp Standard Brain, includes all neuropils listed above, excluding the optic lobe lamina, in addition to the remaining unclassified neuropils in the central brain. The Jewel Wasp Standard Brain will provide a framework to integrate and consolidate the results of future neurobiological studies in *N. vitripennis*, such as cell-type specific neuronal stainings, tracings of electrophysiological recordings. In addition, the volumetric analysis of the segmented neuropils may serve as a baseline for future work on age- and experience-dependent brain plasticity.

Introduction

Standard brains and reference atlases are indispensable resources to understand the three-dimensional functional morphology and, ultimately, the functioning of the brain. They facilitate the continuous integration of results from multidisciplinary studies (such as expression data, neuronal tracings, or pathology) in a common digital framework, allowing the visualization of large datasets and generation of new hypotheses. Indeed, these fundamental tools were created and used for large-scale operations such as the Human Brain Project (e.g. Amunts et al. (2013)) or the BRAIN Initiative (e.g. Lein et al. (2007); Ding et al. (2016)). Although these large initiatives focus mainly on mammalian brains, much can be gained by the study of insect brains as well. Compared to human brains, the complexity of insect brains is orders of magnitude lower, increasing the feasibility of eventually reaching the ultimate goal of understanding their functional morphology in great detail.

At the forefront of insect standard brains is the Virtual Fly Brain of the fruit fly *Drosophila melanogaster* (Milyaev et al., 2012) (RRID:SCR_004229). This database not only serves as a reference for registration of many single neurons, their connectivity, and expression patterns, it also contains high resolution morphological images and detailed structural annotations. Other standard brains have been developed for insect species of various families, highlights of which include the honey bee *Apis mellifera* (Brandt et al., 2005; Rybak et al., 2010), the hawk moth *Manduca sexta* (el Jundi et al., 2009), the tobacco budworm *Heliothis virescens* (Kvello et al., 2009; Zhao et al., 2014), the flour beetle *Tribolium castaneum* (Dreyer et al., 2010), the desert locust *Schistocerca gregaria* (Kurylas et al., 2008; el Jundi et al., 2010), the monarch butterfly *Danaus plexippus* (Heinze et al., 2013), and two *Agrotis* moths (de Vries et al., 2017). These standard brains provide a fundamental basis for studies of the neural systems of these respective species, as well as a framework for large scale comparative neurological studies. A novel example of the latter is the Insect Brain Database (insectbraindb.org), which provides access to models of these brains or subregions thereof, greatly increasing the ease with which they can be compared.

Parasitic wasps are becoming increasingly important as model species for neuroscience. The jewel wasp *Nasonia vitripennis* (Hymenoptera: Pteromalidae), not to be confused with the emerald cockroach wasp *Ampulex compressa*, is a small (1.5-2.5 mm long) pupal parasitoid that develops as a larva inside a host, in this case the puparium of various fly species. *Nasonia vitripennis* has become a hymenopteran model species (Whiting, 1967; Werren and Loehlin, 2009). The

genomes of *N. vitripennis* and two related *Nasonia* species have been sequenced (Werren et al., 2010; Rago et al., 2016) and many genetic tools are being developed (Lynch, 2015; Li et al., 2017).

Recent years have seen multiple studies on *N. vitripennis* that focused on its nervous system: on e.g. genomics and proteomics (Hauser et al., 2010; Hoedjes et al., 2015), learning and memory (Schurmann et al., 2012; Hoedjes and Smid, 2014; Schurmann et al., 2015; Van der Woude and Smid, 2017a), clock cells involved in the photoperiodic response (Mukai and Goto, 2016), the distribution of the neurotransmitter octopamine (Haverkamp and Smid, 2014), and scaling of brain neuropils (Groothuis and Smid, 2017). This diversity of topics, in addition to support and interest from the international *Nasonia* community (JG, personal communication, *Nasonia* Meetings 2013 & 2017), indicate that there is a widespread need for a *Nasonia* standard brain to serve as a framework for integration of such results.

Here, we present the Jewel Wasp Standard Brain: a standard brain for *N. vitripennis* comprising 9 paired and 4 unpaired neuropils of interest, based on data of 10 adult female individuals averaged using the iterative shape averaging method. These brains are a subset of the brains used for a volumetric comparison of *N. vitripennis* of different sizes in our previous work (Groothuis and Smid, 2017). In addition, we provide morphological descriptions of the general neuropil layout.

Materials and methods

Insects and preparation

The isofemale AsymCx strain of *Nasonia vitripennis* was reared as described previously (Hoedjes et al., 2012). In short, 10 mated females were placed with 20 *Calliphora vomitoria* pupae (Kreikamp, Hoevelaken, The Netherlands) in 28.5×95 mm polystyrene rearing vials with foam stoppers at 25±1 °C and 16:8 (L:D) photoperiod. To prevent confounding effects of size- and experience-dependent plasticity, normal sized (head width >750 μm (Groothuis and Smid, 2017)) and unexperienced female wasps were collected within one day after emergence and kept overnight with access to honey and water.

Dissection and immunofluorescence

Cold-sedated female wasps were decapitated in ice-cold Phosphate Buffered Saline (PBS, Oxoid, Dulbecco 'A' tablets). Using fine sharpened tweezers (Dumont no. 5, Sigma) the cuticle was removed and brains were dissected. Dissected brains were kept in freshly prepared ice-cold 4% formaldehyde in 0.1M phosphate buffer (pH 7.2). After obtaining several brains, they were placed in fixative solution at RT and fixed for 2.5 h. After rinsing 6 times for 5 min in PBS, the brains were exposed to 5 mg/ml collagenase (Sigma) in PBS for 1 h at RT, improving permeability of the tissue. Subsequently, the brains were rinsed 4 times for 5 min in PBS containing 0.5% Triton-X100 (PBS-T) and pre-incubated in 10% normal goat serum (NGS, Dako, Glostrup, Denmark) in PBS-T (PBS-T-NGS) for 1 h at RT. The brains were then incubated overnight at RT in the primary antibody (1:250 dilution of mouse anti-Bruchpilot (αBrp, concentrate, DSHB hybridoma product nc82 (Wagh et al., 2006)) in PBS-T-NGS). Brains were rinsed 6 times for 20 min in PBS-T and incubated in 1:200 AlexaFluor®488-conjugated goat anti-mouse (Invitrogen) and 1:500 propidium iodide (Sigma-Aldrich) for 4 h. Brains were rinsed 4 times for 30 min in PBS-T and 2 times for 10 min in PBS. To avoid tissue shrinkage, which could lead to a confounding distortion of relative volumes, brains were not dehydrated and cleared, but mounted in aqueous VectaShield (Vector Laboratories) between two 24×24 mm coverslips with custom spacers and placed in a Cobb slide for imaging.

Brains used for descriptive morphology were obtained with a slightly modified protocol. To boost the detection of the primary αBrp antibody, here we used a secondary 1:100 rabbit-anti-mouse (Dako) antibody (incubation 3 h at RT) with a tertiary 1:200 Alexa Fluor® 488-conjugated goat-anti-rabbit (Invitrogen) antibody (incubation O/N at 4 °C). Brains were dehydrated in ascending EtOH concentration (30, 50, 70, 80, 90, 96, 2×100%, 2 min each), washed in a 50/50 EtOH/xylenes mix for 2 min, cleared in xylenes, and mounted in DPX (Sigma) on a microscope slide, fitted with two stacked strips of double-sided adhesive tape (Henzo, Roermond, The Netherland) as spacer, and an 18 mm x 18 mm #1 cover slip.

Confocal imaging and stack reconstruction

Whole mount preparations were scanned with a Zeiss LSM 510 confocal laser scanning microscope equipped with a 25× (Plan-Neofluar 25×/0.8 oil) objective. Alexa488 staining was imaged using the 488 nm line of an Argon laser with a

505-550 nm band pass filter, the PI nuclear counterstain was imaged using the same wavelength but with a 560 nm long pass filter. To accommodate the entire brain, 10-20% overlapping side-by-side Z-stacks were scanned at 1024×1024 pixels with a zoom of 0.8 and a step size of 2 μm, from both sides of the preparation.

After image acquisition, Z-stacks comprising the entire brain were reconstructed in FIJI (RRID:SCR_002285) (Schindelin et al., 2012). In short, first stacks from each side of the preparation were combined using the Pairwise Stitching plugin (Preibisch et al., 2009). Subsequently, one of the resulting stacks was effectively flipped in the Z-direction and manually rotated in the XY-plane to match the angle of the other stack, after which both sides were again combined by Pairwise Stitching, recalibrated, and saved as a TIFF file. To compensate for the axial scaling due to refraction index mismatch (Bucher et al., 2000) between immersion oil and the mounting medium, a correction of 0.9505 was applied to the voxel depth. Final voxel calibration was 0.4498844×0.4498844×1.901 μm.

Brain preparations used for descriptive morphology were obtained with the same 25× or 40× (Plan-Neofluar 40×/1.3 oil) objective, resulting in voxel calibrations of 0.5089862×0.5089862×2 μm and 0.2249421×0.2249421×0.4498843 μm, respectively. Images used for figures were obtained with FIJI or the VolRen and VolTex modules of Amira 5.4.2 (Visage Imaging; RRID:SCR_014305).

Neuropils were segmented and labeled using standardized insect brain nomenclature (Ito et al., 2014) where possible. We used the Segmentation Editor in Amira to assign voxels to 13 unique materials every 1-5 slices. Segmentations were completed with the Interpolation option and manually checked for correctness. The following neuropils were labeled: lobula (LO), medulla (ME), lamina (LA), anterior optic tubercle (AOTU), lateral horn (LH), antennal lobe (AL), mushroom body calyx (CA) and ventral mushroom body (MB-V), i.e. pedunculus and vertical & medial lobes, fan-shaped body (FB), ellipsoid body (EB), noduli (NO), and protocerebral bridge (PB), and rest of neuropils (RoN). The lamina was not included in the average standard brain.

Generating the average standard brain

To generate the standard brain we selected 10 brains based on staining quality and artefacts, as well as intactness of the overall morphology (e.g. torn or rotated optic lobes do not hamper volumetric analysis, but would impair generation of average shapes). Due to their general fragility, the lamina (the most distal

neuropil of the optic lobes) and the cell body rind were not incorporated in the *Nasonia* Standard Brain.

Standardization of the *Nasonia* brain was carried out by applying the iterative shape averaging protocol (ISA) on the confocal image stacks, using the computational morphometry toolkit (CMTK, Version 3.2.3) as described by Kurylas et al. (2008) and Rohlfing and Maurer (2003). All calculations were carried out on the high performance Linux cluster MaRC2 at the University of Marburg, Germany.

Before the registration process, one of the ten data sets was chosen as reference, based on two criteria: its volume had to approximate the median volume of the source brains and the shape had to be a typical representation of the brains used. To aid registration of the confocal image stacks, all background data more than 10 voxels away from the neuropils of interest (based on the segmented data) were replaced with black voxels. In addition, the bounding box of all files was increased and standardized to the same dimensions (2000×1100×160) and voxel values were normalized.

All registration steps used normalized mutual information as the metric. First, all image stacks were subjected to a two-step affine registration processes. In the first step, a rigid transformation with six degrees of freedom (rotation and translation along/around the x, y, and z axis) was performed, followed by a non-rigid transformation with 9 degrees of freedom (i.e. additional scaling along the three cardinal axes). Next, the average gray values of the ten registered data stacks were calculated for each voxel in space, yielding a first averaged image stack. The result of this operation was then used as the new template for the next registration step. In the following five iterations of the registration, the image stacks were subjected to elastic transformations using a B-spline free-form deformation model. In this process a 3D grid is applied to the image stack and this grid is warped locally to match the local features of the current brain to the template brain. After elastic registration of all 10 brains, a new average was computed which served as the template for the next iteration. This sequence of computations was carried out five times, each time with a finer 3D grid.

For each registration step, the transformation parameters were saved and subsequently applied to the labelfields, i.e. the segmented images, resulting in registration of the labelfield data based on the registration of the confocal image data. Eventually an average labelfield was created by computing a shape-based average using signed Euclidean distance maps computed for each of the voxel values (Rohlfing and Maurer, 2007).

Because the registration process is based on the information content of the confocal grey value images, alignment of large peripheral neuropils with clear borders, like the calyces or the optic lobes is generally better than for small neuropils in the central brain. In the final shape-based average of the labelfields, this can lead to discontinuities and reduced sizes in structures like the central complex. To avoid this problem and obtain the best possible representation of the compartments of the central complex, these neuropils were both standardized together with the rest of the brain as well as individually. The results from the individual standardizations were then registered into the final brain through affine transformations.

The entire ISA protocol for the data set of the ten complete brains took about 10 days and 3 hours to complete on a 64 core node consisting of four AMD Opteron 6276 (interlagos) with 16 cores each, running at 2.3 GHz. The maximum memory usage was 3.86 GB.

Results

The Jewel Wasp Standard Brain (JWSB)

The average standard brain of the jewel wasp *N. vitripennis* females (Jewel Wasp Standard Brain: JWSB) was constructed after 5 passes of iterative shape averaging. As the source material of the JWSB was not dehydrated during the sample preparation, the JWSB is close to *in vivo* volumes, which will be useful for future use of the standard brain.

The current version of the JWSB (Figure 1A) is comprised of 12 distinct neuropils and excludes the lamina. As can be seen in Figure 1B, there is a large potential for further segmentation in the area now labeled 'rest of neuropils'. We expect that future versions of the JWSB will improve as our understanding of the *Nasonia* brain and our ability to discern neuropils increase.

Averaging small structures proved problematic. This is especially true for internal structures, which suffer more from the degradation in signal quality (and therefore lesser contrast) imposed by the lack of tissue dehydration. Averaging of the central complex (composed of several small midline neuropils) could therefore not be performed in the total brain but was instead by itself and later incorporated in the full brain.
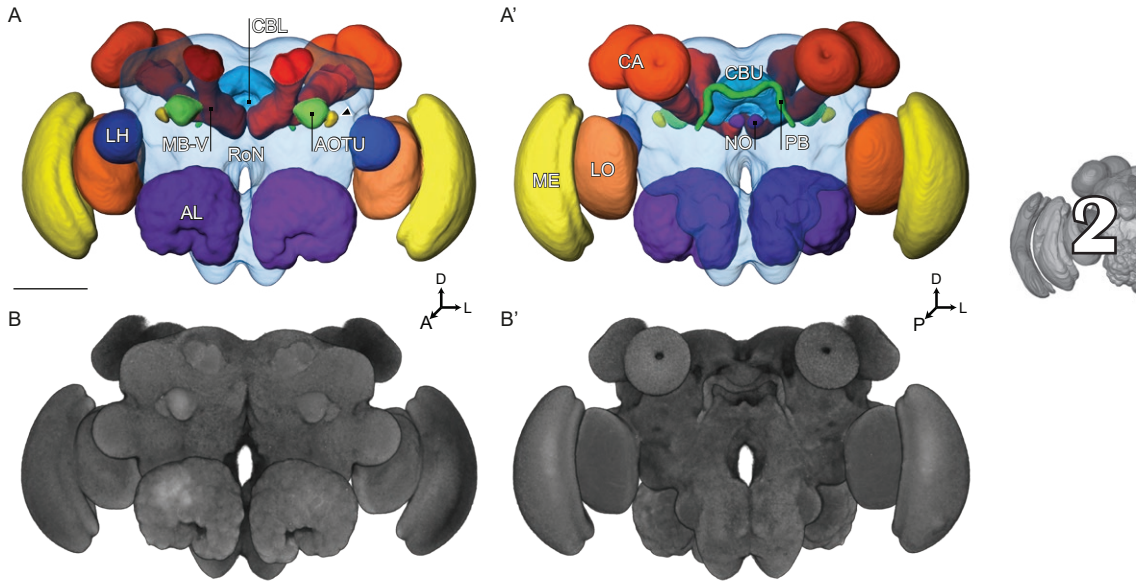
Figure 1. The *Nasonia vitripennis* standard brain, with labeled neuropils. **A.** A surface model from an anterior (A) and posterior (A') perspective. Arrowhead points to AOTU lower unit complex **B.** The averaged raw values of the α-Brp staining, seen as a direct volume rendering in the same orientation as in A. Abbreviations: AL, antennal lobe; AOTU, anterior optic tubercle; CA, calyx (mushroom body); EB, ellipsoid body (central complex); FB, fan-shaped body (central complex); LH, lateral horn; LO, lobula (optic lobes); MB-V, ventral mushroom body; ME, medulla (optic lobes); NO, noduli (central complex); RoN, rest of neuropils. Scale bar depicts 100 μm.

The average shape atlas was based on the sample closest to the median volume of all brains used, as such, the volume of the JWSB is comparable to the average of the source samples (Table 1). The relative volume of neuropils in the dehydrated and cleared brains is comparable to that of the JWSB source brains, though they are close to half the absolute volume of JWSB brains.

Morphology

Relative neuropil volumes are based on the manual segmentation of the JWSB source brain and calculated as percentage of total neuropil (excluding the lamina) and reported as mean ± standard error (*N*=10). For paired structures, the total volume (of both hemispheres) is given. When given, the axis of reference refers to the body axis (Ito et al., 2014).

Table 1. The Jewel Wasp Standard Brain in volume. Neuropil volumes of the iterative shape averaging result (JWSB), the manually segmented (uncleared, in vivo-like) source brains (*N*=10), and cleared and dehydrated *N. vitripennis* brains (HVRx strain, *N*=9, van der Woude et al. (2018)). All relative volumes based on total neuropils volume excluding the lamina. Abbreviations as used in Figure 1, with addition of: OL, optic lobes; MB, mushroom body; CX, central complex.

	Relative volumes (%)			Absolute volumes (µm³)			
	JWSB Volume	Source Mean ± SD	Dehydrated Mean ±SD	JWSB Volume	Source Mean ± SD	Dehydrated Mean ±SD	
				$1.70×10^7$	$1.74×10^7 ± 1.42×10^6$	$1.07×10^7 ± 7.37×10^5$	**Total**
OL	27.11	26.42 ± 0.9		$4.62×10^6$	$4.59×10^6 ± 3.60×10^5$		**OL**
LO	9.17	8.76 ± 0.55	8.59 ± 0.64	$1.56×10^6$	$1.52×10^6 ± 1.51×10^5$	$9.23×10^5 ± 1.28×10^5$	**LO**
ME	17.94	17.66 ± 0.65	18.5 ± 1.04	$3.06×10^6$	$3.07×10^6 ± 2.35×10^5$	$1.99×10^6 ± 2.49×10^5$	**ME**
AOTU	0.45	0.47 ± 0.05		$7.73×10^4$	$8.18×10^4 ± 6.30×10^3$		**AOTU**
AL	11.99	11.92 ± 0.67	11.29 ± 0.25	$2.04×10^6$	$2.07×10^6 ± 1.54×10^5$	$1.21×10^6 ± 7.44×10^4$	**AL**
LH	2.51	2.44 ± 0.33	2.76 ± 0.38	$4.28×10^5$	$4.23×10^5 ± 5.80×10^4$	$2.94×10^5 ± 4.31×10^4$	**LH**
MB	11.24	12.64 ± 0.4		$1.91×10^6$	$2.20×10^6 ± 1.83×10^5$		**MB**
MB-V	4.64	5.02 ± 0.25	5.04 ± 0.36	$7.91×10^5$	$8.72×10^5 ± 6.88×10^4$	$5.37×10^5 ± 3.36×10^4$	**MB-V**
CA	6.59	7.62 ± 0.4	7.45 ± 0.64	$1.12×10^6$	$1.32×10^6 ± 1.32×10^5$	$7.95×10^5 ± 5.90×10^4$	**CA**
CX	1.75	1.24 ± 0.12		$2.99×10^5$	$2.14×10^5 ± 1.45×10^4$		**CX**
FB	1.27	0.85 ± 0.09	0.99 ± 0.16	$2.17×10^5$	$1.47×10^5 ± 1.16×10^4$	$1.06×10^5 ± 1.41×10^4$	**FB**
EB	0.19	0.14 ± 0.03	0.16 ± 0.03	$3.28×10^4$	$2.48×10^4 ± 4.53×10^3$	$1.70×10^4 ± 2.24×10^3$	**EB**
NO	0.08	0.06 ± 0.06	0.08 ± 0.02	$1.41×10^4$	$1.06×10^4 ± 1.81×10^3$	$8.37×10^3 ± 1.68×10^3$	**NO**
PB	0.21	0.18 ± 0.03	0.26 ± 0.06	$3.49×10^4$	$3.20×10^4 ± 4.42×10^3$	$2.77×10^4 ± 6.44×10^3$	**PB**
RoN	44.94	44.87 ± 1.58	44.87 ± 0.96	$7.66×10^6$	$7.81×10^6 ± 8.14×10^5$	$4.80×10^6 ± 2.72×10^5$	**RoN**
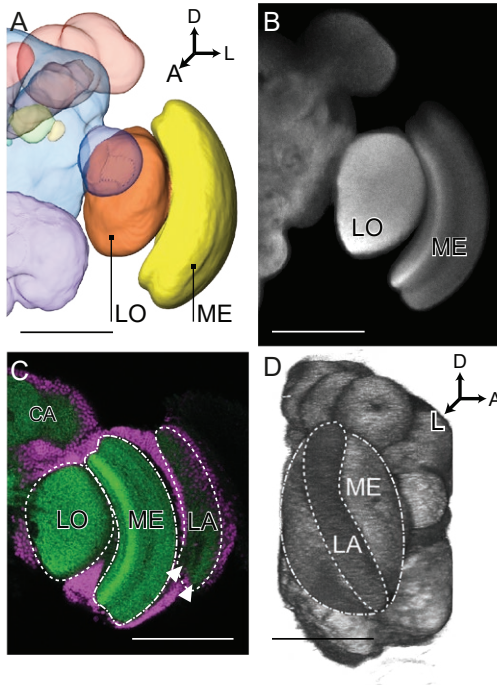
Figure 2. The Optic Lobes. **A.** Anterior view of the optic lobes in the standard brain as a surface reconstruction. **B.** A slice of averaged morphological data. **C.** 2 µm thick slice of α-Brp staining in a single brain, depicting the 3 optic lobes(similar orientation as in B). Obtained at 25× magnification; green: α-Brp, magenta: propidium iodide. Arrowheads point to layers in the lamina. **D.** Lateral view of a direct volume rendering of the preparation depicted in B, showing the relative thinness of the lamina. Abbreviations: CA, calyx (mushroom body); LA, lamina; LO, lobula; ME, medulla. Scale bars depict 100 µm.

Optic Lobes

Lamina

The smallest and most distal structure of the optic lobes, the lamina is a relatively thin layer of neuropil covering the medulla (Figure 2B, B'). The neuropil consists of two layers (arrowheads in Figure 2B) separated by an area of low staining intensity. Each layer appears to consist of many columnar units, called cartridges, which correspond to the ommatidia of the compound eye. The lamina was not included in the JWSB and the volumetric description presented in this work. In a previous analysis its relative volume was 5.23±0.69% (*N*=17) of the total brain (Groothuis and Smid, 2017). Based on our morphological staining, a dorsal rim area and accessory lamina are not evident. Due to its fragile nature, the lamina is often damaged and therefore not included in the standard brain.

Medulla

The medulla (Figure 2) is the largest neuropil of the optic lobes (relative volume of 17.66±0.65%), located between the lamina and lobula. Though gradients in the morphological staining hint at a layered structure as it is found in other insects (Ito et al., 2014), we cannot clearly identify boundaries between such layers. An accessory medulla has not been identified.

Lobula

The lobula (Figure 2) is located medially to the medulla and consists of a single neuropil with a relative volume of 8.76±0.55%. The morphological stainings reveal a layered pattern, though the exact number of layers cannot be determined with these stainings alone.

Mushroom Bodies

Calyx

The mushroom body calyx (Figure 3A, D) is formed by two fused spheroid neuropils: the lateral and medial calyx, together comprising a relative volume of 7.62±0.40%. The calyx neuropil stands out clearly against the surrounding cell bodies and lies slightly posteriorly of the most superior curve of the protocerebrum. Of the two, the lateral calyx lies slightly more anteriorly. There is a clear dorsal invagination visible in both parts of the calyx (e.g. Figure 3D, D"), but there is no clear division in concentric zones (lip, collar, or basal ring), nor are there obvious regions with varying microglomeruli densities.
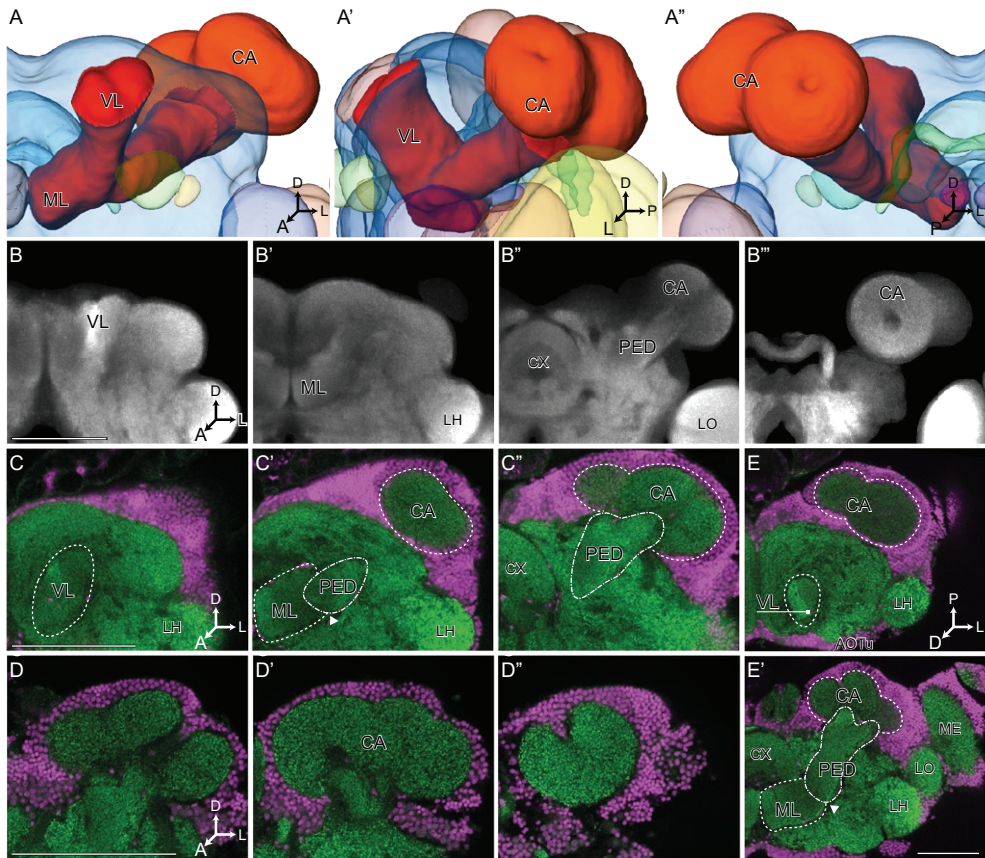
Figure 3. The Mushroom Body. **A.** Anterior (A), lateral (A'), and posterior (A") surface renderings of the mushroom body in the standard brain. **B.** Averaged morphological data of the standard brain at progressive depths from anterior to posterior. **C.** α-Brp staining in a single brain at progressive depths from anterior to posterior. 2 μm thick slices obtained at 25× magnification; green: α-Brp, magenta: propidium iodide. Arrowhead points to the pedunculus divide where it splits in the ML and VL. **D.** Detailed α-Brp slices of the calyx at progressive depths from anterior to posterior. 0.45 μm thick slices obtained at 40× magnification. **E.** The mushroom body from a dorsal perspective. 1 μm thick slices obtained at 25× magnification. Abbreviations: CA, calyx; CX, central complex; LH, lateral horn; LO, lobula; ME, medulla; ML, medial lobe; PED, pedunculus; VL, vertical lobe. Scale bars depict 100 μm.

Ventral Mushroom Body

We define the ventral mushroom body as comprising the pedunculus, vertical lobe, and medial lobe (Figure 3A, C, E). These are grouped together, because a clear boundary between these neuropils (at the pedunculus divide, arrowhead in Figure 3C', E') cannot be reliably made. The pedunculus runs from a more lateral and posterior position (ventral to the calyx) to a more anterior and medial location where it gives rise to the two lobes. The medial lobe is relatively short

and broad, it extends further to the midline where it touches the central complex. The vertical lobe is more slender and extends both superiorly and anteriorly, all the way to the surface of the protocerebrum. Based on the density of the αBrp staining, the ventral mushroom body has the appearance of a layered structure. In the pedunculus these layers appear twisted in a helical fashion, whereas the vertical and medial lobes have a non-twisted structure. In the lobes, these layers likely correspond to, for example, α- and α'-lobes described in other species (Ito et al., 2014). Together, the components of the ventral mushroom body make up 5.02±0.25 % of the total neuropil.

Figure 4. The Central Complex. **A.** α-Brp staining in a single brain at progressive depths from anterior to posterior. 0.45 μm thick slices obtained at 40× magnification; green: α-Brp, magenta: propidium iodide. **B.** Anterior (B), and posterior (B') surface renderings of the central complex in the standard brain. **C.** Averaged morphological data of the standard brain. Abbreviations: EB, ellipsoid body; FB, fan-shaped body; NO, noduli; OCG, ocellar ganglia; PB, protocerebral bridge. Scale bars depict 100 μm.
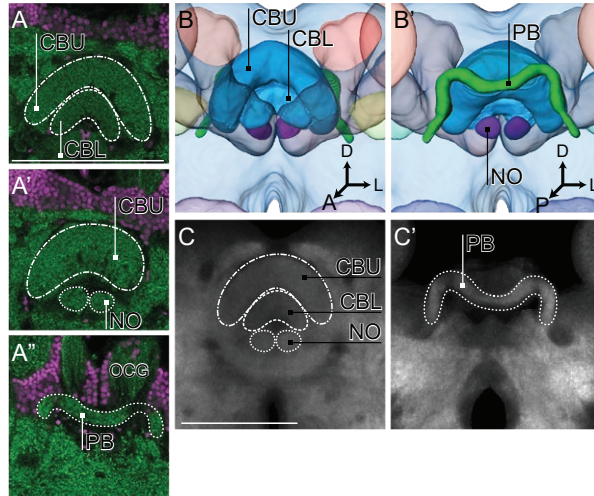
Central Complex

The central complex (Figure 4) stands out centrally in the brain around the midline. Its components are the central body (comprised of the fan-shaped body and the ellipsoid body), the protocerebral bridge, and the noduli.

Fan-shaped Body

The fan-shaped body (or upper part of the central body, Figure 4A, A'), is the largest component of the central complex, measuring 0.85±0.09% of the total neuropil. Its shape is roughly fan- or arch-like; the (paired) base of this arch is the most frontal part of the central body and often lies laterally to the tip of the mushroom body medial lobes, the apex extends to the posterior surface of the brain. As in other species (Ito et al., 2014), the αBrp staining hints towards an arrangement in columnar slices, but lacks consistently visible demarcations in our preparations.

Ellipsoid Body

Within the arch of the fan-shaped body lies the ellipsoid body (or lower part of the central body, Figure 4A), which is shaped like a smaller fan or arch itself rather than an ellipse. Like in the fan-shaped body, a general neuropil staining hints at a sliced structure, but lacks clear demarcations. The ellipsoid body is smaller than the fan-shaped body, measuring 0.14±0.03% of the total neuropil.

Protocerebral Bridge

The protocerebral bridge lies embedded in the cell body rind, slightly posterior from the central body (Figure 4A"). It has the classical handlebar shape and is connected in the midline, forming an unpaired structure instead of two paired neuropils. In most individual brains, the end of its lateral edge is indistinguishable from the start of the posterior optic tubercle, which also lies embedded in the rind. As such, these neuropils were analyzed as one volume in Groothuis and Smid (2017); their relative volume is 0.18±0.03 %.

Noduli

The noduli are paired spherical neuropils that lie directly posterior of the mushroom body medial lobes and ventrally to the central body (Figure 4A'). They comprise only 0.06±0.06% of the total neuropil.

Anterior Optic Tubercle

The anterior optic tubercle (Figure 5) protrudes from the anterior edge of the protocerebrum and is often the most anterior neuropil of the brain. It has a larger upper unit with a smaller lower unit complex at the lateral side. Together they make up 0.47±0.05% of the total neuropil. It is innervated by a thick bundle of fibers from the optic lobes, the anterior optic tract.
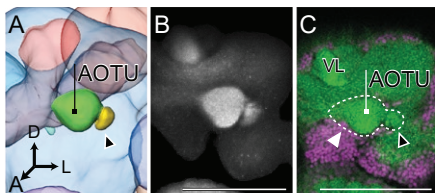
Figure 5. The Anterior Optic Tubercle. **A.** Anterior surface rendering of the anterior optic tubercle in the standard brain. Arrowhead points to the lower unit complex of the AOTU. **B.** Averaged morphological data of the standard brain. **C.** α-Brp staining in a single brain. 1 μm thick slice, obtained at 25× magnification; green: α-Brp, magenta: propidium iodide. Solid white arrowhead points to the upper unit of the AOTU, open arrowhead to the lower unit. Abbreviations: AOTU, anterior optic tubercle; VL, vertical lobe. Scale bars depict 100 μm.

Figure 6. The Lateral Horn. **A.** Anterior (A) and lateral (A') surface rendering of the lateral horn in the standard brain. **B.** Averaged morphological data of the standard brain **C.** α-Brp staining in a single brain. 1 μm thick slice, obtained at 25× magnification; green: α-Brp, magenta: propidium iodide. Abbreviations: AL, antennal lobe; LH, lateral horn; VL, vertical lobe. Scale bars depict 100 μm.
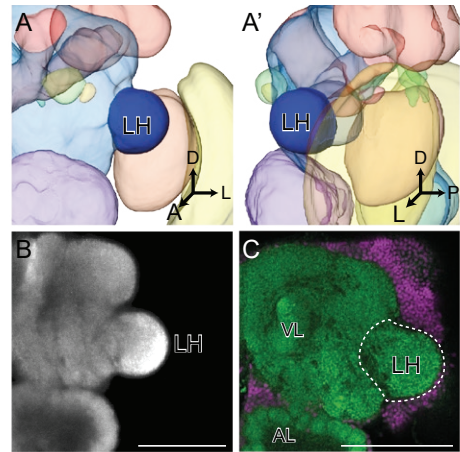
Lateral Horn

The lateral horn (Figure 6) is a second-order olfactory neuropil occupying 2.44±0.33% of the total neuropil. It is an easily-recognized spherical protuberance at the anterior and lateral side of the protocerebrum. Unlike several other neuropils discussed above, it does not have a glial sheath (Ito et al., 2014). As such, the interior boundary with other neuropils is not clearly defined by αBrp staining.

Antennal Lobe

The anteriorly located antennal lobe (Figure 7) consists of approximately 200 separate glomeruli (Figure 7C). There is some variation in glomerular volume that may be associated with specialization (for information pertaining to pheromones, for example), but there is no clear macroglomerular complex in the female

Figure 7. The Antennal Lobe. **A.** α-Brp staining in a single brain at progressive depths through the antennal lobe from anterior to posterior. 0.45 μm thick slices obtained at 40× magnification; green: α-Brp, magenta: propidium iodide. **B.** Anterior surface rendering (B) and averaged morphological data (B') of the antennal lobe in the standard brain. **C.** Anterior surface rendering of individual AL glomeruli in a single brain reconstruction. Colors are randomized. Abbreviations: AL, antennal lobe. Scale bars depict 100 μm.
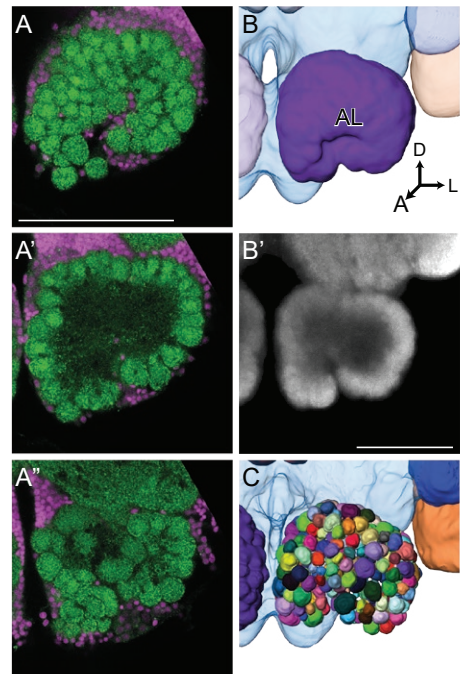
N. vitripennis brain. It seems there is little variation in glomerular volume and location between individuals, as glomeruli can still be recognized after the iterative shape averaging process. The total antennal lobe (the glomeruli and central hub combined) measures 11.92±0.67% of the total neuropil.

Rest of Neuropil

In the current Jewel Wasp Standard Brain, 44.87±1.58% of the total neuropil is not assigned to a specific label, owing to the lack of clearly recognizable demarcations for the remaining subregions. A notable feature of the remaining neuropil is the fusion of the cerebral and gnathal ganglia. The ocellar neuropils are not included in the segmentations.

Discussion

The Jewel Wasp Standard Brain

Here we present the first morphological description of the most prominent neuropils in the *N. vitripennis* brain, as well as the first average shape atlas to serve as a standard brain for these jewel wasps. Care was taken to ensure that the current standard brain will serve as a suitable reference for future studies.

First, the source brains were all from recently eclosed and naïve individuals, reducing effects of age- and experience-dependent plasticity. Second, potential influence of sex and genetic background was avoided by only using female wasps of the isogenic AsymCx line, which is most widely used and has a sequenced genome. Third, the Jewel Wasp Standard Brain is unique among insect standard brains due to one interesting aspect: as we avoided shrinkage of the source brains due to dehydration and clearing (and the potentially confounding effects thereof), the resulting average volumes are closer to those of an *in vivo* brain. This may aid researchers attempting to inject in, or record from, specific brain areas in the living animal (Grabe et al., 2015).

Future versions of the Jewel Wasp Standard Brain, building on better methods and better understanding of the *Nasonia* brain, will likely incorporate improvements such as better boundaries of the lateral horn, protocerebral bridge, and posterior optic tubercle. As in the desert locust *S. gregaria*, where an average central complex (el Jundi et al., 2010) was published to supplement its standard brain (Kurylas et al., 2008), a separate standardization of the central complex will enable better registration for studies that require a more detailed reference than is presented

here. In addition, more research in sexual dimorphism or brain morphology and behavior of the haploid *Nasonia* males may prompt the creation of a male standard brain.

The brain of *N. vitripennis* is, in most aspects, representative of a typical hymenopteran brain, though there are several interesting comparisons to be made on the shape and volume of its neuropils:

Shape-based comparison

In bees or ants, the calyx has a typical 'cup'-shape with elongated collars and obvious input-related subdivisions (Gronenberg, 2001); their lateral and medial calyx are two separate entities. In *Nasonia*, however, these are more globular or spheroid in shape, show no recognizable input-related subdivisions, and are fused where the 'cups' touch. This fusion of the calyces is reminiscent of that in moths (e.g. like the calyx of *Heliothis virescens* (Kvello et al., 2009)), but not as fused seen in *Drosophila* (Ito et al., 2014). The lateral horn has a pronounced and quite anterior position in the brain, compared to *Drosophila*, where it lies posteriorly relative to the optic lobes.

Volume-based comparison

We chose to compare the *N. vitripennis* brain with that of the honey bee (Brandt et al., 2005) and the fruit fly (Rein et al., 2002; Shao et al., 2014) due to their role as model organisms. In addition, we compare it with a group of 12 papers wasps (O'Donnell et al., 2014) as they represent a diverse group of Hymenoptera with varying ecologies. As is evident from the data in Table 2, the total neuropil of the *N. vitripennis* brain is much smaller than that of the honey bee or the group of paper wasps (though we must note that this is an underestimation, as brains of these animals were dehydrated and thus subject to shrinkage). But, despite of comparable body size (2-3 mm in length), the total neuropil volume is larger than that of the fruit fly. However, the compartmentalization of these brains is markedly different.

Comparing relative neuropil volumes, the optic lobes of *N. vitripennis* are of intermediate relative volume in the paper wasp range, but are much smaller than the optic lobes of both the honey bee and the fruit fly. The relative volume of the antennal lobe, on the other hand, is much larger in *N. vitripennis* than all others in this comparison, barring one paper wasp. These differences in optic and antennal lobe volume (and ratios between those and other neuropils)

likely reflect differences in sensory ecology (O'Donnell et al., 2014). Indeed, *N. vitripennis* is known to prioritize olfactory over visual information (Whiting, 1967) and brain architecture has been linked to behavior and ecology in other insects (e.g. Muscedere and Traniello (2012), de Vries et al. (2017), Stöckl et al. (2016)). Whether this one exception of the paper wasps (*Nectarinella championi*) relies more on olfaction than other paper wasps is unknown to us.

N. vitripennis is known as a strong learner (Hoedjes and Smid, 2014). Somewhat surprisingly, its mushroom body calyx in particular is of much smaller relative volume than that of the honey bee or all paper wasps in our comparison. This may be due to differences in the input from the aforementioned optic and antennal lobes to the calyx, but as we cannot distinguish input-specific zones (Gronenberg, 1999) this remains unknown. It must be noted that these other Hymenoptera are all social. Although interactions are required for growth of the mushroom body (Smith et al., 2010; Seid and Junge, 2016), mushroom body size is probably not related to sociality per se (Farris and Schulmeister, 2011). Another explanation may be that these social Hymenoptera require larger mushroom bodies due to an increased load of spatial learning by navigation and foraging (Farris and Van Dyke, 2015).

The relative volumes of the central complex present an interesting case of brain component scaling: the relative volume in *N. vitripennis* is almost twice that in the honey bee, and that in the fruit fly is again almost twice that of *N. vitripennis* (we must note, however, that these differences in relative volume are still within the same order of magnitude). Within species, smaller individuals have relatively larger central complexes (Mares et al., 2005; Gronenberg and Couvillon, 2010; Groothuis and Smid, 2017); we consider it likely that this is the case between species as well.

The anterior optic tubercle has a prominent presence on the anterior face of the brain and is comparable in relative volume to what is reported for *Manduca sexta* moths (0.43-0.44%) (el Jundi et al., 2009). The AOTU maintains its relative volume even with large differences in absolute brain volume (Groothuis and Smid, 2017), hinting at an ecological relevance of this neuropil. The role of this neuropil remains unclear however, though it may be involved with color processing (Mota et al., 2013), object discrimination (Aptekar et al., 2015), and light polarization processing (Pfeiffer and Kinoshita, 2012).

Table 2. Volumetric comparisons between *Nasonia vitripennis* and other insects. Data for *N. vitripennis* (AsymCx) are from the (uncleared, *in vivo*-like) source brains of the JWSB, *N*=10. Data for the honey bee *A. mellifera* are from Brandt et al. (2005), *N*=20. Data for brains of 12 paper wasps, *N*=3-6 per species, are extrapolated from data of worker brains in O'Donnell et al. (2014). Data for the fruit fly *D. melanogaster* females are combined from absolute data of neuropil compartments in Rein et al. (2002), *N*=28, and total brain volume from Shao et al. (2014), *N*=22, relative volumes are extrapolated from these sources. Honeybee and paper wasp tissue was dehydrated. Abbreviations as used in Figure 1, with addition of: OL, optic lobes; MB, mushroom body; CX, central complex.

Relative volumes (%)

	N. vitripennis (JWSB Source) Mean ± SD	*A. mellifera* Mean ± SD	12 Paper wasps Min to Max	*D. melanogaster* Mean ± SD
OL	26.42 ± 0.9		12.3 to 39.37	
LO	8.76 ± 0.55	8.66 ± 0.7		13.29 ± 1.12
ME	17.66 ± 0.65	29.93 ± 3.15		25.78 ± 2.5
AOTU	0.47 ± 0.05			
AL	11.92 ± 0.67	5.67 ± 0.75	3.17 to 14.29	4.59 ± 0.44
LH	2.44 ± 0.33			2.08 ± 0.25
MB	12.64 ± 0.4			3.71 ± 0.47
MB-V	5.02 ± 0.25	8.26 ± 0.77		
CA	7.62 ± 0.4	13.52 ± 0.7	10.59 to 31.65	
CX	1.24 ± 0.12	0.61 ± 0.11		
FB	0.85 ± 0.09			1.25 ± 0.18
EB	0.14 ± 0.03			0.43 ± 0.06
NO	0.06 ± 0.06			0.12 ± 0.02
PB	0.18 ± 0.03			0.24 ± 0.04
RoN	44.87 ± 1.58	33.36 ± 4.04	37.5 to 63.1	

Absolute volumes (µm³)

	N. vitripennis (JWSB Source) Mean ± SD	*A. mellifera* Mean ± SD	12 Paper wasps Min to Max	*D. melanogaster* Mean ± SD
Total	$1.74\times10^7 \pm 1.42\times10^6$	4.65×10^8	8.50×10^7 to 5.25×10^8	$8.30\times10^6 \pm 1.28\times10^6$
OL	$4.59\times10^6 \pm 3.60\times10^5$		2.90×10^7 to 1.99×10^8	
LO	$1.52\times10^6 \pm 1.51\times10^5$	$3.31\times10^7 \pm 2.68\times10^6$		$1.10\times10^6 \pm 9.30\times10^4$
ME	$3.07\times10^6 \pm 2.35\times10^5$	$1.14\times10^8 \pm 1.20\times10^7$		$2.14\times10^6 \pm 2.08\times10^5$
AOTU	$8.18\times10^4 \pm 6.30\times10^3$			
AL	$2.07\times10^6 \pm 1.54\times10^5$	$2.17\times10^7 \pm 2.86\times10^6$	5.00×10^6 to 3.20×10^7	$3.81\times10^5 \pm 3.66\times10^4$
LH	$4.23\times10^5 \pm 5.80\times10^4$			$1.72\times10^5 \pm 2.06\times10^4$
MB	$2.20\times10^6 \pm 1.83\times10^5$			$3.08\times10^5 \pm 3.90\times10^4$
MB-V	$8.72\times10^5 \pm 6.88\times10^4$	$3.15\times10^7 \pm 2.93\times10^6$		
CA	$1.32\times10^6 \pm 1.32\times10^5$	$5.16\times10^7 \pm 2.65\times10^6$	9.00×10^6 to 9.60×10^7	
CX	$2.14\times10^5 \pm 1.45\times10^4$	$2.32\times10^6 \pm 4.10\times10^5$		
FB	$1.47\times10^5 \pm 1.16\times10^4$			$1.04\times10^5 \pm 1.49\times10^4$
EB	$2.48\times10^4 \pm 4.53\times10^3$			$3.56\times10^4 \pm 4.62\times10^3$
NO	$1.06\times10^4 \pm 1.81\times10^3$			$9.97\times10^3 \pm 1.62\times10^3$
PB	$3.20\times10^4 \pm 4.42\times10^3$			$1.98\times10^4 \pm 3.20\times10^3$
RoN	$7.81\times10^6 \pm 8.14\times10^5$	$1.27\times10^8 \pm 1.54\times10^7$	4.10×10^7 to 2.22×10^8	

Conclusion

Members of the *Nasonia* genus are increasingly used in introgression studies, artificial selection studies, as well as developmental modification using RNAi or CRISPR/Cas9. In our own group, the focus has been especially on behavior, learning, and neurotransmitter networks. With this standard brain we have provided a tool that enables integration and consolidation of such studies in *Nasonia*, as well as the ability to provide direct comparisons of shape and volume between *Nasonia* strains or species.

Acknowledgements

Data accessibility

Raw volumetric data of the source brains of the JWSB can be found as supplementary data to Groothuis and Smid (2017).

An interactive 3-dimensional version of the JWSB is available on https://insectbraindb.org

References

Amunts K, Lepage C, Borgeat L, Mohlberg H, Dickscheid T, Rousseau ME, Bludau S, Bazin PL, Lewis LB, Oros-Peusquens AM, Shah NJ, Lippert T, Zilles K, Evans AC. 2013. BigBrain: An ultrahigh-resolution 3D human brain model. Science 340(6139):1472-1475.

Aptekar JW, Keles MF, Lu PM, Zolotova NM, Frye MA. 2015. Neurons forming optic glomeruli compute figure-ground discriminations in *Drosophila*. J Neurosci 35(19):7587-7599.

Brandt R, Rohlfing T, Rybak J, Krofczik S, Maye A, Westerhoff M, Hege HC, Menzel R. 2005. Three-dimensional average-shape atlas of the honeybee brain and its applications. J Comp Neurol 492(1):1-19.

Bucher D, Scholz M, Stetter M, Obermayer K, Pflüger HJ. 2000. Correction methods for three-dimensional reconstructions from confocal images: I. Tissue shrinking and axial scaling. J Neurosci Methods 100(1-2):135-143.

de Vries L, Pfeiffer K, Trebels B, Adden AK, Green K, Warrant E, Heinze S. 2017. Comparison of navigation-related brain regions in migratory versus non-migratory noctuid moths. Front Behav Neurosci 11:158.

Ding SL, Royall JJ, Sunkin SM, Ng L, Facer BAC, Lesnar P, Guillozet-Bongaarts A, McMurray B, Szafer A, Dolbeare TA, Stevens A, Tirrell L, Benner T, Caldejon S, Dalley RA, Dee N, Lau C, Nyhus J, Reding M, Riley ZL, Sandman D, Shen E, van der Kouwe A, Varjabedian A, Write M, Zollei L, Dang C, Knowles JA, Koch C, Phillips JW, Sestan N, Wohnoutka P, Zielke HR, Hohmann JG, Jones AR, Bernard A, Hawrylycz MJ, Hof PR, Fischl B, Lein ES. 2016. Comprehensive cellular-resolution atlas of the adult human brain. J Comp Neurol 524(16):3127-3481.

Dreyer D, Vitt H, Dippel S, Goetz B, el Jundi B, Kollmann M, Huetteroth W, Schachtner J. 2010. 3D standard brain of the red flour beetle *Tribolium castaneum*: a tool to study metamorphic development and adult plasticity. Front Syst Neurosci 4:3.

el Jundi B, Heinze S, Lenschow C, Kurylas A, Rohlfing T, Homberg U. 2010. The locust standard brain: a 3D standard of the central complex as a platform for neural network analysis. Front Syst Neurosci 3:21.

el Jundi B, Huetteroth W, Kurylas AE, Schachtner J. 2009. Anisometric brain dimorphism revisited: implementation of a volumetric 3D standard brain in *Manduca sexta*. J Comp Neurol 517(2):210-225.

Farris SM, Schulmeister S. 2011. Parasitoidism, not sociality, is associated with the evolution of elaborate mushroom bodies in the brains of hymenopteran insects. Proc R Soc B 278(1707):940-951.

Farris SM, Van Dyke JW. 2015. Evolution and function of the insect mushroom bodies: Contributions from comparative and model systems studies. Curr Opin Insect Sci 12:19-25.

Grabe V, Strutz A, Baschwitz A, Hansson BS, Sachse S. 2015. Digital in vivo 3D atlas of the antennal lobe of *Drosophila melanogaster*. J Comp Neurol 523(3):530-544.

Gronenberg W. 1999. Modality-specific segregation of input to ant mushroom bodies. Brain Behav Evol 54(2):85-95.

Gronenberg W. 2001. Subdivisions of hymenopteran mushroom body calyces by their afferent supply. J Comp Neurol 435(4):474-489.

Gronenberg W, Couvillon MJ. 2010. Brain composition and olfactory learning in honey bees. Neurobiol Learn Mem 93(3):435-443.

Groothuis J, Smid HM. 2017. *Nasonia* parasitic wasps escape from Haller's rule by diphasic, partially isometric brain-body size scaling and selective neuropil adaptations. Brain Behav Evol 90(3):243-254.

Hauser F, Neupert S, Williamson M, Predel R, Tanaka Y, Grimmelikhuijzen CJP. 2010. Genomics and peptidomics of neuropeptides and protein hormones present in the parasitic wasp *Nasonia vitripennis*. J Proteome Res 9(10):5296-5310.

Haverkamp A, Smid HM. 2014. Octopamine-like immunoreactive neurons in the brain and subesophageal ganglion of the parasitic wasps *Nasonia vitripennis* and *N. giraulti*. Cell Tissue Res 358(2):313-329.

Heinze S, Florman J, Asokaraj S, el Jundi B, Reppert SM. 2013. Anatomical basis of sun compass navigation II: The neuronal composition of the central complex of the monarch butterfly. J Comp Neurol 521(2):267-298.

Hoedjes KM, Smid HM. 2014. Natural variation in long-term memory formation among *Nasonia* parasitic wasp species. Behav Processes 105:40-45.

Hoedjes KM, Smid HM, Schijlen EG, Vet LEM, van Vugt JJ. 2015. Learning-induced gene expression in the heads of two *Nasonia* species that differ in long-term memory formation.

BMC Genomics 16:162.

Hoedjes KM, Steidle JLM, Werren JH, Vet LEM, Smid HM. 2012. High-throughput olfactory conditioning and memory retention test show variation in *Nasonia* parasitic wasps. Genes Brain Behav 11(7):879-887.

Ito K, Shinomiya K, Ito M, Armstrong JD, Boyan G, Hartenstein V, Harzsch S, Heisenberg M, Homberg U, Jenett A, Keshishian H, Restifo LL, Rossler W, Simpson JH, Strausfeld NJ, Strauss R, Vosshall LB, Grp IBNW. 2014. A systematic nomenclature for the insect brain. Neuron 81(4):755-765.

Kurylas AE, Rohlfing T, Krofczik S, Jenett A, Homberg U. 2008. Standardized atlas of the brain of the desert locust, *Schistocerca gregaria*. Cell Tissue Res 333(1):125-145.

Kvello P, Løfaldli BB, Rybak J, Menzel R, Mustaparta H. 2009. Digital, three-dimensional average shaped atlas of the *Heliothis virescens* brain with integrated gustatory and olfactory neurons. Front Syst Neurosci 3:14.

Lein ES, Hawrylycz MJ, Ao N, Ayres M, Bensinger A, Bernard A, Boe AF, Boguski MS, Brockway KS, Byrnes EJ, Chen L, Chen L, Chen TM, Chin MC, Chong J, Crook BE, Czaplinska A, Dang CN, Datta S, Dee NR, Desaki AL, Desta T, Diep E, Dolbeare TA, Donelan MJ, Dong HW, Dougherty JG, Duncan BJ, Ebbert AJ, Eichele G, Estin LK, Faber C, Facer BA, Fields R, Fischer SR, Fliss TP, Frensley C, Gates SN, Glattfelder KJ, Halverson KR, Hart MR, Hohmann JG, Howell MP, Jeung DP, Johnson RA, Karr PT, Kawal R, Kidney JM, Knapik RH, Kuan CL, Lake JH, Laramee AR, Larsen KD, Lau C, Lemon TA, Liang AJ, Liu Y, Luong LT, Michaels J, Morgan JJ, Morgan RJ, Mortrud MT, Mosqueda NF, Ng LL, Ng R, Orta GJ, Overly CC, Pak TH, Parry SE, Pathak SD, Pearson OC, Puchalski RB, Riley ZL, Rockett HR, Rowland SA, Royall JJ, Ruiz MJ, Sarno NR, Schaffnit K, Shapovalova NV, Sivisay T, Slaughterbeck CR, Smith SC, Smith KA, Smith BI, Sodt AJ, Stewart NN, Stumpf KR, Sunkin SM, Sutram M, Tam A, Teemer CD, Thaller C, Thompson CL, Varnam LR, Visel A, Whitlock RM, Wohnoutka PE, Wolkey CK, Wong VY, Wood M, Yaylaoglu MB, Young RC, Youngstrom BL, Yuan XF, Zhang B, Zwingman TA, Jones AR. 2007. Genome-wide atlas of gene expression in the adult mouse brain. Nature 445(7124):168-176.

Li M, Au LYC, Douglah D, Chong A, White BJ, Ferree PM, Akbari OS. 2017. Generation of heritable germline mutations in the jewel wasp *Nasonia vitripennis* using CRISPR/Cas9. Sci Rep 7(1):901.

Lynch JA. 2015. The expanding genetic toolbox of the wasp *Nasonia vitripennis* and its relatives. Genetics 199(4):897-904.

Mares S, Ash L, Gronenberg W. 2005. Brain allometry in bumblebee and honey bee workers. Brain Behav Evol 66(1):50-61.

Milyaev N, Osumi-Sutherland D, Reeve S, Burton N, Baldock RA, Armstrong JD. 2012. The Virtual Fly Brain browser and query interface. Bioinformatics 28(3):411-415.

Mota T, Gronenberg W, Giurfa M, Sandoz JC. 2013. Chromatic processing in the anterior optic tubercle of the honey bee brain. J Neurosci 33(1):4-U411.

Mukai A, Goto SG. 2016. The clock gene period is essential for the photoperiodic response in the jewel wasp *Nasonia vitripennis* (Hymenoptera: Pteromalidae). Appl Entomol Zool 51(2):185-194.

Muscedere ML, Traniello JF. 2012. Division of labor in the hyperdiverse ant genus *Pheidole* is associated with distinct subcaste- and age-related patterns of worker brain organization. PLoS One 7(2):e31618.

O'Donnell S, Clifford MR, Bulova SJ, DeLeon S, Papa C, Zahedi N. 2014. A test of neuroecological predictions using paperwasp caste differences in brain structure (Hymenoptera: Vespidae). Behav Ecol Sociobiol 68(4):529-536.

Pfeiffer K, Kinoshita M. 2012. Segregation of visual inputs from different regions of the compound eye in two parallel pathways through the anterior optic tubercle of the bumblebee (Bombus ignitus). J Comp Neurol 520(2):212-229.

Preibisch S, Saalfeld S, Tomancak P. 2009. Globally optimal stitching of tiled 3D microscopic image acquisitions. Bioinformatics 25(11):1463-1465.

Rago A, Gilbert DG, Choi JH, Sackton TB, Wang X, Kelkar YD, Werren JH, Colbourne JK. 2016. OGS2: genome re-annotation of the jewel wasp *Nasonia vitripennis*. BMC Genomics 17:678.

Rein K, Zockler M, Mader MT, Grubel C, Heisenberg M. 2002. The *Drosophila* standard brain. Current Biology 12(3):227-231.

Rohlfing T, Maurer CR, Jr. 2003. Nonrigid image registration in shared-memory multiprocessor environments with application to brains, breasts, and bees. IEEE Trans Inf Technol Biomed 7(1):16-25.

Rohlfing T, Maurer CR, Jr. 2007. Shape-based averaging. IEEE Trans Image Process 16(1):153-161.

Rybak J, Kuss A, Lamecker H, Zachow S, Hege HC, Lienhard M, Singer J, Neubert K, Menzel R. 2010. The bigital bee brain: integrating and managing neurons in a common 3D reference system. Front Syst Neurosci 4:30.

Schindelin J, Arganda-Carreras I, Frise E, Kaynig V, Longair M, Pietzsch T, Preibisch S, Rueden C, Saalfeld S, Schmid B, Tinevez JY, White DJ, Hartenstein V, Eliceiri K, Tomancak P, Cardona A. 2012. Fiji: an open-source platform for biological-image analysis. Nat Methods 9(7):676-682.

Schurmann D, Kugel D, Steidle JL. 2015. Early memory in the parasitoid wasp *Nasonia vitripennis*. J Comp Physiol A 201(4):375-383.

Schurmann D, Sommer C, Schinko APB, Greschista M, Smid H, Steidle JLM. 2012. Demonstration of long-term memory in the parasitic wasp *Nasonia vitripennis*. Entomol Exp Appl 143(2):199-206.

Seid MA, Junge E. 2016. Social isolation and brain development in the ant *Camponotus floridanus*. Sci Nat 103(5):1-6.

Shao HC, Wu CC, Chen GY, Chang HM, Chiang AS, Chen YC. 2014. Developing a stereotypical *Drosophila* brain atlas. IEEE Trans Biomed Eng 61(12):2848-2858.

Smith AR, Seid MA, Jimenez LC, Wcislo WT. 2010. Socially induced brain development in a facultatively eusocial sweat bee *Megalopta genalis* (Halictidae). Proc R Soc B 277(1691):2157-2163.

Stöckl A, Heinze S, Charalabidis A, el Jundi B, Warrant E, Kelber A. 2016. Differential investment in visual and olfactory brain areas reflects behavioural choices in hawk moths. Sci Rep 6:26041.

van der Woude E, Groothuis J, Smid HM. 2018. No gains for bigger brains: functional and neuroanatomical consequences of artificial selection on relative brain size in a wasp Submitted.

Van der Woude E, Smid HM. 2017a. Differential effects of brain scaling on memory performance in parasitic wasps. In prep.

Wagh DA, Rasse TM, Asan E, Hofbauer A, Schwenkert I, Durrbeck H, Buchner S, Dabauvalle MC, Schmidt M, Olin G, Wichmann C, Kittel R, Sigrist SJ, Buchner E. 2006. Bruchpilot, a protein with homology to ELKS/CAST, is required for structural integrity and function of synaptic active zones in *Drosophila*. Neuron 49(6):833-844.

Werren JH, Loehlin DW. 2009. The parasitoid wasp *Nasonia*: an emerging model system with haploid male genetics. Cold Spring Harb Protoc 4(10):pdb emo134.

Werren JH, Richards S, Desjardins CA, Niehuis O, Gadau J, Colbourne JK, Group NGW. 2010. Functional and evolutionary insights from the genomes of three parasitoid *Nasonia* species. Science 327(5963):343-348.

Whiting AR. 1967. The biology of the parasitic wasp *Mormoniella vitripennis* [=*Nasonia brevicornis*] (Walker). Q Rev Biol 42(3):333-406.

Zhao XC, Kvello P, Lofaldli BB, Lillevoll SC, Mustaparta H, Berg BG. 2014. Representation of pheromones, interspecific signals, and plant odors in higher olfactory centers; mapping physiologically identified antennal-lobe projection neurons in the male Heliothine moth. Front Syst Neurosci 8:186.

Genetically identical *Nasonia vitripennis* of different size

Chapter 3

Nasonia parasitic wasps escape from Haller's rule by diphasic, partially isometric brain-body size scaling and selective neuropil adaptations

Jitte Groothuis,
Hans M. Smid

Abstract

Haller's rule states that brains scale allometrically with body size in all animals, meaning that relative brain size increases with decreasing body size. This rule applies both on inter- and intraspecific comparisons. Only one species, the extremely small parasitic wasp *Trichogramma evanescens,* is known as an exception and shows an isometric brain-body size relation in an intraspecific comparison between differently-sized individuals. Here, we investigated if such isometric brain-body size relationship also occurs in an intraspecific comparison with a slightly larger parasitic wasp, *Nasonia vitripennis*, a species that may vary ten-fold in body weight upon differences in levels of scramble competition during larval development. We show that *Nasonia* exhibits diphasic brain-body size scaling: larger wasps scale allometrically, following Haller's rule, whereas the smallest wasps show isometric scaling. Brains of smaller wasps are, therefore, smaller than expected and we hypothesized that this may lead to adaptations in brain architecture. Volumetric analysis of neuropil composition revealed that wasps of different sizes differed in relative volume of multiple neuropils. The optic lobes and mushroom bodies in particular were smaller in the smallest wasps. Furthermore, smaller brains had relatively smaller total neuropil volume and larger cellular rind than large brains. These changes in relative brain size and brain architecture suggest that the energetic constraints on brain tissue outweigh specific cognitive requirements in small *Nasonia* wasps.

Introduction

Haller's rule states that small animals have relatively larger brains than larger animals and this has been supported by studies throughout the animal Kingdom (Rensch, 1948). One explanation for this relationship between body size and brain size is that smaller individuals require the same cognitive abilities as larger ones, and hence cannot scale their brain size at the same rate as their body size. This brain-body size relationship is a negative allometry, which can be visualized by a logarithmically transformed plot, where Ln(brain size) scales linearly to Ln(body size) with a slope, or allometric coefficient, 'b' that is smaller than 1. An isometric relationship would have a slope that is not different from 1. The negative allometry between brain size and body size holds true for inter- and intraspecies comparisons (Pagel and Harvey, 1988), but intraspecific comparisons yield lower slope values (indicating stronger allometry) than interspecific comparisons at higher taxonomic levels (Pagel and Harvey, 1988; 1989; Wehner et al., 2007). Diphasic intraspecific allometry has been described in ants, where small ants had a higher slope value than larger ants (Seid et al., 2011).

The smallest animal with a described intraspecific brain-body size relation is the wasp *Trichogramma evanescens*, an egg parasitoid with 0.3-0.9 mm body length. Remarkably, brain and body volume scaling shows isometry in this species (van der Woude et al., 2013). To our knowledge, *T. evanescens* is the only animal described that exhibits this isometry, thereby "escaping" Haller's rule. This may be because their brain volume comprises on average 8% of the body volume (van der Woude et al., 2013), which likely entails high metabolic costs that strongly constrain brain development in smaller individuals. Thus, isometry in *Trichogramma* wasps, and diphasic brain-body size scaling in small ants (with a higher allometric coefficient for the smallest individuals) may both be a consequence of miniaturized body size and the resulting high metabolic costs of their relatively large brain (Chittka and Niven, 2009; Eberhard and Wcislo, 2011).

Development of smaller brains, especially in cases where brains develop smaller than expected from Haller's rule, may be accommodated by a reduction in complexity, such as disproportionate scaling of neuropils. Such compensatory changes may be seen as the outcome of a trade-off between the energy requirements of neural tissue, which become larger in smaller individuals as relative brain size increases, and the requirement to maintain cognitive functions in the smallest wasps determined by their ecological relevance (Riveros and Gronenberg, 2010; Muscedere and Traniello, 2012; Stöckl et al., 2016; van der Woude and Smid, 2017b). Examples of absolute brain size influencing neuropil

composition include *Drosophila melanogaster*, for which the optic lobe size is relatively smaller in smaller individuals (Lanet et al., 2013). A decrease in relative optic lobe volume in smaller brains is also observed in a comparison of 13 paper wasp species (O'Donnell et al., 2013). In *T. evanescens*, the relative volume of antennal lobe glomeruli is smaller in the smallest wasps, although their number is constant (van der Woude and Smid, 2016), whereas relative antennal lobe volume is not influenced by brain or body size in much larger species like bumblebees and honeybees (Mares et al., 2005; Gronenberg and Couvillon, 2010).

Here, we investigated whether isometric brain-body size scaling and disproportionate neuropil scaling occurs in a parasitic wasp species with a less extreme level of body miniaturisation, the jewel wasp *Nasonia vitripennis* Walker, 1836 (Hymenoptera: Pteromalidae). *Nasonia vitripennis* are small parasitic wasps, generally 1.5-2.5 mm in length (Werren and Loehlin, 2009). They are ectoparasitoids of various fly species and the size of emerging wasps depends on size and quality of the host (Hoedjes et al., 2014a) and the number of eggs laid inside a host puparium (Charnov and Skinner, 1984; Sykes et al., 2007) . Increasing the number of eggs per puparium increases scramble competition between the developing larvae, which can result in a ten-fold reduction in body dry weight [this study, Figure 1]. Comparable body size differences may also be obtained in other species or lines such as *N. giraulti* or the outbred *N. vitripennis* HVRx line (Van de Zande et al., 2014), see Supplement S1. In nature, host quality and abundance likely varies profoundly, as well as the number of competing *Nasonia* females laying eggs.

The strong plasticity of body size in *N. vitripennis* permits the study of Haller's rule in this wasp species as a comparison to the minute *Trichogramma* wasp (van der Woude et al., 2013). Moreover, by using an isogenic *Nasonia* strain we exclude an effect of genetic variation on brain-body scaling. Assuming that the isometric

Figure 1. Two genetically identical individuals of the isogenic *Nasonia vitripennis* AsymCx line, subjected to different rearing conditions. The body (thorax + abdomen) length of the smallest wasp is 1375 μm and its head width is 469 μm. The largest wasp measures 2438 μm and 773 μm, respectively. Scale bar represents 1 mm.

brain-body size relation in *T. evanescens* is related to its extremely small size, we expected to find an allometric, but possibly diphasic, brain-body size relation in the bigger wasp *N. vitripennis*.

To investigate the effect of size variation on brain complexity in *N. vitripennis*, we compared relative volumes of specific neuropils of the largest wasps with the smallest wasps. We hypothesized that neuropil regions in the brains of differently sized *N. vitripennis* wasps show different degrees of scaling. Based on the knowledge that olfaction is of greater ecological relevance than vision for host location in *N. vitripennis* (Whiting, 1967) and the examples mentioned above, we expected to find larger effects of size plasticity in the optic lobes than the other neuropil regions, such as the antennal lobe.

Material and methods

Insect rearing

Nasonia vitripennis Walker, 1836 (Hymenoptera: Pteromalidae) wasps of the isogenic AsymCx strain were kept as described previously (Hoedjes et al., 2012). In short, for a rearing of regular sized wasps, wasps were reared on *Calliphora vomitoria* pupae (Kreikamp BV, Hoevelaken, The Netherlands) using 10 mated females to 20 fly pupae at 25±1 °C and 16:8 (L:D) photoperiod. To induce more size variation, wasps were reared as above, except at 50 female wasps to 5 fly pupae. Wasps could oviposit for 24 hours. After emergence, all wasps were kept overnight in vials with H_2O and honey prior to experiments. Only female wasps were considered for this study. Only naive wasps of 1-2 days old were used to prevent any confounding factors and minimise the influence of ontogenetic plasticity.

Head and body measurements

Measuring brain volume as wet tissue weight in *N. vitripennis* was expected to generate large errors, because of the small size and fragile nature of the brains (Haverkamp and Smid, 2014). Previous studies avoided this problem and investigated the brain volume by using confocal laser scanning microscopy and subsequent 3D volume reconstruction through the intact head capsule, which was either transparent by nature (van der Woude et al., 2013) or after clearing (Smolla et al., 2014). The latter procedure did not yield satisfactory results to unveil the brain in the black head capsule of *N. vitripennis* because of strong

deformation of the brain tissue (data not shown). However, van der Woude *et al.* (van der Woude et al., 2013) show a strong correlation between head and brain volume in *T. evanescens*. In this species, the head capsule is tightly connected to the brain. Such a correlation could be lower in larger insects with more glands or musculature (such as ant major workers or Vespid wasps, where head capsule volume is used as a proxy for body size (Bulova et al., 2016; O'Donnell and Bulova, 2017)). In Supplement 4 we show that this is not the case for *N. vitripennis*. Accordingly, we decided to use head capsule volume and body dry weight, respectively, as proxies for brain and body volume. These proxies allowed analysis of many wasps at high accuracy, yielding a robust data set while maintaining the ability to correlate individual head and body measurements.

Nasonia vitripennis individuals reared with induced size plasticity have a larger variation in size than those reared under standard conditions. Therefore, to obtain a complete representation of size variation in this species, 60 randomly selected wasps from this population were analyzed, in addition to 24 wasps reared under standard conditions. Following sedation on a CO_2 pad (Genesee Scientific), body (thorax + abdomen) length, hind tibia length, and head width were determined using an ocular micrometer. Wasps were decapitated with sharp tweezers (Dumont no. 5, Sigma) and the bodies were transferred to a 96-well plate (Greiner Bio-One), while heads were processed as described below. The bodies were dried at 65 °C for 1 hour and subsequently weighed on a Sartorius CP2P microbalance. Weighing was performed twice and the average was used in analyses. There was a very low measurement error for these measurements, with a high correlation between 1st and 2nd weighing (Pearson's $r = 0.9998$).

To measure head capsule volume of these decapitated wasps, an adaptation of previously used methods (Smolla et al., 2014; Werren et al., 2016) was used. After removal of the antennae, heads were placed in a 96-well plate and fixed for 24 hours at room temperature (RT) in 4% formaldehyde in 0.1M phosphate buffer (pH 7.2), freshly prepared from paraformaldehyde (PFA). After fixation, heads were washed for 24 hours in Phosphate Buffered Saline (PBS, Oxoid, Dulbecco 'A' tablets) at RT, followed by incubation in 30% H2O2 (Sigma) for 7-10 days at RT until the cuticle was an opaque white. Heads were then washed 4 times over 2 hours in PBS at RT and subsequently dehydrated through ethanol solutions of increasing concentration (30%, 50%, 70%, 80%, 90%, 96%, 100%, 2 minutes each) followed by an incubation in 50/50 ethanol/xylene, and 100% xylene for clearing. Heads were mounted in DPX mounting medium (Sigma) between two #1 cover slips, separated by a custom spacer (two stacked strips of adhesive tape, Henzo, Roermond, The Netherlands).

For confocal laser scanning microscopy, preparations were placed in a Cobb slide (Cobb, 1917) (purchased from Laboratory of Nematology, Wageningen University & Research). A Zeiss LSM510 microscope equipped with a 10× objective (Plan-Apochromat 10×/0.45) with a 512×512 px resolution was used for image acquisition. Excitation was induced with the 488 nm line of an Argon laser. Emission of autofluorescence was captured with 505-550 nm BP and 560 nm LP filters. Heads were scanned with a step size of 5 μm from both directions. To compensate for axial scaling due to refraction index mismatch (Bucher et al., 2000) between air and DPX, the voxel depth was scaled with a correction factor of 1.52. Final voxel calibration was 1.7995×1.7995×7.6 μm.

Anterior and posterior Z-stacks were flipped and rotated to the same orientation in FIJI (Schindelin et al., 2012) and fused with the Pairwise Stitching plugin (Preibisch et al., 2009). The head capsule was segmented every 4-5 slices using the segmentation editor in Amira 5.4.2 (Visage Imaging) with the Threshold and Brush tools. Interpolation was used to label the entire head; to ensure correct interpolation, all slices were inspected and corrected, if necessary. Head capsule volume was calculated with the MaterialStatistics module.

Neuropil stainings

To compare the neuropil distribution in *N. vitripennis* wasps of different sizes, two extreme groups of new wasps were analyzed. We selected Small wasps with a head width under 500 μm, and Large wasps with heads of more than 750 μm wide. As brains were pooled per size class during staining procedures, no further individual measurements were performed on these wasps.

Cold-sedated wasps were decapitated in ice-cold PBS. Using fine sharpened tweezers the cuticle was removed and brains dissected. Dissected brains were kept in freshly prepared ice-cold 4% formaldehyde. After obtaining several brains, brains in fixative solution were placed at RT and fixed for 2.5 hours. After rinsing 6 times for 5 min in PBS, the brains were treated in 5 mg/ml collagenase (Sigma) in PBS for 1 hour at RT, improving permeability of the tissue. Subsequently, brains were rinsed 4 times for 5 min in PBS containing 0.5% Triton-X100 (PBS-T) and pre-incubated in 10% normal goat serum (NGS, Dako, Glostrup, Denmark) in PBS-T (PBS-T-NGS) for 1 hour at RT. Brains were then incubated overnight at RT in the primary antibody (1:250 dilution of mouse anti-Bruchpilot (concentrate, DSHB hybridoma product nc82 (Wagh et al., 2006)) in PBS-T-NGS). Brains were rinsed 6 times for 20 min in PBS-T and incubated in 1:200 AlexaFluor®488-conjugated goat anti-mouse (Invitrogen)

and 1:500 propidium iodide (Sigma-Aldrich) for 4 hours. Brains were rinsed 4 times for 30 min in PBS-T and 2 times for 10 min in PBS. To avoid tissue shrinkage, which could lead to a confounding distortion of relative volumes, brains were not dehydrated and cleared. Instead, brains were mounted in aqueous VectaShield (Vector Laboratories) between two 24×24 mm coverslips with custom spacers and placed in a Cobb slide for imaging. Although the lack of clearing slightly diminished image quality, this does not outweigh the advantage we gained by comparing *in situ* volumes and posed no problem in segmenting neuropils.

Preparations were scanned with a Zeiss LSM510 microscope equipped with a 25× oil immersion objective (Plan-Neofluar 25×/0.8). AlexaFluor®488 staining was imaged using the 488 nm line of an Argon laser with a 505-550 nm BP filter, the propidium iodide nuclear counterstain was imaged using the same excitation wavelength but with a 560 nm LP filter. To accommodate the entire brain, 10-20% overlapping side-by-side Z-stacks were scanned from both sides of the preparation at 1024×1024 px with a digital magnification of 0.8 and a step size of 2 μm. To compensate for axial scaling due to refraction index mismatch (Bucher et al., 2000) between immersion oil and VectaShield, a correction of 0.9505 was applied to the voxel depth. Final voxel calibration was 0.4498844×0.4498844×1.901 μm. After image acquisition, the entire brain was reconstructed in FIJI as described for whole head mounts above.

Neuropil analysis

Complete image stacks were imported in Amira and the nc82 channel was used in the Segmentation Editor to assign voxels to 13 distinct neuropil regions. Standardized nomenclature (Ito et al., 2014) was used where possible. We included optic lobes (OL, i.e. lobula (LO), medulla (ME), lamina (LA)), anterior optic tubercle (AOTu), lateral horn (LH), antennal lobe (AL), mushroom body (MB, i.e. calyx (CA) and ventral MB (MB-V, i.e. pedunculus (PED), vertical (VL), medial lobes (ML))), central complex (CX, i.e. fan-shaped body (FB), ellipsoid body (EB), noduli (NO), and protocerebral bridge (PB)), and rest of neuropils (RoN). When possible, the cell body rind (the outermost layer of the arthropod brain, containing all neuronal cell bodies) was also segmented. For an overview, see Figure 3. Labels were assigned every 1-5 slices and completed with the Interpolation option. All slices were inspected and interpolation errors corrected when necessary. The MaterialStatistics module was used to compute absolute neuropil volumes. Volumetric data was imported in MS Excel and used to calculate relative volumes by dividing a neuropil volume by the total neuropil

volume of that brain. For confocal slices selected as illustration in Figure 3 the image contrast was optimized for viewing in FIJI. Surface models of individual brains selected for illustration were generated using the Amira SurfaceGen module.

Statistics

There is considerable discussion on the use of different regression methods in the study of allometry (e.g. (Smith, 2009; Voje et al., 2014; Kilmer and Rodríguez, 2017)). A particular topic of interest is the choice between ordinary least-squares (OLS) and (standardized) major axis (SMA) regression and what is actually described by slopes determined by these methods. In this work, we followed the advice of Kilmer and Rodríguez (2017) and use OLS regression to describe the relationship between *N. vitripennis* body size and brain size.

Piecewise regression analyses were performed as described by Crawley (2007). This method compares a linear regression model to a model that consists of two parts with distinct slopes. The break point where the slope changes was found by developing several regression models, each using a break point at a different value based on the unique weights in the dataset. The model with the lowest residual standard error was selected as the 2-slope model that described the data best. One-way Analysis of Variance (ANOVA) tests were used to compare the 1-slope and 2-slope regression models, and test which one provided a better fit. Similar analyses were used to test if a model with 3 slopes explained the data better than a 2-slope model.

We used ordinary least squares (OLS) regression models to estimate the coefficients of the 1-slope and 2-slope relationships between brain size and body size. To test for isometry, we tested if the slope was significantly different from 1 using the SMATR package (Warton et al., 2012). All regression analyses were performed in R version 3.3.2.

To compare volumes of brain compartments we used a multivariate linear model with the absolute or relative volume of the various neuropils as dependent variables and the size class (small or large) as fixed factor. This analysis was performed in R version 3.3.2. As we tested many variables (neuropils) at once, we corrected *p*-values of pairwise comparisons by means of the Holm-Bonferroni method for multiple comparisons (Holm, 1979). For supercategories (Ito et al., 2014) we used $m = 7$, for separate neuropils this was $m = 13$. This correction was performed in MS Excel. An α level of 0.05 was used for all analyses.

Results

Intraspecific brain-body size scaling in isogenic *N. vitripennis*

Body dry weights ranged from 40 to 438 μg, corresponding to body lengths of 1200 to 2420 μm. Head volumes measured from 11.4×10^6 to 81.1×10^6 μm³, corresponding to head widths of 414.5 to 803.1 μm. These results (Figure 2A) indicate that, under high scramble competition, *N. vitripennis* females have an adult (dry) body weight range spanning at least one order of magnitude. An overview of all measurements is given in Supplemental Table S2.

Ordinary Least Squares (OLS) regression on the natural logarithms of body dry weight and head capsule volume revealed a negatively allometric brain-body size relationship. The allometric coefficient (0.87, 95% CI [0.80, 0.94]) was significantly different from 1 ($p = 0.0006$).

(I) Ln(Head volume) = 0.87 × Ln(Body dry weight) + 12.97   ($R^2 = 0.87$)

A two-segment piecewise regression model with a break point at 183 μg ($R^2 = 0.91$, see Figure 2B for the break point analysis) explained the data better than a linear regression model (ANOVA, $F_{2,80} = 14.618$, $p < 0.001$) and showed a significant interaction between body dry weight and wasp size group ($p < 0.0001$). A separate OLS regression on small and large *N. vitripennis* wasps resulted in the relationships described in formulas II and III, respectively. The allometric coefficient of the small wasp regression (0.94, 95% CI [0.76, 1.13]) was not significantly different from 1 ($p = 0.54$). The allometric coefficient of the large wasp regression (0.22, 95% CI [0.00, 0.44]) was different from 1 ($p < 0.0001$) but not from 0 ($p = 0.053$). This indicates that wasps with a body dry weight lower than 183 μg show isometric brain-body size scaling, whereas larger wasps show negative allometry, or have an invariable brain size. We note that the fit of the allometric line in the larger wasps is not optimal ($R^2 = 0.09$), which may be caused in part by insufficient variation of the larger wasps on the Ln-transformed X-axis.

(II) Ln(Head volume) = 0.94 × Ln(Body dry weight) + 12.6   ($R^2 = 0.74$)

(III) Ln(Head volume) = 0.22 × Ln(Body dry weight) + 16.72   ($R^2 = 0.09$)

Three-segment piecewise regression was found to be no improvement over the model with two slopes (ANOVA, $F_{2,78} = 0.6921$, $p = 0.50$), therefore no three-segment OLS regression was performed. A two-segment model with the breakpoint at the second lowest residual standard error (at 302 μg) was also

Figure 2. Brain-body size scaling in *Nasonia vitripennis* depicted by logarithmic plots of body dry weight and head capsule volume. **A.** the result of single-slope Ordinary Least-Squares (OLS) regression (formula I). **B.** Residual standard error of multiple regression models (Y-axis), plotted for all unique body dry weights (index on X-axis). The lowest error is found at index 40, corresponding to 183 µg. The second lowest error is at index 52, corresponding to 302 µg. **C.** Diphasic allometry. solid line: OLS regression on wasps under 183 µg (formula II). Dashed line: OLS regression on wasps over 183 µg (formula III).

A. Single slope OLS regression

(I) Ln(HV) = 0.87 × Ln(BDW) + 12.97
(R^2=0.87)

B. Breakpoint analysis

C. Dual slope OLS regression

(III) Ln(HV) = 0.22 × Ln(BDW) + 16.72
(R^2=0.09)

(II) Ln(HV) = 0.94 × Ln(BDW) + 12.6
(R^2=0.74)
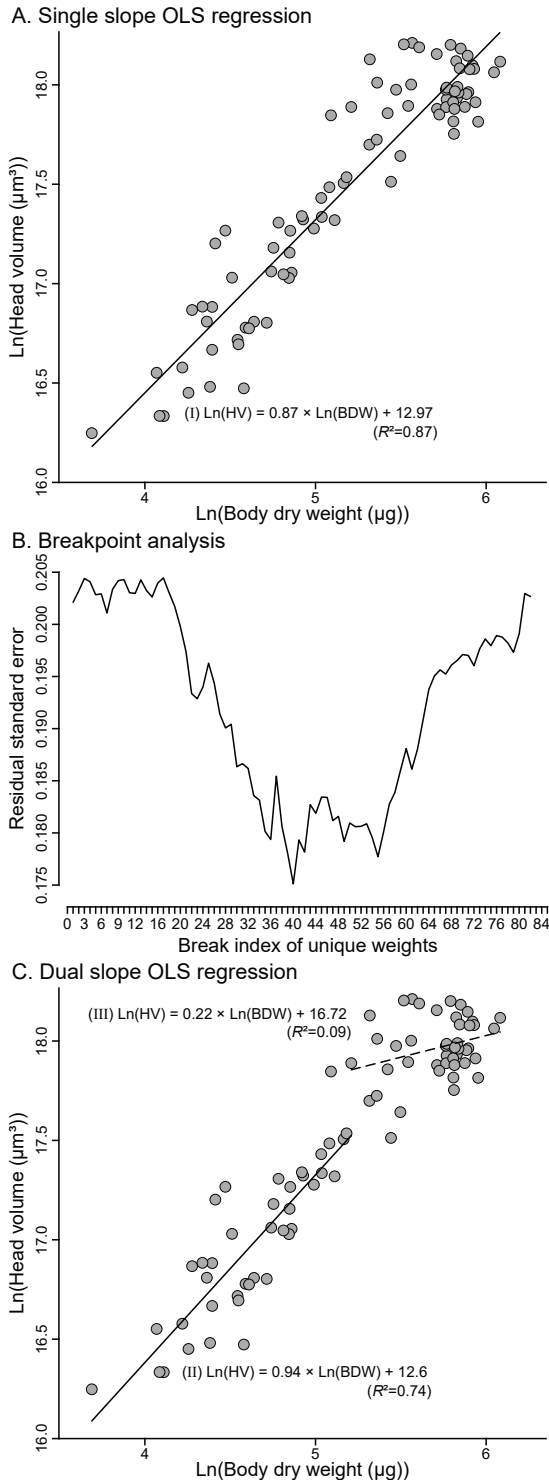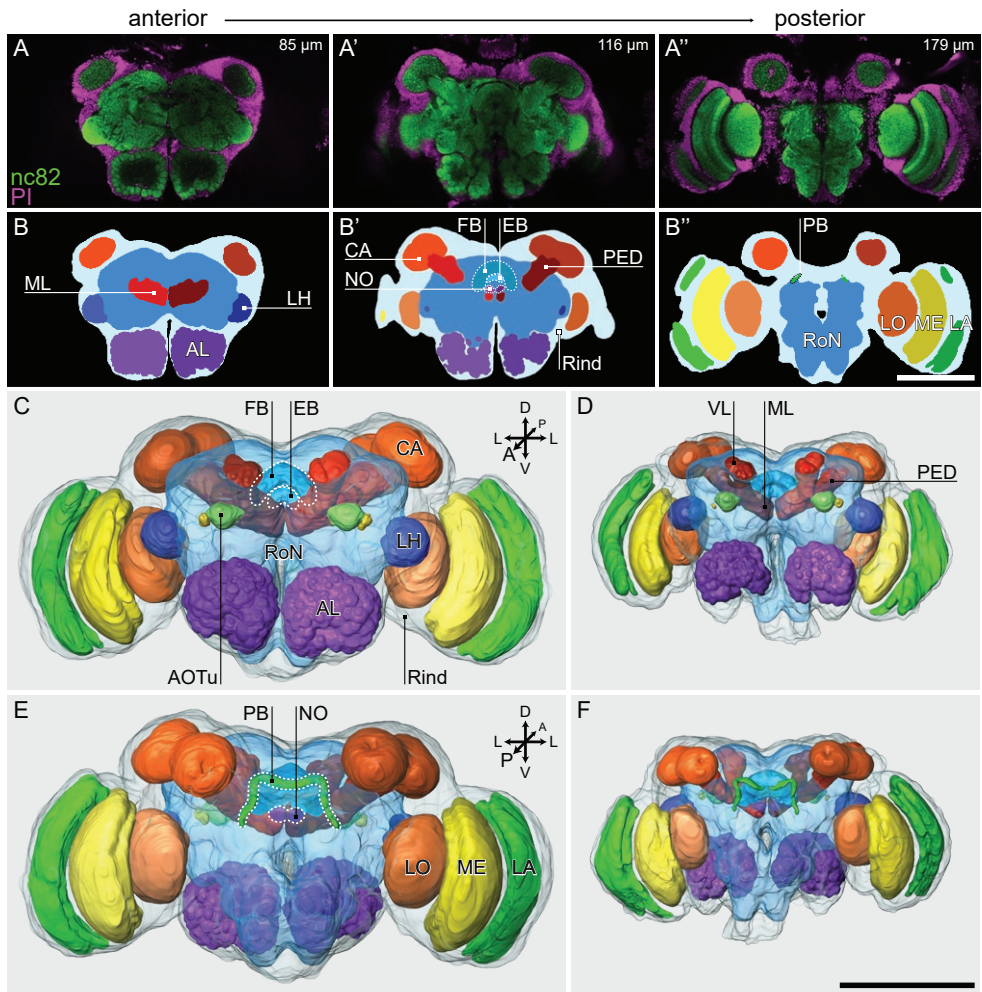
Figure 3. Overview of analyzed neuropils. **A.** Slices through a single *N. vitripennis* brain from the large population, fluorescently labeled with nc82 (green) and propidium iodide (magenta). Top-right notation depicts slice depth in μm. Slice orientation in panels A and B as in panel C, and refers to the body axis (Haverkamp and Smid, 2014; Ito et al., 2014). **B.** Corresponding labels of the cell body rind and segmented neuropils. Optic lobes (OL), i.e. lobula (LO), medulla (ME), and lamina (LA); mushroom body (MB), i.e. calyx (CA), pedunculus (PED), vertical lobe (VL, not visible in panel B), and medial lobe (ML). PED, VL, and ML were segmented as one label, the ventral mushroom body (MB-V); central complex (CX), i.e. fan-shaped body (FB), ellipsoid body (EB), protocerebral bridge (PB), and noduli (NO); lateral horn (LH); antennal lobe (AL); and rest of neuropil (RoN). Scale bar in panel B represents 200 μm and is representative for panel A as well. **C, D.** Anterior surface renderings based on the large brain shown in panel B (panel C), and a small brain (panel D). The cell body rind and RoN are transparent. **E, F.** Posterior views of the same brains as in panel C and D, respectively. Lettering in panels C-F as in panel B, with addition of the anterior optic tubercle (AOTu, not visible in panel B). These individual brains differ 2.1-fold in total volume, but the large brain is 61.8% neuropil, whereas the small brain is 47.1% neuropil. Scale bar in panel F represents 200 μm and is representative for panels C-F.

no better than the 183 μg model. In addition, we checked if other (non-linear) functions in log space could better describe the brain-body size scaling. A power law, as well as multiple degrees of polynomial functions, did not have a better fit than the two-segment piecewise regression presented above.

Total brain composition

Small wasps with a head width under 500 μm and Large wasps with heads of more than 750 μm wide had an average 2.3-fold difference in absolute total brain volume (i.e. neuropil with cell body rind) ($F_{1,22} = 459.32$, $p < 0.001$, Figure 4). Due to its fragility, the cell body rind was too damaged for segmentation in 4 large brains. Data for total brain volume of large brains are therefore reported for $N = 13$, whereas neuropil volumes of these brains are reported with $N = 17$. The largest *N. vitripennis* wasps ($N = 13$) measured $30.4 \pm 0.59 \times 10^6$ μm³ (mean±SE) in total brain volume, consisting of $60.45 \pm 0.74\%$ ($18.1 \pm 0.33 \times 10^6$ μm³) neuropil, with $39.55 \pm 0.74\%$ ($12.1 \pm 0.37 \times 10^6$ μm³) dedicated to the rind. Total brain in the smallest wasps ($N = 11$) was $13.3 \pm 0.52 \times 10^6$ μm³, of which $54.52 \pm 0.86\%$ ($7.2 \pm 0.31 \times 10^6$ μm³) was neuropil and $45.48 \pm 0.86\%$ ($6.0 \pm 0.27 \times 10^6$ μm³) rind. In terms of absolute neuropil volume, this is a 151.73% increase (i.e. approximately 2.5-fold) in the large wasps compared to the smallest wasps. The differences in relative total neuropil and relative cell body rind are significant, $F_{1,22} = 27.72$, $p < 0.001$.

Figure 4. Total brain volume. **A.** Differences in total brain volume. **B.** The proportion of the brain devoted to neuropil or cell body rind. Bar colors match the colors of neuropil and rind in Figure 3A. $N_{large} = 13$, $N_{small} = 11$. Error bars depict the SE. Asterisks depict significant differences, ***: p < 0.001.
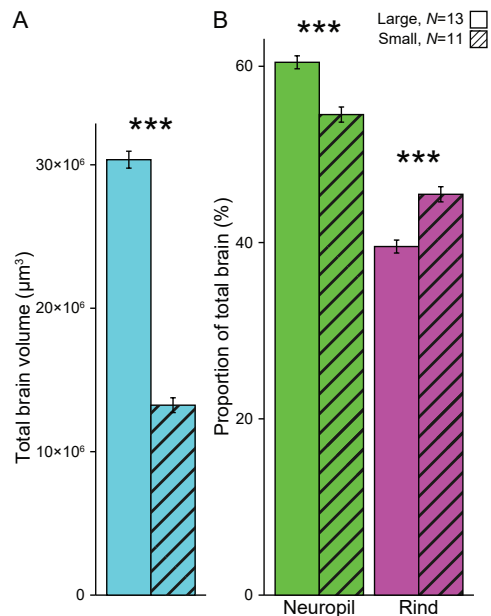
Neuropil scaling

At the level of neuropil supercategories (Figure 5), small wasps had a smaller relative volume of the optic lobes ($F_{1,26}$ = 40.93, corrected p < 0.001) and mushroom bodies ($F_{1,26}$ = 96.00, corrected p < 0.001). By contrast, relative volume of the central complex ($F_{1,26}$ = 25.36, corrected p < 0.001) and rest of the neuropil ($F_{1,26}$ = 64.86, corrected p < 0.001) were larger in small wasps. Complete data are reported in Supplemental Table S3.
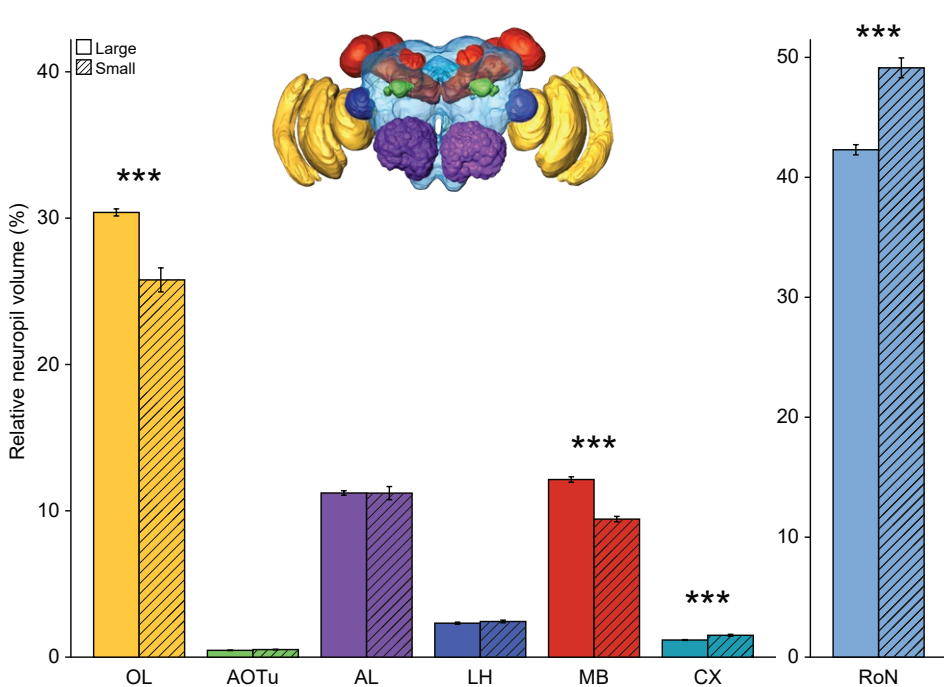
Figure 5. Relative neuropil volumes at supercategory level in large and small *N. vitripennis*. N_{large} = 17, N_{small} = 11. Abbreviations and bar colors as in Figure 3B-F and the brain inset. Error bars depict SE. Asterisks depict significant differences after Holm-Bonferroni correction (m = 7), ***: p < 0.001.

Further analysis (Figure 6) revealed that relative volumes of all neuropils of the optic lobes were significantly smaller in small wasps: the lobula ($F_{1,26}$ = 32.24, corrected p < 0.001), medulla ($F_{1,26}$ = 30.64, corrected p < 0.001), and lamina ($F_{1,26}$ = 9.60, corrected p = 0.03). Analysis of the mushroom body subunits revealed that the difference shown in Figure 5 was largely due to smaller relative volume of the calyx in small wasps ($F_{1,26}$ = 113.44, corrected p < 0.001) rather than the ventral mushroom body (peduncle and lobes), which showed a smaller and marginally insignificant difference ($F_{1,26}$ = 7.73, corrected p = 0.06). The

larger relative volume of the central complex in small wasps reported in Figure 5 was attributed to the fan-shaped body and ellipsoid body ($F_{1,26} = 22.89$, corrected $p < 0.001$ and $F_{1,26} = 32.83$, corrected $p < 0.001$, respectively), with no difference in relative volume of the noduli and protocerebral bridge. As in our previous analysis, the relative volume of the rest of the neuropil was larger in small wasps ($F_{1,26} = 64.86$, corrected $p < 0.001$) and no difference was found for the antennal lobe and lateral horn (primary and secondary olfactory neuropils, respectively). Complete data are reported in Supplemental Table S3.
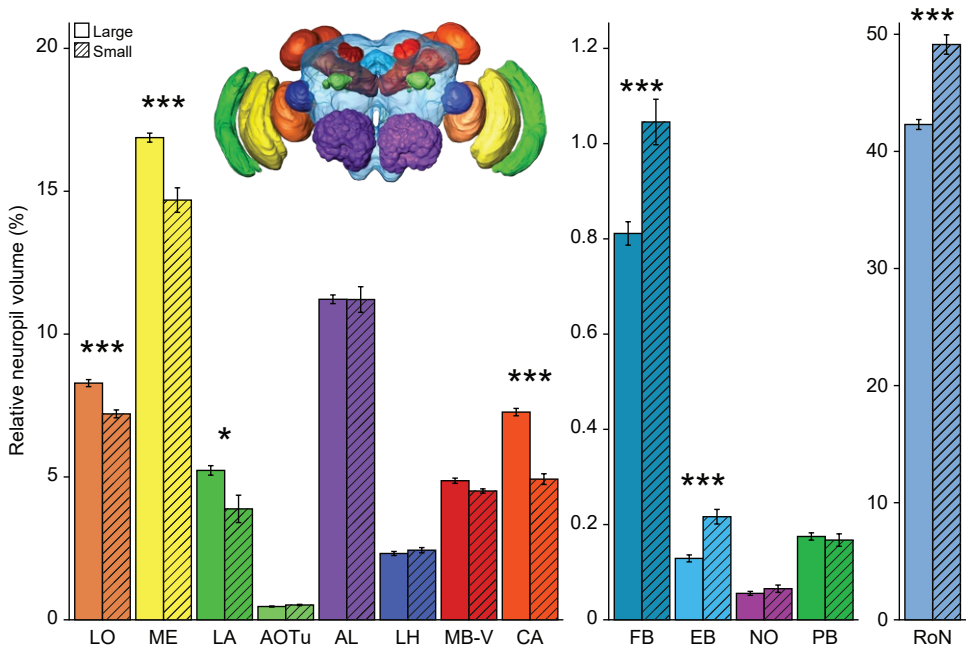
Figure 6. Relative neuropil volumes for individual neuropils in large and small *N. vitripennis*. $N_{large} = 17$, $N_{small} = 11$. Abbreviations and bar colors as in Figure 3B-F and the brain inset. Error bars depict SE. Asterisks depict significant differences after Holm-Bonferroni correction ($m = 13$), *: $0.01 < p < 0.05$, ***: $p < 0.001$.

Discussion

We induced a large degree of body size variation in an isogenic line of the parasitic wasp *Nasonia vitripennis* and found for the first time a diphasic brain-body size relationship where the smallest wasps showed isometry. Though diphasic scaling has been described in insects before (Seid et al., 2011), both phases described there show negative allometry. By contrast, diphasic brain scaling in *N. vitripennis* combines an isometric (b = 0.94) and a negative allometric (b = 0.22) phase for smaller and larger wasps, respectively. Our results indicate that *N. vitripennis* may

represent a link between isometric scaling in minute wasps (van der Woude et al., 2013) and diphasic allometry in larger insects (Seid et al., 2011). We present an overview of brain-body size scaling coefficients in several small hymenoptera showing that if body size becomes smaller, and relative brain size larger, a threshold is reached where negative allometry switches to isometry (Figure 7).
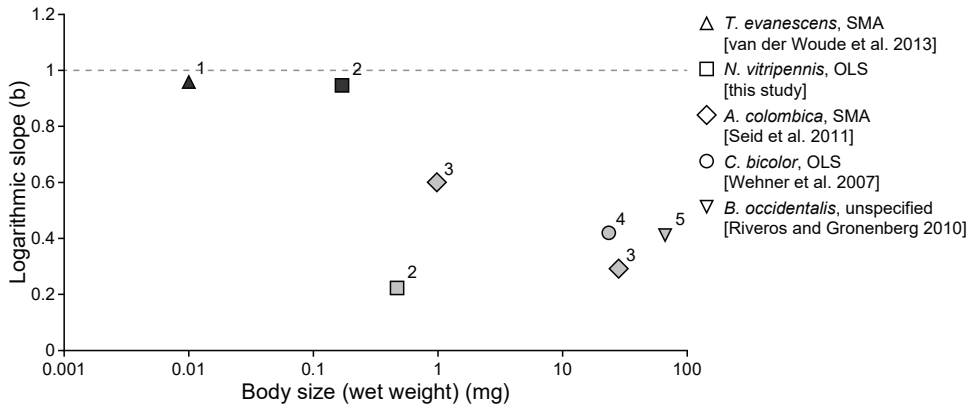
Figure 7. Brain-body size scaling depends on body size in insects. The five species shown here span several orders of magnitude in body size. Brain scaling coefficients are plotted against a common body size measurement: wet weight. For some species this weight was approximated as indicated. Scaling coefficients are isometric (dotted line at b = 1) in extremely small Hymenoptera (black data points), but allometric when body size increases (grey data points). Slopes reported here were obtained using different regression methods (see our notes in the M&M section), this is indicated in the figure legend. **1.** *Trichogramma evanescens* wasps, wet weight approximated using the density of water. **2.** *Nasonia vitripennis wasps*, wet weight approximated by weighing several sedated wasps (data not shown). Note that the two data points correspond to two size classes due to the diphasic scaling in this species. SMA regression would result in slightly different slopes values (b_{small} = 1.09 and b_{large} = 0.74), without affecting our main conclusions. **3.** *Atta colombica ants*. Two (allometric) data points due to diphasic scaling, as in species (2). **4.** *Cataglyphis bicolor* ants. **5.** *Bombus occidentalis* bumblebees.

Although we acknowledge the suboptimal allometric fit (R^2 = 0.09) for the larger wasps, statistical evidence for the fact that the scaling coefficient for larger wasps differs from 1 is strong. Moreover, we posit that this low fit only strengthens the notion that brain size is more strongly constrained at smaller body sizes than at larger body sizes. As evidenced by the very low allometric coefficient in the large phase and the fact that this value was different from 1 but not from 0, there is hardly any or no increase in brain size for larger wasps.

Due to the large variation in size in *N. vitripennis*, we expected to find compensatory changes in neuropil composition in extremely small brains. This expectation was strengthened by the isometric brain body size relation that we found in small wasps. We compared volumetric measurements for brains of small and

large wasps and indeed found specific neuropils with different relative volumes, whereas others had similar relative volume (Figure 6).

As expected, smaller individuals have reduced investment in the optic lobes. This correlates with our observation that smaller *N. vitripennis* have fewer and smaller ommatidia (see Supplement S5) and with developmental plasticity of the optic lobes observed in smaller *Drosophila melanogaster* (Lanet et al., 2013). The inverse was true for visually navigating *Cataglyphis bicolor* ants, where smaller individuals have relatively larger optic lobes (Kühn-Bühlmann and Wehner, 2006). Our finding that smaller *N. vitripennis* had a similar relative volume of the AL than larger conspecifics was also in line with our expectations, and with the lack of differences in AL cell lineages of smaller *D. melanogaster* (Lin et al., 2013) and constant relative AL volume in *Apis mellifera* of different sizes (Gronenberg and Couvillon, 2010). Direct links between antennal and optic lobe volumes and behavioral patterns have recently been reported for two moth species (Stöckl et al., 2016), suggesting that the importance of certain cues may be inferred from relative neuropil size. As mentioned above, *N. vitripennis* primarily uses olfaction, not vision for host finding (Jacobi, 1939; Whiting, 1967). This is reflected in our measurements on the developmental plasticity of the antennal and optic lobes: the antennal lobe is of higher importance and does not decrease in relative volume, whereas the optic lobes have fewer functional constraints and could grow to a smaller final relative volume. This confirms that relative neuropil volumes can give important insights into animal behavior.

Of particular interest is the unexpected finding of a relatively smaller mushroom body calyx in small *N. vitripennis*. This structure receives input of the antennal and optic lobes in most hymenopteran species (Gronenberg, 2001). Part of the reduction in relative calyx volume in smaller individuals may thus have resulted from a reduced input from the smaller optic lobe, although ants did not show a decrease in mushroom body volume after a decrease in the primary sensory neuropils (Waxman et al., 2017). Vision- or olfaction-specific calyx subunits that are visible in honeybees (i.e. lip and collar) are, however, not distinguishable in *N. vitripennis*. Therefore, we are unable to attribute this smaller relative calyx volume to changes in modality-specific subunits and must consider calyx volume as a whole. Interestingly, the lateral horn, which is more important for naive odor preferences (Parnas et al., 2013; Strutz et al., 2014), remained constant in relative volume. This suggests that smaller individuals (with a relatively smaller calyx) rely more on naive than on learned behavior. This was indeed demonstrated in a parallel study on the same AsymCx strain of *N. vitripennis* wasps (Van der Woude and Smid, 2017a). Small and large wasps were reared in the same way

as in our study, and it was shown that small individuals exhibited reduced visual and olfactory memory performance (Van der Woude and Smid, 2017a). Others have shown that *Pieris* butterflies with smaller calyces have reduced learning performance compared to individuals with larger calyces (Snell-Rood et al., 2009).This finding, however, is in contrast to miniature spiders and *T. evanescens*, which lack behavioral consequences of being small (Eberhard, 2011; Van der Woude and Smid, 2017a).

The central complex, important for e.g. locomotion and flight (Pfeiffer and Homberg, 2014), was relatively larger in the smallest *N. vitripennis* individuals, which is in line with studies investigating the brains of *Bombus impatiens* bumblebees (Mares et al., 2005), the honeybee *A. mellifera* (Gronenberg and Couvillon, 2010), and an interspecific analysis of 3 minute wasps (Makarova and Polilov, 2013b). Unlike the primary visual neuropils, the anterior optic tubercle did not vary in relative volume in our study. Maintaining relative optic tubercle size hints towards a relevance of polarized light (el Jundi et al., 2014) that, to our knowledge, has not been studied for this species.

The neuropil compartments grouped into 'rest of the neuropil', which comprised 43% to 50% of the total neuropil volume, also had a larger relative volume in small *N. vitripennis* wasps. Consequences of the large variation in brain and body volume may remain hidden, as this grouping contains a multitude of brain regions that cannot be segmented with the current level of knowledge on the *Nasonia* brain. For example, in *D. melanogaster,* at least 30 more neuropil regions may be specified in the central brain (Ito et al., 2014).

In addition to differences in relative neuropil volumes, the cell body rind is relatively larger in small *N. vitripennis* than in large individuals (Figure 4). This indicates that the level of volumetric plasticity is lower in cell bodies than in neuropils. Animals of different species, or orders, may use different rules for cellular scaling (Herculano-Houzel et al., 2014b). Depending on the species, changes in total brain volume may affect both cell number or size. The arthropod brain, especially one of this minute size, may pose some unique challenges in uncovering how it responds to the variation we described. For instance, specific neuron subtypes in brains of small and larger *T. evanescens* do not differ in number, but do differ in size, (van der Woude and Smid, 2017b). For *N. vitripennis*, more detailed studies are required to ascribe the difference in cell body rind volume to a variation in neuron numbers, neuron/glia ratio, cell body size, or a combination of these factors.

In this study, we used the isogenic AsymCx *N. vitripennis* line. This allowed for analysis of the phenotypic range of developmental plasticity only, in the absence of genotypic variation. This also implies that our results may be genotype-specific. Genotype does influence the brain-body size relationship to some extent in isogenic *T. evanescens* lines; however, all those lines exhibited similar (i.e. isometric) brain-body size relations (van der Woude et al., 2013). A comparison of body length and head width between the AsymCx line and the outbred HVRx line(Van de Zande et al., 2014) (outlined in Supplement S1) showed that AsymCx is not an "oddball" regarding its size range; equal variation is found in the *N. vitripennis* outbred line, as well as in a related species, *N. giraulti*.

Conclusion

In this study we provided evidence that brain-body size isometry is not restricted to *T. evanescens* wasps, but also exists in the small individuals of the slightly larger wasp species *N. vitripennis*. We expect brain-body size isometry to be more common than currently known; it may be present in other minute invertebrates, e.g. certain species of beetles, springtails, or ants. This trait may be linked to extreme reduction in arthropod body size beyond a certain threshold, where relative brain volume constitutes too large an energetic cost. This novel and unexpected finding sheds new light on the evolutionary constraints on brains in small bodies, which may be reflected in the changes in neuropil volume, selective adaptation in total cell body and total neuropil volume, and their effect on cognition, for instance on memory.

Data accessibility

The dataset supporting brain-body size scaling is part of Supplementary Table S2. Raw and analyzed volumetric data for all brains are part of Supplementary Table S3.

Acknowledgements

use of the confocal laser scanning microscope, and the helpful comments of anonymous reviewers. This work was supported by NWO Open Competition grant 820.01.012.

References

Bucher D, Scholz M, Stetter M, Obermayer K, Pflüger HJ. 2000. Correction methods for three-dimensional reconstructions from confocal images: I. Tissue shrinking and axial scaling. J Neurosci Methods 100(1-2):135-143.

Bulova S, Purce K, Khodak P, Sulger E, O'Donnell S. 2016. Into the black and back: the ecology of brain investment in Neotropical army ants (Formicidae: Dorylinae). Sci Nat 103(3):1-11.

Charnov EL, Skinner SW. 1984. Evolution of host selection and clutch size in parasitoid wasps. Fla Entomol 67(1):5-21.

Chittka L, Niven J. 2009. Are bigger brains better? Curr Biol 19(21):R995-R1008.

Cobb N. 1917. Notes on nemas. Contrib Sci Nematol 5:117-228.

Crawley MJ. 2007. Regression. The R Book: John Wiley & Sons, Ltd. p 387-448.

Eberhard WG. 2011. Are smaller animals behaviourally limited? Lack of clear constraints in miniature spiders. Anim Behav 81(4):813-823.

Eberhard WG, Wcislo WT. 2011. Grade changes in brain-body allometry: morphological and behavioural correlates of brain size in miniature spiders, insects and other invertebrates. In: Casas J, ed. Advances in Insect Physiology. Vol 40: Elsevier Limited. p 155-214.

el Jundi B, Pfeiffer K, Heinze S, Homberg U. 2014. Integration of polarization and chromatic cues in the insect sky compass. J Comp Physiol A 200(6):575-589.

Gronenberg W. 2001. Subdivisions of hymenopteran mushroom body calyces by their afferent supply. J Comp Neurol 435(4):474-489.

Gronenberg W, Couvillon MJ. 2010. Brain composition and olfactory learning in honey bees. Neurobiol Learn Mem 93(3):435-443.

Haverkamp A, Smid HM. 2014. Octopamine-like immunoreactive neurons in the brain and subesophageal ganglion of the parasitic wasps *Nasonia vitripennis* and *N. giraulti*. Cell Tissue Res 358(2):313-329.

Herculano-Houzel S, Manger PR, Kaas JH. 2014b. Brain scaling in mammalian evolution as a consequence of concerted and mosaic changes in numbers of neurons and average neuronal cell size. Front Neuroanat 8:77.

Hoedjes KM, Kralemann LEM, van Vugt JJFA, Vet LEM, Smid HM. 2014a. Unravelling reward value: the effect of host value on memory retention in *Nasonia* parasitic wasps. Anim Behav 96:1-7.

Hoedjes KM, Steidle JLM, Werren JH, Vet LEM, Smid HM. 2012. High-throughput olfactory conditioning and memory retention test show variation in *Nasonia* parasitic wasps. Genes Brain Behav 11(7):879-887.

Holm S. 1979. A simple sequentially rejective multiple test procedure. Scand J Stat 6(2):65-70.

Ito K, Shinomiya K, Ito M, Armstrong JD, Boyan G, Hartenstein V, Harzsch S, Heisenberg M, Homberg U, Jenett A, Keshishian H, Restifo LL, Rossler W, Simpson JH, Strausfeld NJ, Strauss R, Vosshall LB, Grp IBNW. 2014. A systematic nomenclature for the insect brain. Neuron 81(4):755-765.

Jacobi EF. 1939. Über Lebensweise, Auffinden des Wirtes und Regulierung der Individuenzahl von *Mormoniella vitripennis* Walker. Arch Neer Zool 3(2):139-282.

Kilmer JT, Rodríguez RL. 2017. Ordinary least squares regression is indicated for studies of allometry. J Evol Biol 30(1):4-12.

Kühn-Bühlmann S, Wehner R. 2006. Age-dependent and task-related volume changes in the mushroom bodies of visually guided desert ants, *Cataglyphis bicolor*. J Neurobiol 66(6):511-521.

Lanet E, Gould AP, Maurange C. 2013. Protection of neuronal diversity at the expense of neuronal numbers during nutrient restriction in the *Drosophila* visual system. Cell Rep 3(3):587-594.

Lin S, Marin EC, Yang CP, Kao CF, Apenteng BA, Huang Y, O'Connor MB, Truman JW, Lee T. 2013. Extremes of lineage plasticity in the *Drosophila* brain. Curr Biol 23(19):1908-1913.

Makarova AA, Polilov AA. 2013b. Peculiarities of the brain organization and fine structure in small insects related to miniaturization. 2. The smallest Hymenoptera (Mymaridae, Trichogrammatidae). Entomological review 93(6):714-724.

Mares S, Ash L, Gronenberg W. 2005. Brain allometry in bumblebee and honey bee workers. Brain Behav Evol 66(1):50-61.

Muscedere ML, Traniello JF. 2012. Division of labor in the hyperdiverse ant genus *Pheidole* is associated with distinct subcaste- and age-related patterns of worker brain organization. PLoS One 7(2):e31618.

O'Donnell S, Bulova S. 2017. Development and evolution of brain allometry in wasps (Vespidae): size, ecology and sociality. Curr Opin Insect Sci 22:54-61.

O'Donnell S, Clifford MR, DeLeon S, Papa C, Zahedi N, Bulova SJ. 2013. Brain size and visual environment predict species differences in paper wasp sensory processing brain regions (Hymenoptera: Vespidae, Polistinae). Brain Behav Evo:177-184.

Pagel MD, Harvey PH. 1988. The taxon-level problem in the evolution of mammalian brain size - facts and artifacts. Am Nat 132(3):344-359.

Pagel MD, Harvey PH. 1989. Taxonomic differences in the scaling of brain on body-weight among mammals. Science 244(4912):1589-1593.

Parnas M, Lin AC, Huetteroth W, Miesenbock G. 2013. Odor discrimination in *Drosophila*: from neural population codes to behavior. Neuron 79(5):932-944.

Pfeiffer K, Homberg U. 2014. Organization and functional roles of the central complex in the insect brain. Annu Rev Entomol 59:165-184.

Preibisch S, Saalfeld S, Tomancak P. 2009. Globally optimal stitching of tiled 3D microscopic image acquisitions. Bioinformatics 25(11):1463-1465.

Rensch B. 1948. Histological changes correlated with evolutionary changes of body size. Evolution 2(3):218-230.

Riveros AJ, Gronenberg W. 2010. Brain allometry and neural plasticity in the bumblebee *Bombus occidentalis*. Brain Behav Evol 75(2):138-148.

Schindelin J, Arganda-Carreras I, Frise E, Kaynig V, Longair M, Pietzsch T, Preibisch S, Rueden C, Saalfeld S, Schmid B, Tinevez JY, White DJ, Hartenstein V, Eliceiri K, Tomancak P, Cardona A. 2012. Fiji: an open-source platform for biological-image analysis. Nat Methods 9(7):676-682.

Seid MA, Castillo A, Wcislo WT. 2011. The allometry of brain miniaturization in ants. Brain Behav Evol 77(1):5-13.

Smith RJ. 2009. Use and misuse of the reduced major axis for line-fitting. Am J Phys Anthropol 140(3):476-486.

Smolla M, Ruchty M, Nagel M, Kleineidam CJ. 2014. Clearing pigmented insect cuticle to investigate small insects' organs in situ using confocal laser-scanning microscopy (CLSM). Arthropod Struct Dev 43(2):175-181.

3

Snell-Rood EC, Papaj DR, Gronenberg W. 2009. Brain size: a global or induced cost of learning? Brain Behav Evol 73(2):111-128.

Stöckl A, Heinze S, Charalabidis A, el Jundi B, Warrant E, Kelber A. 2016. Differential investment in visual and olfactory brain areas reflects behavioural choices in hawk moths. Sci Rep 6:26041.

Strutz A, Soelter J, Baschwitz A, Farhan A, Grabe V, Rybak J, Knaden M, Schmuker M, Hansson BS, Sachse S. 2014. Decoding odor quality and intensity in the *Drosophila* brain. eLife 3.

Sykes EM, Innocent TM, Pen I, Shuker DM, West SA. 2007. Asymmetric larval competition in the parasitoid wasp *Nasonia vitripennis*: a role in sex allocation? Behav Ecol Sociobiol 61(11):1751-1758.

Van de Zande L, Ferber S, De Haan A, Beukeboom LW, Van Heerwaarden J, Pannebakker BA. 2014. Development of a *Nasonia vitripennis* outbred laboratory population for genetic analysis. Mol Ecol Res 14(3):578-587.

van der Woude E, Smid HM. 2016. How to escape from Haller's rule: olfactory system complexity in small and large *Trichogramma evanescens* parasitic wasps. J Comp Neurol 524(9):1876-1891.

Van der Woude E, Smid HM. 2017a. Differential effects of brain scaling on memory performance in parasitic wasps. In prep.

van der Woude E, Smid HM. 2017b. Effects of isometric brain-body size scaling on the complexity of monoaminergic neurons in a minute parasitic wasp. Brain Behav Evol 89(3):185-194.

van der Woude E, Smid HM, Chittka L, Huigens ME. 2013. Breaking Haller's rule: brain-body size isometry in a minute parasitic wasp. Brain Behav Evol 81(2):86-92.

Voje KL, Hansen TF, Egset CK, Bolstad GH, Pélabon C. 2014. Allometric constraints and the evolution of allometry. Evolution 68(3):866-885.

Wagh DA, Rasse TM, Asan E, Hofbauer A, Schwenkert I, Durrbeck H, Buchner S, Dabauvalle MC, Schmidt M, Olin G, Wichmann C, Kittel R, Sigrist SJ, Buchner E. 2006. Bruchpilot, a protein with homology to ELKS/CAST, is required for structural integrity and function of synaptic active zones in *Drosophila*. Neuron 49(6):833-844.

Warton DI, Duursma RA, Falster DS, Taskinen S. 2012. smatr 3-an R package for estimation and inference about allometric lines. Methods Ecol Evol 3(2):257-259.

Waxman HK, Muscedere ML, Traniello JFA. 2017. Behavioral performance and neural systems are robust to sensory injury in workers of the ant *Pheidole dentata*. Brain Behav Evol 89(3):195-208.

Wehner R, Fukushi T, Isler K. 2007. On being small: brain allometry in ants. Brain Behav Evol 69(3):220-228.

Werren JH, Cohen LB, Gadau J, Ponce R, Baudry E, Lynch JA. 2016. Dissection of the complex genetic basis of craniofacial anomalies using haploid genetics and interspecies hybrids in *Nasonia* wasps. Dev Biol 415(2):391-405.

Werren JH, Loehlin DW. 2009. The parasitoid wasp *Nasonia*: an emerging model system with haploid male genetics. Cold Spring Harb Protoc 4(10):pdb emo134.

Whiting AR. 1967. The biology of the parasitic wasp *Mormoniella vitripennis* [=*Nasonia brevicornis*] (Walker). Q Rev Biol 42(3):333-406.

SUPPLEMENT

Supplement S1. Comparing lines

Introduction

In the main paper we studied the body-brain relationship in the isogenic AsymCx *N. vitripennis* line. In this supplement, we compare the range of size plasticity of the AsymCx line with that of a genetically diverse outbred line, HVRx (Van der Zande et al., 2014), as well as an isogenic line of the closely related species, *Nasonia giraulti* (R2VUx). A completely new dataset was generated using rearing conditions as described in the Methods section and plotted in figure S1. A trendline (MS Excel uses OLS regression) is provided for easier comparison. For this supplemental analysis, we measured Body Length (BL) and Head Width (HW) on sedated wasps. As such, the regressions provided here are different from the analysis provided in Figure 1 of the main text. For easier comparison to existing data, a BLxHW plot of the dataset used in the main text (Supplement S2) is provided in figure S2.

N. giraulti R2VUx
y = 0.9341x - 0.5446
R² = 0.9509

N. vitripennis HVRx
y = 0.949x - 0.719
R² = 0.9574

N. vitripennis AsymCx
y = 0.9663x - 0.864
R² = 0.9845

■ Nv AsymCx
▲ Nv HVRx
◆ Ng R2VUx
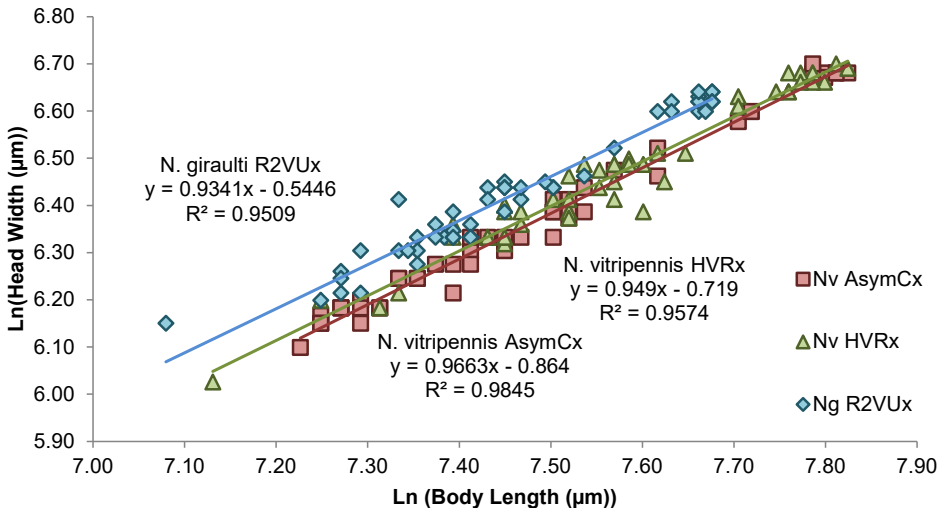
**Figure S1.** Ln(BL)xLn(HW) in 3 *Nasonia* lines with OLS regression.
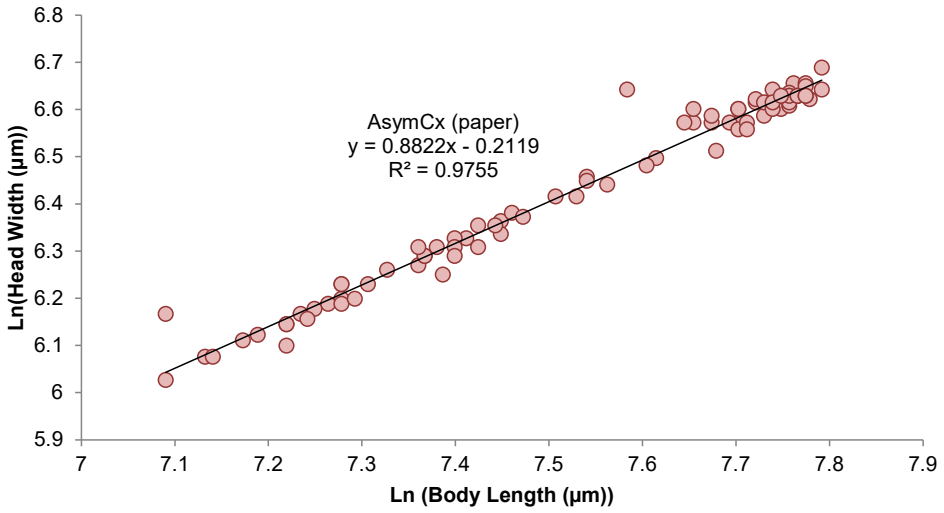
Figure S2. Ln(BL)xLn(HW) in AsymCx, paper.

Conclusion

The possible spread in body size is about equal for all studied lines. I.e. the AsymCx line is not unique in its potential size plasticity. Extremely small wasps remain outliers.

The full dataset is available online (https://dx.doi.org/10.6084/m9.figshare.5531839)

Supplement S2.

Table S1. Size measurements of individual wasps. TL, tibia length; BL, body length; BDW, body dry weight; HW, head width; HV, head volume.

TL (μm)	BL (μm)	BDW (μg)	weight1	weight2	HW (μm)	HV (μm³)
455.96	1572.41	129	130	128	528.5	25522356.48
398.96	1200	40	40	40	414.51	11385509.84
461.14	1655.17	119.5	120	119	559.59	32835483.84
455.96	1717.24	161	160	162	580.31	39227737.44
414.51	1448.28	98.5	98	99	492.23	19360323.6
383.42	1365.52	81	82	80	466.32	17316928.32
404.15	1448.28	103.5	104	103	507.77	19942161.36
435.23	1427.59	81	81	81	487.05	21483382.08
580.31	1882.76	226.5	228	225	637.31	56939376.32
424.87	1520.69	111.5	113	110	523.32	19838550.56
518.13	1634.48	154	155	153	559.59	33781407.2
393.78	1386.21	78.5	79	78	476.68	19957258
590.67	1882.76	203.5	202	205	632.12	48594652.32
544.04	1737.93	147	148	146	590.67	31867386.72
585.49	1820.69	175	177	173	611.4	40055410.88
466.32	1489.66	100.5	99	102	507.77	19286444
538.86	1675.86	138	139	137	549.22	33364431.68
580.31	1603.45	128	128	128	549.22	31515780.32
461.14	1200	76.5	75	78	476.68	21512175.44
435.23	1251.73	58.5	58	59	435.23	15426782.48
424.87	1262.07	61	62	60	435.23	12407932.52
471.5	1406.9	72	70	74	481.87	21152914.32
455.96	1448.28	91	91	91	507.77	24885733.36
461.14	1396.55	80	80	80	471.5	14373880
704.66	2213.79	320	318	322	715.03	61010386.24
652.85	2317.24	338.5	340	337	735.75	73966367.68
652.85	2110.35	238	238	238	715.03	64060241.92
704.66	2275.86	363.5	364	363	725.39	63291863.68
663.21	2255.17	340	339	341	746.11	61458956.48
652.85	2193.1	302.5	303	302	715.03	58173433.92
746.11	2337.93	318.5	319	318	740.93	64102820.16
756.48	2358.62	261.5	261	262	756.48	81089191.04
611.4	1924.14	212.5	212	213	626.94	49837793.44
715.03	2213.79	302	304	300	735.75	76657874.24
725.39	2255.17	347.5	349	346	751.3	78805123.52
704.66	2151.73	319	320	318	715.03	58704941.44
544.04	1634.48	127.5	128	127	549.22	28231875.04
476.68	1448.28	94	94	94	487.05	18206667.92
585.49	1758.62	153.5	155	152	585.49	37166264.8
518.13	1582.76	87.5	87	88	538.86	31534309.12
512.95	1582.76	116	116	116	538.86	28923450.72
590.67	1862.07	178	178	178	611.4	41259570.08
533.68	1634.48	82.5	82	83	538.86	29566690.4
554.4	1717.24	137	136	138	564.77	33924591.2
518.13	1613.79	127	126	128	518.13	24852288.8
569.95	1706.9	166	166	166	575.13	33243084
533.68	1572.41	123	122	124	549.22	25314326.24
538.86	1675.86	114.5	114	115	575.13	25679965.28
756.48	2348.28	359.5	360	359	777.2	62692205.44
683.94	2337.93	327.5	327	328	761.66	80275541.12

Table S1. (cont.)

TL (µm)	BL (µm)	BDW (µg)	weight1	weight2	HW (µm)	HV (µm³)
709.84	2110.35	183	184	182	735.75	58740448.64
683.94	2151.73	162.5	163	162	725.39	56321897.6
787.56	2420.69	272.5	273	272	803.11	79299518.72
683.94	2089.66	255.5	254	257	715.03	59051185.28
715.03	2275.86	306.5	308	305	746.11	56543762.88
471.5	1365.52	97.5	97	98	466.32	14261483.6
445.6	1365.52	70.5	72	69	445.6	13946988
497.41	1468.97	94.5	94	95	492.23	17801358.4
440.41	1303.45	59.5	60	59	450.78	12417506.24
445.6	1324.14	68	67	69	455.96	15838193.28
663.21	2337.93	372.5	373	372	756.48	72413748.48
694.3	2213.79	385	385	385	704.66	54550915.2
715.03	2389.66	422.5	422	423	751.3	69930640
694.3	2337.93	332.5	333	332	746.11	60187421.76
746.11	2420.69	345.5	346	345	766.84	71344951.36
704.66	2317.24	376	376 [1]		756.48	71148214.72
715.03	2234.48	333	333		715.03	54630137.6
642.49	2027.59	231	231		663.21	40325730.72
746.11	2296.55	204	204		766.84	74645126.72
756.48	2379.31	213	213		777.2	66386905.92
642.49	2296.55	343	343		735.75	63146807.04
735.75	2337.93	356	356		756.48	58762847.36
652.85	2162.07	334	334		673.58	51306906.88
663.21	2358.62	362	362		756.48	76027700.48
642.49	2006.9	244	244		652.85	45905629.44
715.03	2213.79	320	320		735.75	64744643.2
683.94	2234.48	335	335		704.66	58170381.76
725.39	2296.55	260	260		746.11	65769457.6
735.75	1965.52	438	438		766.84	73778586.88
735.75	2379.31	366	366		772.02	71019993.6
761.66	2317.24	341	341		756.48	64978036.16
740.93	2358.62	336	336		756.48	63563755.2
720.21	2379.31	379	379		756.48	60154784.32
746.11	2379.31	249	249		756.48	80485982.08

$y = 0.997x + 0.3103$
$R^2 = 0.9997$
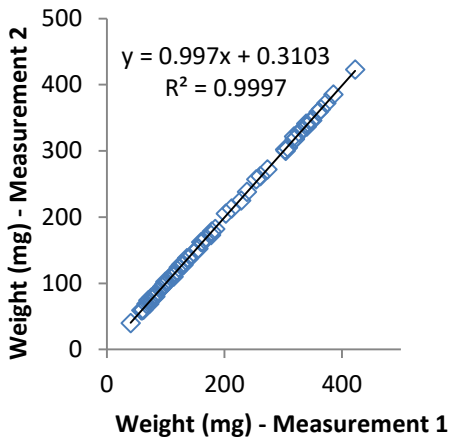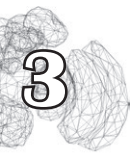
Figure S3. Correlation between dry body weight measurement 1 and 2 of the first 65 measurements.

Supplement S3.

Table S2. Relative ([Neuropil]/[Total Neuropil]*100) and absolute volumetric data on several neuropil regions in small and large *Nasonia vitripennis* wasps.

	Size Class (Head width)	Relative volume			Absolute volume		
		Statistics	N	Mean (%) ± SE	Statistics	N	Mean (µm³) ± SE
Total Brain	> 750 µm				$F_{1,22}=459.32$	13	$3.04×10^7 ± 5.90×10^5$
	< 500 µm				$p<0.001$	11	$1.32×10^7 ± 5.15×10^5$
Cell Body Rind [1]	> 750 µm	$F_{1,22}=27.72$	13	39.55 ± 0.736		13	$1.21×10^7 ± 3.71×10^5$
	< 500 µm	$p<0.001$	11	45.48 ± 0.862		11	$6.04×10^6 ± 2.73×10^5$
Total Neuropil [1]	> 750 µm	$F_{1,22}=27.72$	13	60.45 ± 0.736		17	$1.81×10^7 ± 3.35×10^5$
	< 500 µm	$p<0.001$	11	54.52 ± 0.862		11	$7.20×10^6 ± 3.05×10^5$
Optic Lobe (OL)	> 750 µm	$F_{1,26}=40.93$	17	30.39 ± 0.243		17	$5.52×10^6 ± 8.55×10^4$
	< 500 µm	$p<0.001$ [2]	11	25.78 ± 0.821		11	$1.86×10^6 ± 8.98×10^4$
Lobula (LO)	> 750 µm	$F_{1,26}=32.24$	17	8.28 ± 0.123		17	$1.51×10^6 ± 3.57×10^4$
	< 500 µm	$p<0.001$ [3]	11	7.21 ± 0.139		11	$5.19×10^5 ± 1.56×10^4$
Medulla (ME)	> 750 µm	$F_{1,26}=30.64$	17	16.88 ± 0.157		17	$3.07×10^6 ± 5.11×10^4$
	< 500 µm	$p<0.001$ [3]	11	14.69 ± 0.43		11	$1.07×10^6 ± 5.76×10^4$
Lamina (LA)	> 750 µm	$F_{1,26}=9.60$	17	5.23 ± 0.166		17	$9.48×10^5 ± 2.87×10^4$
	< 500 µm	$p=0.03$ [3]	11	3.88 ± 0.479		11	$2.79×10^5 ± 3.53×10^4$
Anterior Optic Tubercle [4] (AOTu)	> 750 µm	N.S.	17	0.47 ± 0.018		17	$8.42×10^4 ± 3.11×10^3$
	< 500 µm	$F_{1,26}=3.48$ $p=0.37$ [3]	11	0.52 ± 0.022		11	$3.74×10^4 ± 2.20×10^3$
Antennal Lobe (AL) [4]	> 750 µm	N.S.	17	11.22 ± 0.15		17	$2.04×10^6 ± 3.69×10^4$
	< 500 µm	$F_{1,26}=0.00$ $p=0.98$ [3]	11	11.21 ± 0.449		11	$8.16×10^5 ± 5.98×10^4$
Lateral Horn (LH) [4]	> 750 µm	N.S.	17	2.32 ± 0.07		17	$4.22×10^5 ± 1.39×10^4$
	< 500 µm	$F_{1,26}=1.00$ $p=0.98$ [3]	11	2.44 ± 0.091		11	$1.77×10^5 ± 1.19×10^4$
Mushroom Body (MB)	> 750 µm	$F_{1,26}=96.00$	17	12.14 ± 0.186		17	$2.21×10^6 ± 4.86×10^4$
	< 500 µm	$p<0.001$ [2]	11	9.43 ± 0.187		11	$6.78×10^5 ± 1.98×10^4$
Ventral MB (MB-V) (Lobes&Peduncle)	> 750 µm	N.S.	17	4.87 ± 0.09		17	$8.84×10^5 ± 1.93×10^4$
	< 500 µm	$F_{1,26}=7.73$ $p=0.060$ [3]	11	4.51 ± 0.075		11	$3.25×10^5 ± 1.24×10^4$
MB Calyx (CA)	> 750 µm	$F_{1,26}=113.44$	17	7.27 ± 0.13		17	$1.32×10^6 ± 3.38×10^4$
	< 500 µm	$p<0.001$ [3]	11	4.92 ± 0.188		11	$3.53×10^5 ± 1.26×10^4$
Central Complex (CX)	> 750 µm	$F_{1,26}=25.36$	17	1.17 ± 0.028		17	$2.12×10^5 ± 4.82×10^3$
	< 500 µm	$p<0.001$ [2]	11	1.49 ± 0.068		11	$1.07×10^5 ± 5.15×10^3$
Fan-Shaped Body (FB)	> 750 µm	$F_{1,26}=22.89$	17	0.81 ± 0.025		17	$1.47×10^5 ± 4.13×10^3$
	< 500 µm	$p<0.001$ [3]	11	1.05 ± 0.048		11	$7.51×10^4 ± 3.96×10^3$
Ellipsoid Body (EB)	> 750 µm	$F_{1,26}=32.83$	17	0.13 ± 0.007		17	$2.33×10^4 ± 1.24×10^3$
	< 500 µm	$p<0.001$ [3]	11	0.22 ± 0.015		11	$1.55×10^4 ± 1.01×10^3$
Noduli (NO)	> 750 µm	N.S.	17	0.06 ± 0.004		17	$1.01×10^4 ± 8.07×10^2$
	< 500 µm	$F_{1,26}=1.48$ $p=0.94$ [3]	11	0.07 ± 0.008		11	$4.66×10^3 ± 5.52×10^2$
Protocerebral Bridge (PB)	> 750 µm	N.S.	17	0.18 ± 0.008		17	$3.19×10^4 ± 1.49×10^3$
	< 500 µm	$F_{1,26}=0.29$ $p=1.20$ [3] [5]	11	0.17 ± 0.013		11	$1.20×10^4 ± 8.63×10^2$
Rest of neuropil (RoN) [4]	> 750 µm	$F_{1,26}=64.86$	17	42.3 ± 0.43		17	$7.71×10^6 ± 1.99×10^5$
	< 500 µm	$p<0.001$ [3]	11	49.13 ± 0.829		11	$3.56×10^6 ± 1.73×10^5$

[1]) The relative volumes of the rind and neuropil refer to the percentage of Total Brain, whereas subsequent neuropil percentages refer to Total Neuropil as 100%.
[2]) Comparison on the level of supercategories (OL,AOTu,AL,LH,MB,CX,RoN) was performed with Holm-Bonferroni correction of $m = 7$, Figure 5 in the paper.
[3]) Comparison on the level of individual neuropils (LO,ME,LA,AOTu,AL,LH,MB-V,CA,FB,EB,NO,PB, RoN) was performed with Holm-Bonferroni correction of $m = 13$, Figure 6 in the paper.
[4]) Though used in both analyses (note 2&3), reported p-values are from the (more detailed) comparison at individual neuropil level.
[5]) p-value >1 due to the Holm-Bonferroni multiple comparisons correction.

Supplement S4. Head capsule volume as proxy for brain size

To determine the brain-body size correlations we considered various options to quantify the weight or volume of the brains of *Nasonia vitripennis*. Due to its small size, we expected that wet weight would introduce a large error. Previous work on *Trichogramma evanescens* was performed by using 3D segmentation data of entire heads, which was possible because the head capsule of this species is transparent (van der Woude et al., 2013). This method provided highly accurate volumetric data, but could not be used for our study because the head capsule of *N. vitripennis* is not transparent. Unpublished analyses of the *T. evanescens* dataset showed, however, that the brains of these parasitoid wasps were tightly connected to the head capsule, filling the majority of the volume. In three isogenic strains of this species, the ratio between head capsule and brain volume varied between 1.60 to 1.62 with an average correlation (R^2)of 0.984 between head capsule volume and brain volume. These data suggest that head capsule volume may be an excellent proxy for brain volume, if the brains of *N. vitripennis* would be tightly connected to the head capsule in a similar way as in *T. evanescens*. To show that this is indeed the case, we prepared serial paraplast sections of the heads of *N. vitripennis*.

Wasps reared as described for induction of size plasticity (section Materials and Methods in the main text) were cooled on ice and decapitated. Heads were immersed in freshly prepared fixative, containing 4% formaldehyde and 0.1M phosphate buffer at pH of 7.2. To enable penetration of chemicals into the tissues in the head, openings were made in the eyes using fine tweezers. After fixation overnight at RT, heads were dehydrated using graded series of ethanol, cleared in amyl acetate and embedded in paraplast plus (Sigma-Aldrich). Serial sections of 10 μm were cut and mounted on poly-L-lysine coated slides (Sigma-Aldrich). Sections were deparaffinized in xylene, rehydrated to PBS and stained with eosin-haematoxylin (Ehrlich) solution (Sigma-Aldrich) for 5 mins, washed with tap water for 5 mins and dehydrated to xylene. Sections were mounted in DPX (Sigma) under cover glass and photographed.

Results show that the brain is indeed tightly connected to the head capsule in both the small and the large heads (Figure S3). There are few muscles in the head capsule, mainly posterior to the brain and ventro-anterior to the brain, attached to the mandibles. This is similar to the results obtained with confocal laser scanning microscopy on the transparent heads of *T. evanescens*. Not all sections were entirely intact, due to the difficulties with sectioning of the hard cuticle of the head capsule, which prevented volumetric analysis by image segmentation

to determine the exact ratio between head capsule volume and brain volume. However, given the high correlation with brain volume in the *T. evanescens* study, and the similarity in the position of the brain in the head capsule, we chose head volume as the best available option to be used as a reliable proxy for brain volume, since its volume can be determined with great precision and it allows for a large sample size using the methodology described in this study.
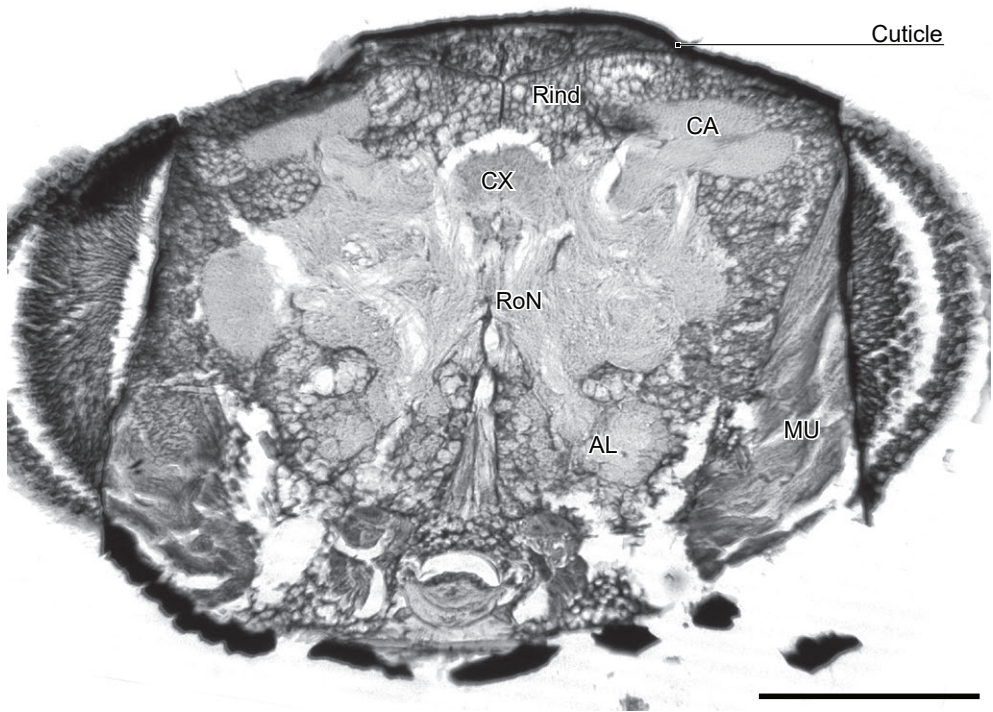
Figure S4. Paraplast section through the head of *Nasonia vitripennis*, showing the tight connection between brains and head capsule. Several notable neuropils are indicated. Scale bar represents 200 μm. CA, calyx; CX, central complex, RoN, rest of neuropil; AL, antennal lobe; MU, muscle fibers.

Supplementary references

van der Woude E, Smid HM, Chittka L, Huigens ME. 2013. Breaking Haller's rule: brain-body size isometry in a minute parasitic wasp. Brain Behav Evol 81(2):86-92.

Supplement S5. Eye size in large and small *N. vitripennis*

Eyes (Figure S5) were carefully removed whole during dissection of the brain for wasps with head width wider than 750 μm (large wasps) and smaller than 500 μm (small wasps). After fixation in 4% formaldehyde and 0.1M phosphate buffer at pH of 7.2 for 2.5 h at RT, eyes were washed 4 times 5 min in phosphate buffered saline (Oxoid, Dulbecco 'A' tablets) containing 0.5% Triton-X100 (PBS-T) and kept in PBS-T at 4 °C until processing. To enhance the image quality, the eyes were incubated in 1:500 propidium iodide (PI) in PBS-T for 4h at RT, then washed 2 times 5 min in PBS-T, followed by dehydration in a graded series of EtOH. The eyes were cleared in xylene and were mounted, convex side up, on a microscope slide in DPX (Sigma) under an 18×18 mm coverslip. Eye preparations were scanned with a Zeiss LSM 510 confocal laser scanning microscope equipped with a 25× oil immersion objective (Plan-Neofluar 25×/0.8). The tissue was imaged using the 488 nm line of an Argon laser to excite autofluorescence and PI. We found that using a 505-550 nm BP filter mainly resulted in emission from remains of the head capsule cuticle, and a 560 nm LP filter mainly imaged the ommatidia. Both signals were used to assess quality of the eye preparation. Eyes were scanned with an image size of 512×512 pixels. In the event that an eye would not fit the frame, overlapping
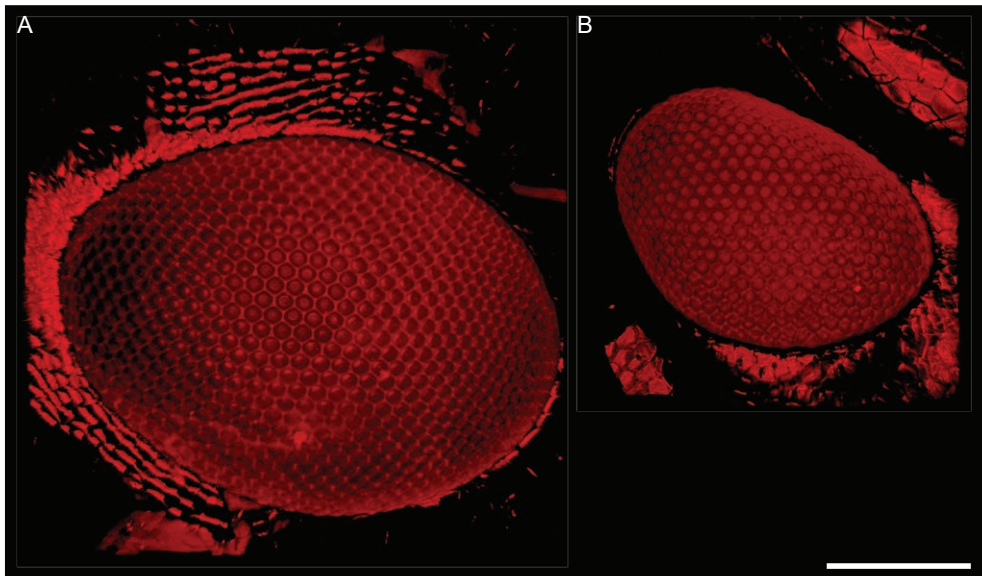

Figure S5. 3D volume of autofluorescence in *N. vitripennis* eyes from wasps with head width wider than 750 μm (panel **A**, large wasps) and smaller than 500 μm (panel **B**, small wasps). Images exported from the 3D Viewer plugin in FIJI. Scale bar represents 100 μm in the most anterior plane.

stacks were made and later combined with the Stitching plugin in FIJI (Preibisch et al., 2009). For analysis, stacks were loaded in FIJI (Schindelin et al., 2012) and analyzed using the 3D Viewer plugin (Schmid et al., 2010). After optimization of the stack histogram, the point tool was used to mark individual ommatidia on the eye surface (improper optimization would result in points floating far above the eye). The line tool was used to measure ommatidia diameter of a septet at the convex tip of the eye. Data were exported and analyzed in MS Excel, statistical comparisons were made using a Welch's T-test.

Our data show that large *N. vitripennis* females have 695.8±1.52 ommatidia (mean±SD, $N = 5$) that measure 13.33±0.73 μm ($N = 5$ averaged septets) in diameter, whereas small wasps have 447.2±50.26 ommatidia ($N = 5$) with a diameter of 11.8±0.44 μm. Large and small wasps differed significantly for both ommatidia count ($p < 0.001$) and ommatidia diameter ($p = 0.006$).

Supplementary references

Preibisch S, Saalfeld S, Tomancak P. 2009. Globally optimal stitching of tiled 3D microscopic image acquisitions. Bioinformatics 25(11):1463-1465.

Schindelin J, Arganda-Carreras I, Frise E, Kaynig V, Longair M, Pietzsch T, Preibisch S, Rueden C, Saalfeld S, Schmid B, Tinevez JY, White DJ, Hartenstein V, Eliceiri K, Tomancak P, Cardona A. 2012. Fiji: an open-source platform for biological-image analysis. Nat Methods 9(7):676-682.

Schmid B, Schindelin J, Cardona A, Longair M, Heisenberg M. 2010. A high-level 3D visualization API for Java and ImageJ. BMC Bioinformatics 11.

Nasonia giraulti

Chapter 4

Species- and size-related differences in dopamine-like immunoreactive clusters in the brain of *Nasonia vitripennis* and *N. giraulti*

Jitte Groothuis,
Krista van den Heuvel,
Hans M. Smid

Abstract

An extreme reduction in body size has been shown to negatively impact the memory retention level of the parasitic wasp *Nasonia vitripennis*. In addition, *N. vitripennis* and *Nasonia giraulti*, a closely related parasitic wasp, differ markedly in the number of conditioning trials required to form long-term memory. These differences in memory dynamics may be associated with differences in the dopaminergic clusters in the *Nasonia* brains. Here we used dopamine-like immunoreactivity to identify and count the number of cell bodies in dopaminergic clusters of normal- and small-sized *N. vitripennis* and normal-sized *N. giraulti*. We counted 9 identifiable clusters (D1a, D1b, D2, D3, D4a, D45b, D6, and D7), but were unable to reliably trace the projections of these clusters. Our analysis revealed that *N. giraulti* had fewer cells in the D2 and D4a clusters, but more in D4b, compared with normal-sized *N. vitripennis*. In addition, we found fewer cells in the D5 and D7 cluster of small-sized *N. vitripennis* compared to normal-sized *N. vitripennis*. These findings contrast a study on octopaminergic cells in *N. giraulti* and *N. vitripennis*, where no differences were observed.

A comparison of our findings with the literature on dopaminergic clusters in the fruit fly *Drosophila melanogaster* and the honey bee *Apis mellifera* indicates that clusters D2, D3, and D5 may play a role in memory formation in *Nasonia* wasps. The results from both the species comparison and the size comparison are therefore of high interest and importance for our understanding of the complex intricacies that underlie the memory dynamics of insects.

Introduction

Nasonia is a genus of emerging hymenopteran model organisms (Werren and Loehlin, 2009). *Nasonia* wasps parasitize various fly species and lay egg clutches inside the puparium of their fly host, where the wasps develop gregariously. Laying eggs in a host is a highly rewarding and ecologically relevant experience for the female wasps. As such, it is suitable for use as an appetitive unconditioned stimulus in classical conditioning and can be used to make lasting associations with conditioned stimuli such as odors (Hoedjes et al., 2012). Interestingly, there are strong and distinct differences in the memory dynamics of such conditioning within the *Nasonia* genus. *Nasonia vitripennis* wasps consolidate protein synthesis-dependent long-term memory after a single conditioning event, whereas in *N. giraulti* wasps a single event leads to short-lasting, protein synthesis-independent, memory. Three repeated conditioning events, however, do lead to formation of long-term memory in *N. giraulti* (Hoedjes and Smid, 2014).

In addition to these interspecies differences, different strains also differ in their memory strength (Schurmann et al., 2012; Koppik et al., 2015), as do size-related differences within one genotype. *Nasonia* wasps have a large potential for size plasticity, being able to scale their body size over at least one order of magnitude when forced to deal with strong scramble competition. In *N. vitripennis*, this leads to several structural adaptations in the brains of the smallest wasps (Groothuis and Smid, 2017). These small *N. vitripennis* individuals have inferior memory retention when compared to larger conspecifics (Van der Woude and Smid, 2017a).

Memory dynamics in insect brains are mediated by the modulating neurotransmitters octopamine (OA) and dopamine (DA) (Das et al., 2016). Whereas previous theories ascribed appetitive conditioning to octopaminergic cells and aversive conditioning to dopaminergic cells (Schwaerzel et al., 2003), it is currently assumed that dopamine in fact plays a role in both aversive as well as appetitive learning (Waddell, 2013). This implies that differences in memory dynamics may relate to the functioning of these modulatory neurotransmitter networks. They may, for example, differ in the number of octopaminergic or dopaminergic cells or in their projections. As a previous description of the octopaminergic network showed no evidence for differences between *N. vitripennis* and *N. giraulti* (Haverkamp and Smid, 2014), the focus of this study is on the dopaminergic network.

Dopaminergic neurons (DANs) heavily innervate the mushroom body, a multimodal integration center which is thought to be the basis of memory in insects. In *Drosophila melanogaster* fruit flies, this dopaminergic innervation derives from cells in the protocerebral posterior lateral (PPL1 and PPL2ab), and protocerebral anterior medial (PAM) clusters, with various cells showing discrete topological innervation of specific areas in the mushroom body (Mao and Davis, 2009; Waddell, 2013; Das et al., 2016). Of these PPL and the PAM clusters, specific DANs (PPL1-MV1, PPL1-MP1, and PAM-M3 cells (Claridge-Chang et al., 2009; Aso et al., 2012)) are thought to signal aversion, whereas other DANs in the PAM cluster are assumed to signal reward (Aso et al., 2012; Burke et al., 2012; Liu et al., 2012; Lin et al., 2014). In addition, appetitive memory is associated with PPL1-MP1 DANs. These cells block appetitive memory formation by their tonic activity; however, this activity may be inhibited by signaling of neuropeptide F (the arthropod analog of mammalian neuropeptide Y) (Krashes et al., 2009). Thus, the PPL and the PAM cluster are clearly relevant for appetitive memory dynamics in the fruit fly. As their *Nasonia* homologs may serve similar functions, it is crucial to study this.

Here, we investigate whether the behavioral differences found between normal- and small-sized *N. vitripennis* individuals and those between *N. vitripennis* and *N. giraulti* are associated with differences in their dopaminergic networks.

First, by analyzing dopamine-like immunoreactivity (DA-L-IR) we will provide a comparison of DA-L clusters in the *Nasonia* brain with the clusters known from the fruit fly (Mao and Davis, 2009) and the honey bee (Tedjakumala et al., 2017). This comparison will be based mainly on the comparative location of the clusters within the cell body rind, relative to specific neuropils, as well as the putative projection targets of these clusters. We hypothesize to find an overall similar number of clusters and DA-L neurons as in the *D. melanogaster* brain, as this is closest in size to the brain of *Nasonia* species. Second, we will compare the number of DA-L neurons present in the various clusters between normal-sized *N. vitripennis* and *N. giraulti*, as well as between normal- and small-sized *N. vitripennis*. We hypothesize that differences in oviposition-based appetitive conditioning are associated with differences in neuron number in the clusters relevant to appetitive memory. Specifically, in normal-sized *N. vitripennis*, we expect to find more DA-L neurons corresponding to the fruit fly PAM cluster, or less DA-L neurons corresponding to the fruit fly PPL cluster.

Materials & Methods

Insects

Isogenic strains of *N. vitripennis* (AsymCx) and *N. giraulti* (RV2x(U)) were used. Both strains have previously been used to study memory formation (Hoedjes and Smid, 2014). They have a sequenced genome and genetic tools have been developed for these strains (Werren et al., 2010; Rago et al., 2016). Rearing was performed and differences in body size were induced by varying levels of scramble competition as described previously (Groothuis and Smid, 2017). In short, normal-sized wasps were obtained by rearing on *Calliphora vomitoria* pupae (Kreikamp BV, Hoevelaken, The Netherlands) at a ratio of 10 female wasps to 20 pupae. Small-sized *N. vitripennis* were obtained by rearing at a ratio of 50:5. Females were allowed to oviposit for 24 h in both cases. For experiments, female wasps were collected within one day of eclosion and kept in vials with access to water and honey. The 50:5-rearing shows large variation in female body size; for the experiments only small-sized *N. vitripennis* wasps with a head width under 500 μm were used. The heads of normal-sized *N. vitripennis* and *N. giraulti* were not measured but generally have head widths of approximately 750 μm (Groothuis and Smid, 2017).

Immunohistochemistry

Cold-sedated wasps were decapitated in ice-cold fixative: one part 25% glutaraldehyde (Sigma) and three parts saturated picric acid with 0.1% acetic acid (GPA). To allow penetration of the fixative, the antennae were removed and small openings made in the eyes. Heads were fixed for 4 h at RT and then washed overnight in 70% EtOH prior to dissection of the brains in 70% EtOH.

After dissection, brains were dehydrated in a graded series of EtOH concentrations (70-90-96-100-100%, 50% EtOH/xylene, 2 minutes each), degreased in 100% xylene, and rehydrated to phosphate buffered saline (PBS; Oxoid, Dulbecco "A" tablets) (via 50% EtOH/xylene, 100-96-90-80-70-50-30% EtOH). To reduce oxidized dopamine, brains were incubated for 20 minutes in freshly prepared 1% sodium borohydrate in PBS. After rinsing four times for 5 min and 3 times for 15 min in PBS, the brains were treated with 5 mg/mL collagenase (Sigma) in PBS for 1 h at RT, improving the permeability of the tissue. Subsequently, the brains were rinsed four times for 5 min in PBS containing 0.5% Triton-X100 (PBS-T) and preincubated in 10% normal goat serum (NGS; Dako, Glostrup, Denmark) in PBS-T (PBS-T-NGS) for 1 h at RT. The primary mouse anti-

dopamine antiserum (Millipore, catalogue no. MAB5300, RRID:AB_94817) was incubated overnight at RT at dilutions of 1:200 for normal-sized brains or 1:66.7 for small brains in PBS-T-NGS. After five 30-min washes in PBS-T, a secondary rabbit anti-mouse antibody (Dako, catalogue no. Z0259, RRID:AB_2532147) was applied at a 1:200 dilution in PBS-T-NG for 3 h at room temperature. Finally, following four 30-min washes in PBS-T, a tertiary antiserum of goat anti-rabbit antibodies linked to AlexaFluor® 488 (Jackson ImmunoResearch Labs, catalogue no. 115–545-003, RRID:AB_2338840) was used at a dilution of 1:100 together with propidium iodide at a dilution of 1:200 in PBS-T-NGS overnight at 4 °C.

Whole-mount preparations were made by washing four times for 30 min in PBS-T and dehydration and degreasing to xylenes (via 30-50-70-80-90-96-100-100% EtOH, 50% EtOH/xylene, 2 min each), followed by mounting on a microscope slide in a drop of DPX mounting medium (Sigma) under a No. 1 cover slip.

Antiserum specificity

Cross-reactivity of the mouse anti-dopamine antibody was determined as specified by the manufacturer: DA-G-BSA 1; L-DOPA-G-BSA 1:10,000; Tyrosine-G-BSA 1:36,000; Tyramine-G-BSA 1:>50,000; Noradrenaline-G-BSA 1:>50,000; OA-G-BSA 1:>50,000; Adrenaline-G-BSA 1:>50,000; DA 1:>50,000. We performed additional control experiments by using preparations without primary antisera. These did not reveal any immunolabeling.

Microscopy

Preparations were scanned with a Zeiss LSM510 microscope equipped with a 40× oil immersion objective (Plan-Neofluar 40×/1.3) and 63× oil immersion objective (Plan-Apochromat 63×/1.4). AlexaFluor® 488 staining was imaged using the 488-nm line of an Argon laser with a 505- to 550-nm BP filter; the propidium iodide nuclear counterstain was imaged using the same excitation wavelength but with a 560-nm LP filter. Scanning was performed at 8 bit with a resolution of 1024×1024, with voxel dimensions ranging from 0.36×0.36×2 μm to 0.14×0.14×0.38 μm.

Nomenclature

Nomenclature of neuropils in the *N. vitripennis* and *N. giraulti* brains was used

as described previously (Groothuis et al., 2018) and according to standardized nomenclature (Ito et al., 2014). Orientation and positions in the brain are given using the body axis. Dopamine-like immunoreactive (DA-L-IR) clusters were numbered from anterior to posterior, as was done previously in the honey bee *Apis mellifera* (Schürmann et al., 1989; Tedjakumala et al., 2017), the parasitic wasp *Trichogramma evanescens* (van der Woude and Smid, 2017c), and for octopaminergic clusters in *N. vitripennis* and *N. giraulti* (Haverkamp and Smid, 2014). When clusters were found at comparable depths, preference was given to dorsal clusters. As there is no clear boundary of the fusion between the supra- and suboesophageal ganglia in *Nasonia* brains, we did not consider this division in naming the DA-L clusters.

Neuron analysis

The counting of DA-L-IR neurons was performed blinded to the identity (species or body size) of the brain sample by randomization of files after image acquisition. The initial sample consisted of 51 brains, based on a visual assessment of staining quality; during analysis several more samples were removed, bringing the total to 38 analyzed brains. The number of cell bodies was only analyzed in brains in which DA-L-IR clusters were clearly visible and the best-stained hemisphere was selected for analysis of individual clusters. Cell bodies were counted by means of image segmentation in Amira 5.4 (Visage Imaging, Berlin, Germany), assigning each cluster a separate LabelField and each cell an individual Material. During this process, the propidium iodide counterstain could be used for orientation, but is not used for other purposes. Due to tissue damage, not all identified clusters could be counted in every sample. After segmentation, results were exported with the MaterialStatistics module and collected in a spreadsheet for further analysis.

Statistics

We compared the number of DA-L cell bodies for all identified clusters separately and in a pairwise fashion for the following combinations: *N. vitripennis* (normal-sized) × *N. giraulti* (normal-sized) and *N. vitripennis* (normal-sized) × *N. vitripennis* (small-sized).

Comparison between cluster-species combinations were analyzed with a non-parametric Mann-Whitney-Wilcoxon test ($\alpha = 0.05$). All statistical analyses were performed in R version 3.3.2.

Results

Overall tissue and labeling quality

The triple labeling protocol ensured sufficient staining quality in most brains. However, the glutaraldehyde fixation of the brains in the head capsule before dissection (required for the conjugation and subsequent detection of the antigen) caused relatively fragile brains that are difficult to dissect from the head capsule, as the tissue is more brittle than after formaldehyde fixation or in unfixed dissections. In many preparations, this led to a damaged cell body rind or loss of tissue, mainly of the optic lobes. In addition, the rind at the anterior and the central sides of the brain was found to be especially fragile; which on occasion caused either damage to or removal of the rind, or an occlusion of relevant clusters by non-neural and strongly autofluorescent tissues.

Prior to the blinded DA-L-IR analysis, 51 brains were selected (blind to their identity) from the available preparations; of those, 20 were normal-sized *N. vitripennis*, 15 small-sized *N. vitripennis*, and 26 *N. giraulti*. These numbers were reduced to 15, 9, and 14 brains, respectively, after closer examination during the analysis. The low number of small *N. vitripennis* brains was striking in particular and was probably due to the added brittleness of glutaraldehyde fixation, as these brains proved more resilient when dissected as unfixed tissue (Groothuis and Smid, 2017).

DA-L-IR clusters in the *N. vitripennis* brain

Our analysis of DA-L-IR in *N. vitripennis* and *N. giraulti* resulted in the identification of nine uniquely identifiable cell groups, two of which we consider a subdivision of another cluster, see Figures 1, 2, and 3A for an overview. Cell numbers are given as average count ± SD (N = number of hemispheres analyzed) and based on normal-sized *N. vitripennis*:

Cluster D1a (Figure 3B) is the most anterior cell cluster, located laterally of the anterior optic tubercle. In all cases it comprises at least two large and heavily stained cell bodies; in some brains several additional cells can be identified near this location, which we considered as belonging to D1a. On average we counted 3.7±0.7 (N = 13) D1 cells in the *N. vitripennis* brain.

Cluster D1b (Figure 3C) is a small cluster that always consists of 2 small DA-L cells. It lies at the same level and laterality as cluster D1, but more ventrally. This cluster is only found in a minority of preparations (N = 4).
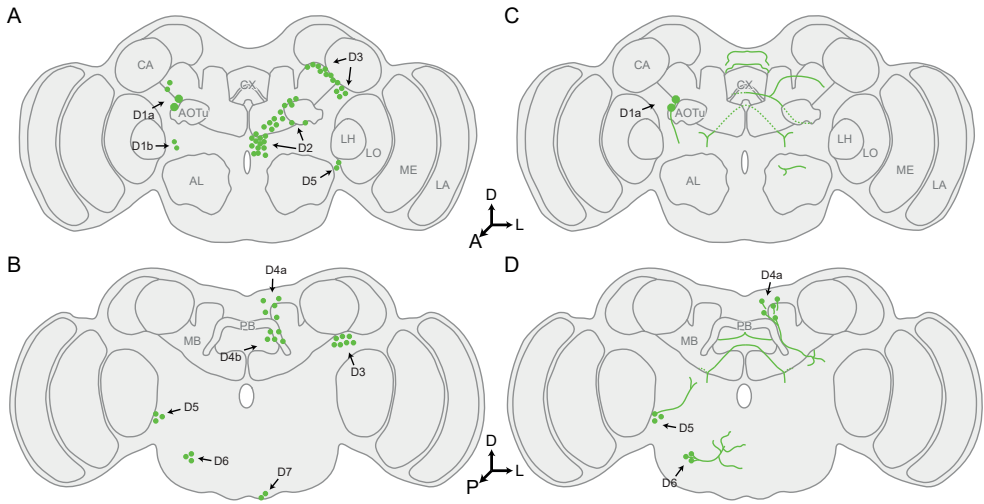
Figure 1. Schematic representation of DA-L-IR cluster locations (**A.** Anterior; **B.** Posterior) and major arborizations (**C.** Anterior; **D.** Posterior) in the brains of *N. vitripennis* and *N. giraulti*. Locations and arborizations are only drawn for one brain hemisphere. The antennal lobes are scaled to 80% of the original size to reveal the subesophageal zone neuropils. Abbreviations: A, anterior; AL, antennal lobe; AOTu, anterior optic tubercle; CA, calyx ; CX, central complex; D, dorsal; FB, fan-shaped body (part of CX); L, lateral; LH, lateral horn; LO lobula; MB, mushroom body; ME, medulla; P, posterior. Arrows point to clusters.
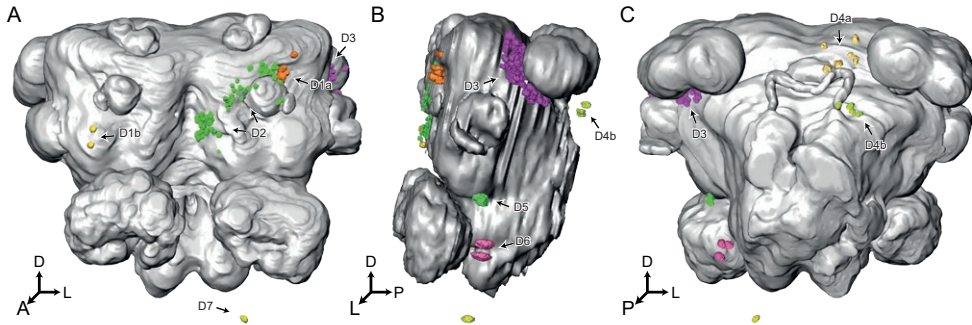
Figure 2. Location of DA-L-IR somata in the cell body rind (not shown) of a single *N. vitripennis* brain seen from an anterior (**A**), lateral (**B**), and posterior (**C**) perspective. The combined neuropil of the brain is shown in grey. Each cluster is shown with randomized colors in only one of the hemispheres. Note that the optic lobes are omitted from the neuropil reconstruction. Abbreviations: A, anterior; D, dorsal; L, lateral; P, posterior. Arrows point to clusters

Cluster D2 (Figure 3D) is the largest cluster, containing 59.6±11.1 cells ($N = 13$). The largest concentration of DA-L cells in this cluster is found at the midline, approximately halfway between the antennal lobe and the distal end of the vertical lobe of the mushroom body, from which more cell bodies are scattered laterally towards and surrounding the anterior optic tubercle. Cell bodies may lie more dorsal or ventral to the tubercle in individual brains. The neurilemma at the midline forms a clear boundary between hemispheres, so the cluster cannot be confused for an unpaired cluster. In several brains we observed a gap between the population of more laterally scattered cells and the concentrated mass near the midline, indicating that cluster D2 can probably be subdivided into 2 subclusters. The majority of brains, however, did not show this, so all cell bodies were grouped into cluster D2 in this study.

Cluster D3 (Figure 3E) lies at the posterior side of the protocerebrum, where it surrounds the proximal end of the mushroom body pedunculus, wedged between the neuropils of the protocerebrum and mushroom body calyx. With 42.5±7.1 ($N = 11$) cell bodies, it is the second largest cluster. Most cells are found at the anterior and lateral side of the pedunculus. Results from a minority of preparations hint at a gap between the anterior and lateral groupings of cells in this cluster, suggesting that, like in cluster D2, a subdivision of cluster D3 may be warranted.

Cluster D4a (Figure 3F) is a relatively small (5.6±1.0 cell bodies, $N = 13$) cluster, located posteriorly of the superior protocerebral neuropils and surrounding the ocellar neuropils in the dorsal cell body rind.

Cluster D4b (Figure 3G) lies at the most posterior edge of the cell body rind, at a similar dorsal level as cluster D4a. It consists of 5.9±1.3 ($N = 8$) slightly scattered cell bodies.

Cluster D5 (Figure 3H) consists of several (3.75±1.2 cell bodies, $N = 8$) cells posterior in the brain, located in the thin layer of cell body rind between the neuropil of the central brain and the optic lobe lobula.

Figure 3. ▶ DA-L-IR cell body clusters in the *N. vitripennis* brain, with visible neuropils and midline (M) annotated. Each panel is oriented dorsal side up, and contains a maximum intensity projection of varying thickness, highlighting a single cluster. **A.** An overview of DA-L-IR in a single brain: four 30 μm thick maximum intensity projections through the brain from anterior (A) to posterior (A'''), annotations only in one of the hemispheres. **B.** cluster D1a. **C.** cluster D1b. **D.** cluster D2. **E.** cluster D3. **F.** cluster D4a. **G.** cluster D4b. **H.** cluster D5. **I.** cluster D6. **J.** cluster D7. Abbreviations: AL, antennal lobe; AOTu, anterior optic tubercle; CA, calyx (MB); CX, central complex; EB, ellipsoid body (CX); FB, fan-shaped body (CX); LH, lateral horn; LO lobula; M, midline; MB, mushroom body; ME, medulla; ML, medial lobe (MB); NO, nodulus (CX); OCN, ocellar neuropils; PED, pedunculus (MB); SEZ, subesophageal zone. Arrows point to cell clusters, white arrowheads point to staining artefacts, black arrowheads point to cell body fibers. Scale bars depict 100 μm in panels A-A''', 50 μm in panels B-J.

Cluster D6 (Figure 3I) always consists of 3 (*N* = 8) large cell bodies, ventrally in the brain, flanking the subesophageal zone.

Cluster D7 (Figure 3J) lies at the most ventral edge of the subesophageal zone and consists of 2 (*N* = 3) neurons. The cell body rind at its location is easily damaged and this cluster is often lost in preparations.
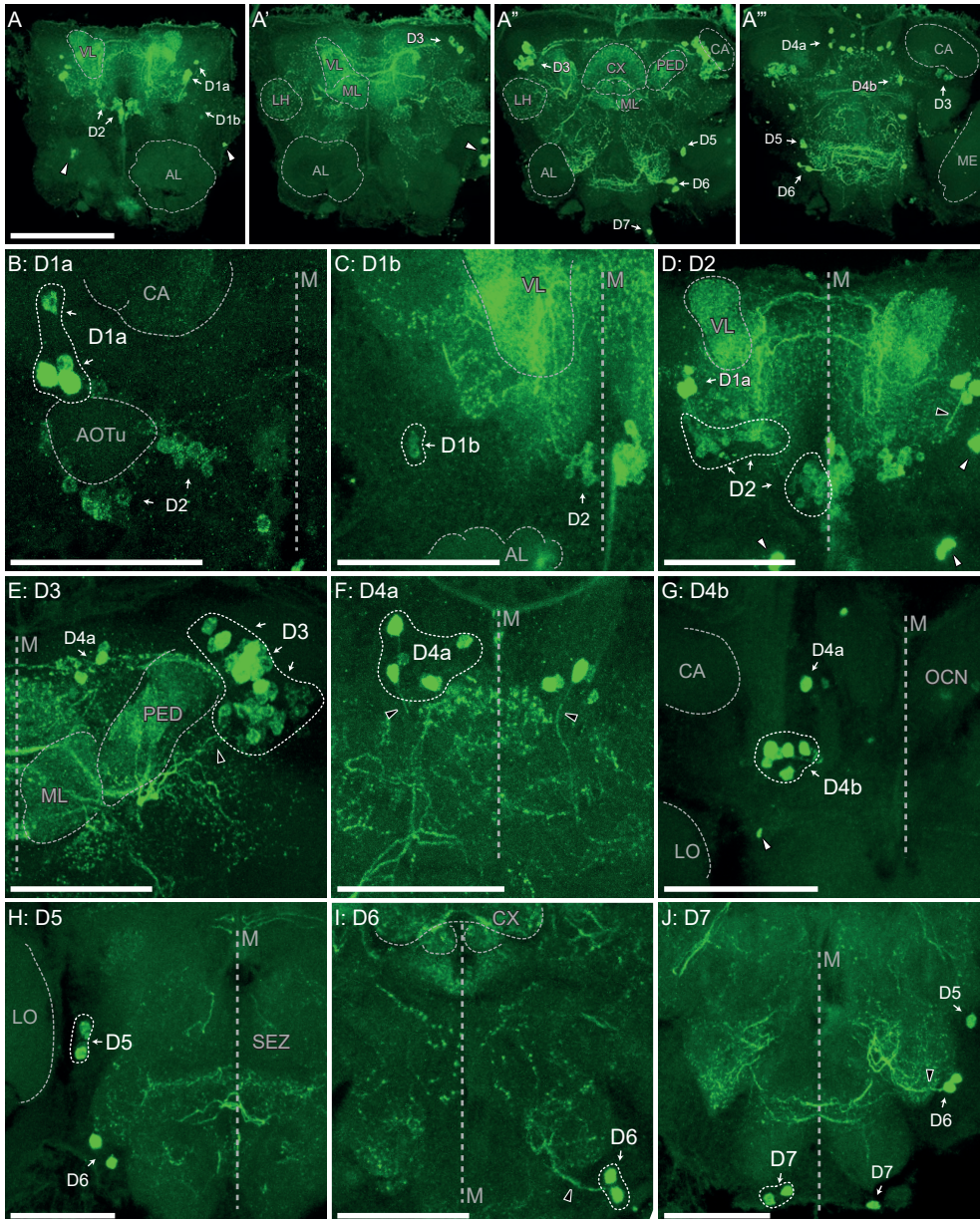
DA-L-IR innervation in the *N. vitripennis* brain

Many neuropils in the central brain are highly innervated by DA-L-IR fibers. Due to their abundance, as well as the varicose nature of the immunofluorescence, these fibers cannot be traced back to the cell body clusters from which they project. In a limited number of cases, however, cell body fibers (also described as primary neurites) can be observed in samples. Here, we describe the innervation of several landmark neuropils and, if possible, the location of DA-L-IR fibers projecting towards these neuropils:

The antennal lobe (Figure 4A) is largely devoid of DA-L-IR innervation, though in most preparations a low number of small fibers was observed in the central non-glomerular antennal lobe hub.

We found no evidence of DA-L-IR innervation in the optic lobes (Figure 4B).

The anterior optic tubercle (Figure 4C) contains many varicose DA-L-IR terminals. Although the AOTu is surrounded by cell bodies of cluster D1a and D2, its innervation does not originate from these clusters.

The mushroom body (Figure 4D-G) is strongly innervated in the peduncle (Figure 4D), medial lobe (Figure 4E), and vertical lobe (Figure 4F). We have, however, not reliably observed innervation in the calyx (Figure 4G).

The central complex (Figure 4H, I) is strongly innervated in the fan-shaped body and the noduli, and less in the ellipsoid body (Figure 4H). No innervation was observed in the protocerebral bridge (Figure 4I).

The lateral horn (Figure 4J) is innervated with many varicose terminals. The projections entering the lateral horn were rarely visible, and could not reliably be traced back to cell bodies.

Figure 4. ▶ DA-L-IR projections in the *N. vitripennis* brain, focusing on innervations of landmark neuropils, with visible clusters and midline (M) annotated. Each panel is oriented dorsal side up, and contains a maximum intensity projection of varying thickness, highlighting a single neuropil. When visible, (parts of) the clusters are annotated. **A.** Antennal lobe. **B.** Optic lobe (lobula and medulla). **C.** Anterior optic tubercle. **D-G.** Mushroom body peduncle, medial lobe, vertical lobe, and calyx. **H.** Central complex (fan-shaped body, ellipsoid body, and noduli) **I.** Protocerebral bridge. **J.** Lateral horn. **K.** Subesophageal zone. Abbreviations: AL, antennal lobe; AOTu, anterior optic tubercle; CA, calyx (MB); CX, central complex; EB, ellipsoid body (CX); FB, fan-shaped body (CX); LH, lateral horn; LO lobula; M, midline; MB, mushroom body; ME, medulla; ML, medial lobe (MB); NO, nodulus (CX); OCN, ocellar neuropils; PED, pedunculus (MB); SEZ, subesophageal zone. Arrows point to cell clusters, white arrowheads point to staining artefacts, black arrowheads point to cell body fibers. Scale bars depict 50 μm.

The subesophageal zone (Figure 4K) is home to an extensively branched DA-L-IR arborization that is strongly stained in most preparations. It originates from cluster D6.
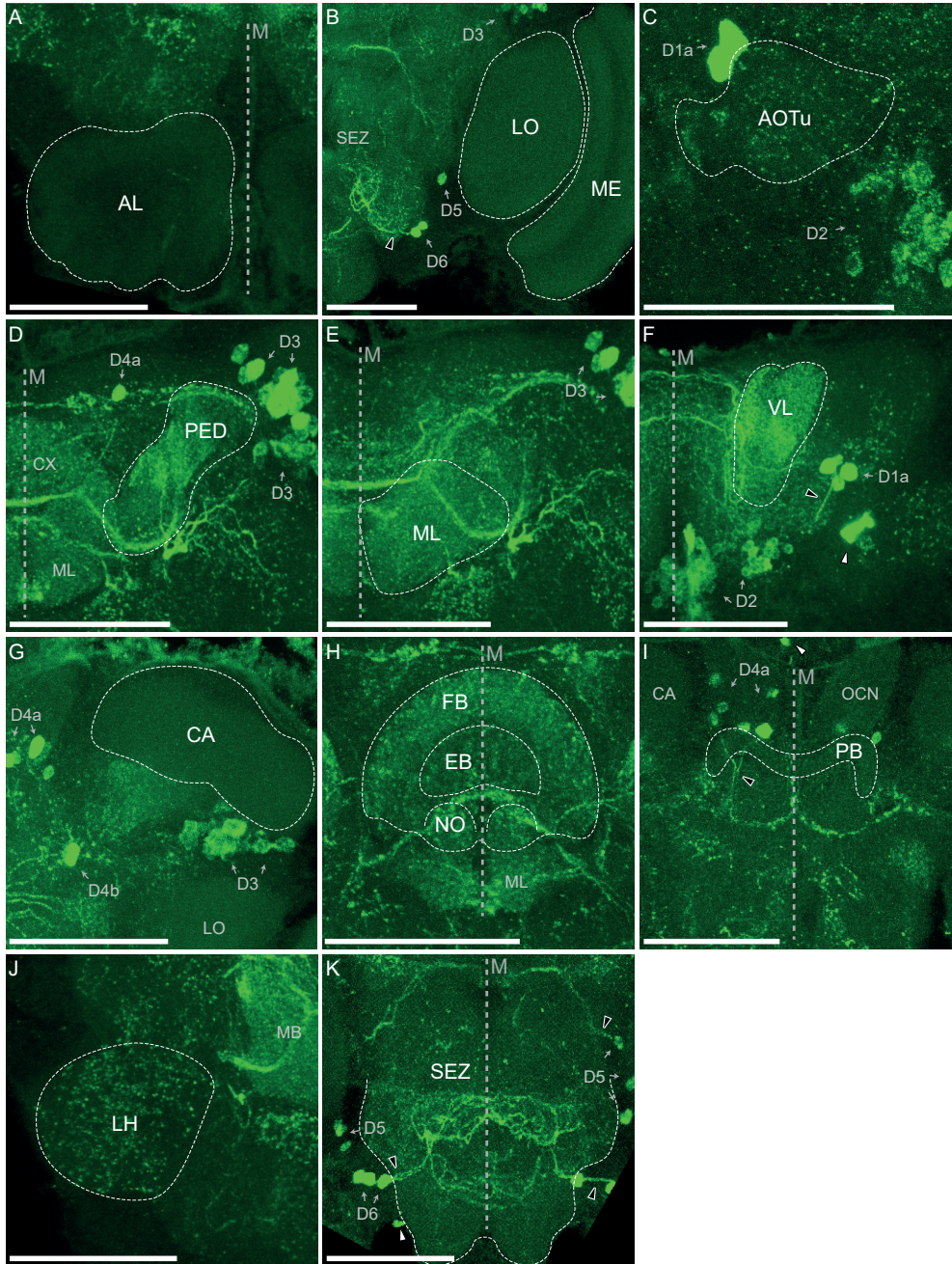
Species-specific differences

Nasonia vitripennis and *N. giraulti* did not show any outwardly recognizable morphological differences in their neuropils, nor did we note differences in the location or projection patterns of the DA-L-IR clusters. Most clusters showed a similar number of cells counted per cluster for the two *Nasonia* species (Table 1, Figure 5) and the maximum number of DA-L-IR cells observed in a single

Table 1. Mean number of cells per cluster for the three groups of *Nasonia* studied. *N* = number of hemispheres counted per cluster. Standard deviation for clusters for which no variation in cell body number was counted is labeled as n.a.

|		*Nasonia giraulti*		*N. vitripennis* (normal)		*N. vitripennis* (small)		
		Number of cells Mean ± SD	*N =*	Number of cells Mean ± SD	*N =*	Number of cells Mean ± SD	*N =*	
	D1a	3.43 ± 0.82	14	3.77 ± 0.7	13	3.11 ± 0.74	9	**D1a**
	D1b	2 n.a.	4	2 n.a.	4	2 n.a.	3	**D1b**
	D2	47.08 ± 11.15	13	59.85 ± 11.11	13	50.88 ± 13.13	8	**D2**
Cluster	**D3**	42.07 ± 5.24	14	42.55 ± 7.14	11	44.25 ± 9.12	8	**D3**
	D4a	4.58 ± 0.95	12	5.77 ± 0.97	13	5.56 ± 0.68	9	**D4a**
	D4b	7.67 ± 2.05	6	5.88 ± 1.27	8	5.5 ± 1.12	4	**D4b**
	D5	3.14 ± 1.64	7	3.75 ± 1.2	8	2.38 ± 0.7	8	**D5**
	D6	3 n.a.	10	3 n.a.	8	2.78 ± 0.63	9	**D6**
	D7	1.33 ± 0.47	3	2 n.a.	3	1 n.a.	4	**D7**
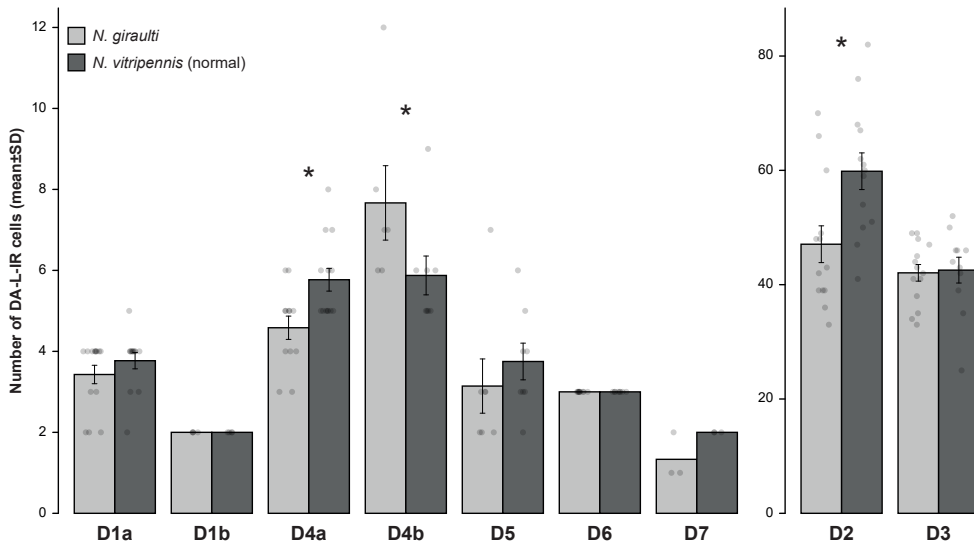
Figure 5. DA-L-IR cell bodies in brains of normal-sized *N. vitripennis* and *N. giraulti*. Due to the relative abundance of cell bodies in clusters D2 and D3, these are given separately. Bars depict average number of cells ± standard deviation, dots depict raw counts. *: $p < 0.05$ (Wilcoxon).

brain was also similar (*N. vitripennis*: 143. *N. giraulti*: 138). However, we found a significant difference indicating fewer cells in the D2 cluster of *N. giraulti* than in that of *N. vitripennis* (Wilcoxon, W = 34.5, p = 0.011). In addition, we found fewer cells for *N. giraulti* than for *N. vitripennis* in the D4a cluster (Wilcoxon, W = 34.5, p = 0.013), but more in the D4b cluster (Wilcoxon, W = 40, p = 0.038).

Effect of brain size on DA-L-IR cell bodies in *N. vitripennis*

Despite the large difference in total brain size between normal-sized and small *N. vitripennis* (Groothuis and Smid, 2017), the maximum number of DA-L-IR cell bodies counted in a single brain was similar in these groups (*N. vitripennis* (normal): 143. *N. vitripennis* (small): 138). We did find several differences in numbers of cells per cluster. Our analysis indicates fewer cells in the D5 cluster of small *N. vitripennis* (Wilcoxon, W = 52.5, p = 0.027), as well as fewer cells in D7 (Wilcoxon, W = 12, p = 0.025). However, this D7 cluster could be counted in only three and four brains, for normal-sized and small *N. vitripennis*, respectively. In addition, we found a marginally significant lower number of D1a cells in small versus normal-sized *N. vitripennis* (Wilcoxon, W = 85.5, p = 0.0502).
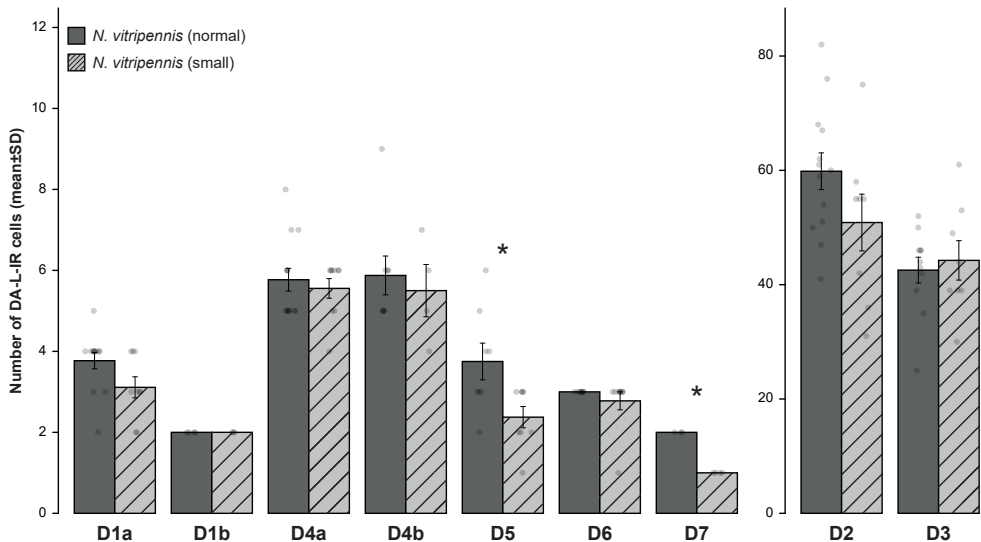

Figure 6. DA-L-IR cell bodies in brains of normal- and small-sized *N. vitripennis*. Due to the relative abundance of cell bodies in clusters D2 and D3, these are given separately. Bars depict average number of cells ± standard deviation, dots depict raw counts. *: $p < 0.05$ (Wilcoxon).

Discussion and conclusion

Previous studies have identified differences in memory dynamics between *Nasonia* species, as well as *N. vitripennis* of different sizes. Understanding the factors that underlie these differences may lead to novel insights that could be translated to mammalian studies. To that end, this study aimed to find potential correlations between the observed differences in memory dynamics and the morphology of the dopaminergic network in *Nasonia*.

To accomplish this, we first described the dopaminergic clusters in *Nasonia* brains, providing examples from *N. vitripennis*. In total, we identified 9 distinct clusters, two of which we consider subclusters. The two largest clusters, D2 and D3, can likely be further subdivided, but we were unable to reliably do so in this study.

We then compared the number of cell bodies in these dopaminergic clusters between the species *N. vitripennis* and *N. giraulti*, as well between normal- and small-sized *N. vitripennis*. We found significant differences in clusters that may explain the differences in memory dynamics of these groups, as they likely correspond to clusters projecting to the mushroom bodies and are involved with associative learning in other insects, as we will discuss below.

Comparison with other insects

In order to verify our hypotheses regarding differences in DA-L-IR clusters for our *Nasonia* species and size groups we need to determine potential homologs of the clusters we identified. Here we present a comparison of the identified *Nasonia* clusters with those of three other species: the honey bee *A. mellifera*, the fruit fly *D. melanogaster*, and the egg parasitoid *T. evanescens*. This comparison (Table 2) is based mainly on the location of these clusters in the cell body rind relative to landmark neuropils. For example, both the PAM cluster in the fruit fly and the C1 and C2 clusters in the honey bee are located at the anterior side of the brain, between the antennal lobe and the distal end of the vertical lobe of the mushroom body; a cluster found at this location in the *Nasonia* brain may be considered homologous to these clusters. Better comparisons can be made based on the projection patterns of the DA-L neurons in the clusters; unfortunately, our staining method targets all dopaminergic cells, which leads to many fibers crossing or running in parallel. The varicose nature of the immunolabeling further restricts the tracing of these fibers.

In *D. melanogaster*, the PAM, PPL1, and PPL2ab clusters project to the mushroom body (Mao and Davis, 2009) and are relevant for memory formation (Waddell, 2013). As such, we expect that the D2, D3, and D5 clusters in *Nasonia* fulfill similar roles. These clusters are therefore of particular importance for this study.

Comparing dopamine-like immunoreactivity in *Nasonia* with these other species results in several interesting observations.

First is the diversity of DA-L-IR clusters between the compared species. Although we were able to make global comparisons, the location of these clusters does not appear to be very conserved. The clusters located at the ventral side of the brain, in particular, seem quite divergent. Multiple small clusters have been described for the honey bee, and several in *T. evanescens*, but in the *Nasonia* species studied here we only found a few clusters with a low number of cells.

The relative abundance of cell bodies per cluster follows the same pattern in *Nasonia*, *A. mellifera*, and *D. melanogaster*: the clusters that likely correspond to D2 and D3 are most abundant. With a low number of cells in each cluster, *T. evanescens* appears to be the outlier. This may be an adaptation to the miniaturization in this tiny egg parasitoid (van der Woude and Smid, 2017c).

We did not observe innervation of the mushroom body calyx or the optic lobes, and only low levels of innervation of the antennal lobes. This is comparable

Table 2. A comparison of dopaminergic clusters in normal-sized *N. vitripennis* (DA-L-IR, this study), *A. mellifera* (Tyrosine hydroxylase (TH)-IR, Tedjakumala et al. (2017)), *D. melanogaster* (TH-IR, TH-Gal4, Mao and Davis (2009)), and *T. evanescens* (DA-L-IR, van der Woude and Smid (2017c)). Clusters are grouped by location of somata in the cell body rind and, when possible, projection patterns. This grouping is tentative and does not guarantee homology between the clusters. *: confirmed innervation of the mushroom bodies.

N. vitripennis		A. mellifera		D. melanogaster		T. evanescens	
Cluster	Cells	Cluster	Cells	Cluster	Cells	Cluster	Cells
D1a	3.77	ST/AOTu	2-3	PAL	5	DA-1	2.6
D1b	2						
D2	59.85	*C1	75	*PAM	~100	DA-3?	2.7
		*C2	75				
D3	42.55	*C3	140	*PPL1	12	DA-5a	
				PPL2c	4.6		3.9
				PPL4	0.91	DA-5b	
				PPL5	0.54		
D4a	5.77	SP	15-20	PPM1	5.46	DA-6	3.2
D4b	5.88			PPM2	8.07		
D5	3.75	SL	5-8	*PPL2ab	6.1	DA-2	2.3
D6	3	S1-2	4			DA-7	1.4
D7	2	S7-8	2-4			DA-4	2.5

to results in the other small parasitoid *T. evanescens*, but not with *A. mellifera* and *D. melanogaster*, where innervation of these neuropils was clearly visible, albeit to a lesser extent than in the rest of the brain. Based on our current results, we cannot attribute the apparent lack of DA-L-IR in the calyx to a functional difference, or to differences in methodology, as will be discussed below.

It has been shown that choosing the method to detect dopaminergic cells is a non-trivial matter: in *A. mellifera* different results were obtained with an immunostaining against tyrosine hydroxylase (TH), the rate-limiting enzyme in dopamine synthesis (Tedjakumala et al., 2017) or against dopamine (Schäfer and Rehder, 1989); likewise, Mao and Davis (2009) found different results by making use of the GAL4/UAS system or anti-TH staining. It could be that the overall low number of DA-L-IR cells in *T. evanescens*, as well as the apparent lack of an equivalent cluster to the D2/C1,2/PAM clusters, could be ascribed to this methodology. As we only assessed DA-L-IR with the anti-dopamine antibody, future studies may obtain different results with anti-TH.

Species differences in *Nasonia*

Nasonia vitripennis and *N. giraulti* differ in their memory dynamics, with *N. giraulti* requiring multiple, spaced experiences before consolidating protein synthesis-dependent long-term memory (Hoedjes et al., 2012). A previous study comparing the octopaminergic network in these wasps was unable to show differences in this system (Haverkamp and Smid, 2014). Contrary to that study, we show here that normal-sized *N. vitripennis* and normal-sized *N. giraulti* do indeed differ in their dopaminergic network. Our analysis revealed that *N. vitripennis* had more cells in the D2 and D4a clusters, but fewer in the D4b cluster.

As discussed above, the D2 cluster corresponds to mushroom body-projecting clusters in other species, such as the PAM cluster in *D. melanogaster* and the C1 and C2 clusters in *A. mellifera*. This PAM cluster contains both cells associated with aversive and reward signaling. Although perhaps overly simplified, an increase in D2 cell number in *N. vitripennis* could be attributed to more cells associated with reward signaling. Though these results are not enough to imply causation, this is worthy of further study.

The D4 clusters are most similar to clusters that project to and around the central complex in *A. mellifera* (SP cluster) and *D. melanogaster* (PPM1/2 clusters). Although dopaminergic innervation in the central complex is important for motor control (reviewed by Pfeiffer and Homberg (2014)), the behavioral implications of *N. vitripennis* having more cells in D4a and less in D4b are unclear.

It may be that our arbitrary distinction of these subclusters (based on distance) is incorrect, and that the effects we found cancel out.

Our comparison of DA-L-IR clusters, the previous comparison of octopaminergic clusters (Haverkamp and Smid, 2014), and the difference in memory dynamics that instigated these comparisons (Hoedjes et al., 2012) were all described for the isogenic AsymCx and R2VU(x) strains of *N. vitripennis* and *N. giraulti*, respectively. As genetic variation may influence *N. vitripennis* memory dynamics (Koppik et al., 2015), the use of isogenic lines helps to minimize variation and pinpoint potential causalities. Both the AsymCx and R2VU(x) strains have a sequenced genome (Werren et al., 2010) which may aid further characterization of dopaminergic cluster size. Of particular interest for further investigation is that this particular difference in memory dynamics has been introgressed by hybridization of these strains, yielding *N. giraulti*-like memory in an *N. vitripennis* genetic background (Hoedjes et al., 2014b).

Size-related differences in *N. vitripennis*

To our knowledge, this is the second study to compare the dopaminergic system in relation to body size in insects (the first being a comparison of the highly diverse body sizes in *T. evanescens* (van der Woude and Smid, 2017b)). Despite the almost threefold differences in absolute brain volume between normal- and small-sized *N. vitripennis* (Groothuis and Smid, 2017), we observe no difference in the overall number of DA-L-IR cells. This is comparable to the effects of extreme (fivefold) brain scaling in *T. evanescens*, where no difference in DA-L-IR neuron number was found (van der Woude and Smid, 2017b). However, in *T. evanescens* these neurons are significantly smaller in the smallest individuals. Though we intended to analyze similar measurements in *N. vitripennis*, we found we could not reliably label the entire cell body in every instance. It may be that dopamine is not sufficiently present throughout the cell bodies of *N. vitripennis*, restricting the use of an anti-dopamine stain.

In contrast to the *T. evanescens* study, we did find cluster-specific differences between *N. vitripennis* of different size. Small individuals had fewer cells in the D5 and in the D7 cluster. We do not know the functional role of the D7 cluster, nor could we observe its projections. Therefore, we cannot speculate regarding the implications of this difference at this time. We note, however, that the D7 cluster could only be counted in a very small number of brains in both size classes (see Table 1).

On the other hand, the D5 cluster seems homologous to the PPL2ab cluster of *D. melanogaster*, which is known to project to the mushroom body calyx and the lateral horn (Mao and Davis, 2009). These neuropils that are known to be involved with learned and naïve odor preferences, respectively (Strutz et al., 2014). The probable projection pattern of this cluster therefore hints at a role for the D5 cluster in the memory dynamics of *N. vitripennis*. However, the exact functional mechanics of the D5/PPL2ab cluster have, to our knowledge, not been described in other species.

Future prospects

Owing to the hymenopteran male haploid genetics, introgression of traits that differ between strains and species is relatively easy in *Nasonia* (Hoedjes et al., 2014b; Werren et al., 2016). As mentioned above, the memory dynamics central to this study have been introgressed, yielding *N. giraulti*-like memory linked to two specific quantitative trait loci in a predominantly *N. vitripennis* genetic background (Hoedjes et al., 2014b). Although this trait is still undergoing further introgression, future lines of research may focus on the dopaminergic networks of the resulting interspecies hybrid wasps. If the differences found in our work indeed explain the difference in memory dynamics, these future studies may find similar differences in the dopaminergic system of introgressed hybrid lines, such as *N. giraulti*-like numbers of D2 cells.

The methodology that was used in this study restricts the potential of incorporating the results into a common reference, such as the Jewel Wasp Standard Brain (Groothuis et al., 2018). This effect is predominantly due to the tissue fixation by glutaraldehyde, which strongly shrinks the tissue and restricts the use of other antibodies raised against formaldehyde-fixed antigens. Future studies may therefore opt to try anti-TH in combination with a counterstain such as NC82 (Wagh et al., 2006; Groothuis and Smid, 2017). Even further advancements in the study of dopaminergic neurons may be made by individually or clonally targeted single-cluster projections, which may also be incorporated into the Jewel Wasp Standard Brain. These future developments will contribute to a better understanding of the projection patterns and potential interactions of the many dopaminergic neurons in the *Nasonia* brain.

Synthesis

In this study we found differences in the dopaminergic system in the comparison between two *Nasonia* species and two *N. vitripennis* size classes. Both comparisons

showed differences in memory dynamics: *N. giraulti* needs more experiences than *N. vitripennis* to form long-term memory (Hoedjes et al., 2012), whereas small *N. vitripennis* show reduced memory performance (Van der Woude and Smid, 2017a). It is therefore not too surprising that we found effects on different dopaminergic clusters for these comparisons, but it is promising that in both cases these effects are (in part) in clusters that likely project to the mushroom bodies, lending credibility to the role of these findings in explaining the memory dynamics of these groups.

Acknowledgements

References

Aso Y, Herb A, Ogueta M, Siwanowicz I, Templier T, Friedrich AB, Ito K, Scholz H, Tanimoto H. 2012. Three dopamine pathways induce aversive odor memories with different stability. Plos Genetics 8(7).

Burke CJ, Huetteroth W, Owald D, Perisse E, Krashes MJ, Das G, Gohl D, Silies M, Certel S, Waddell S. 2012. Layered reward signalling through octopamine and dopamine in *Drosophila*. Nature 492(7429):433-437.

Claridge-Chang A, Roorda RD, Vrontou E, Sjulson L, Li HY, Hirsh J, Miesenbock G. 2009. Writing memories with light-addressable reinforcement circuitry. Cell 139(2):405-415.

Das G, Lin S, Waddell S. 2016. Remembering components of food in *Drosophila*. Front Integr Neurosci 10:4.

Groothuis J, Pfeiffer K, Smid HM. 2018. The Jewel Wasp Standard Brain: average shape atlas and morphology of the female *Nasonia vitripennis brain*. In prep.

Groothuis J, Smid HM. 2017. *Nasonia* parasitic wasps escape from Haller's rule by diphasic, partially isometric brain-body size scaling and selective neuropil adaptations. Brain Behav Evol 90(3):243-254.

Haverkamp A, Smid HM. 2014. Octopamine-like immunoreactive neurons in the brain and subesophageal ganglion of the parasitic wasps *Nasonia vitripennis* and *N. giraulti*. Cell Tissue Res 358(2):313-329.

Hoedjes KM, Smid HM. 2014. Natural variation in long-term memory formation among *Nasonia* parasitic wasp species. Behav Processes 105:40-45.

Hoedjes KM, Smid HM, Vet LEM, Werren JH. 2014b. Introgression study reveals two quantitative trait loci involved in interspecific variation in memory retention among *Nasonia* wasp species. Heredity 113(6):542-550.

Hoedjes KM, Steidle JLM, Werren JH, Vet LEM, Smid HM. 2012. High-throughput olfactory conditioning and memory retention test show variation in *Nasonia* parasitic wasps. Genes Brain Behav 11(7):879-887.

Ito K, Shinomiya K, Ito M, Armstrong JD, Boyan G, Hartenstein V, Harzsch S, Heisenberg M, Homberg U, Jenett A, Keshishian H, Restifo LL, Rossler W, Simpson JH, Strausfeld NJ, Strauss R, Vosshall LB, Grp IBNW. 2014. A systematic nomenclature for the insect brain. Neuron 81(4):755-765.

Koppik M, Hoffmeister TS, Brunkhorst S, Kieß M, Thiel A. 2015. Intraspecific variability in associative learning in the parasitic wasp *Nasonia vitripennis*. Animal Cogn 18(3):593-604.

Krashes MJ, DasGupta S, Vreede A, White B, Armstrong JD, Waddell S. 2009. A neural circuit mechanism integrating motivational state with memory expression in *Drosophila*. Cell 139(2):416-427.

Lin S, Owald D, Chandra V, Talbot C, Huetteroth W, Waddell S. 2014. Neural correlates of water reward in thirsty *Drosophila*. Nat neurosci 17(11):1536-1542.

Liu C, Placais PY, Yamagata N, Pfeiffer BD, Aso Y, Friedrich AB, Siwanowicz I, Rubin GM, Preat T, Tanimoto H. 2012. A subset of dopamine neurons signals reward for odour memory in *Drosophila*. Nature 488(7412):512-516.

Mao ZM, Davis RL. 2009. Eight different types of dopaminergic neurons innervate the *Drosophila* mushroom body neuropil: anatomical and physiological heterogeneity. Front Neural Circuit 3.

Pfeiffer K, Homberg U. 2014. Organization and functional roles of the central complex in the insect brain. Annu Rev Entomol 59:165-184.

Rago A, Gilbert DG, Choi JH, Sackton TB, Wang X, Kelkar YD, Werren JH, Colbourne JK. 2016. OGS2: genome re-annotation of the jewel wasp *Nasonia vitripennis*. BMC Genomics 17:678.

Schäfer S, Rehder V. 1989. Dopamine-like immunoreactivity in the brain and suboesophageal ganglion of the honeybee. J Comp Neurol 280(1):43-58.

Schurmann D, Sommer C, Schinko APB, Greschista M, Smid H, Steidle JLM. 2012. Demonstration of long-term memory in the parasitic wasp *Nasonia vitripennis*. Entomol Exp Appl 143(2):199-206.

Schürmann FW, Elekes K, Geffard M. 1989. Dopamine-like immunoreactivity in the bee brain. Cell Tissue Res 256(2):399-410.

Schwaerzel M, Monastirioti M, Scholz H, Friggi-Grelin F, Birman S, Heisenberg M. 2003. Dopamine and octopamine differentiate between aversive and appetitive olfactory memories in *Drosophila*. J Neurosci 23(33):10495-10502.

Strutz A, Soelter J, Baschwitz A, Farhan A, Grabe V, Rybak J, Knaden M, Schmuker M, Hansson BS, Sachse S. 2014. Decoding odor quality and intensity in the *Drosophila* brain. eLife 3.

Tedjakumala SR, Rouquette J, Boizeau ML, Mesce KA, Hotier L, Massou I, Giurfa M. 2017. A tyrosine-hydroxylase characterization of dopaminergic neurons in the honey bee brain. Front Syst Neurosci 11:47.

Van der Woude E, Smid HM. 2017a. Differential effects of brain scaling on memory performance in parasitic wasps. In prep.

van der Woude E, Smid HM. 2017b. Effects of isometric brain-body size scaling on the complexity of monoaminergic neurons in a minute parasitic wasp. Brain Behav Evol 89(3):185-194.

van der Woude E, Smid HM. 2017c. Maximized complexity in miniaturized brains: morphology and distribution of octopaminergic, dopaminergic and serotonergic neurons in the parasitic wasp, *Trichogramma evanescens*. Cell Tissue Res 369(3):477-496.

Waddell S. 2013. Reinforcement signalling in *Drosophila*; dopamine does it all after all. Curr Opin Neurobiol 23(3):324-329.

Wagh DA, Rasse TM, Asan E, Hofbauer A, Schwenkert I, Durrbeck H, Buchner S, Dabauvalle MC, Schmidt M, Olin G, Wichmann C, Kittel R, Sigrist SJ, Buchner E. 2006. Bruchpilot, a protein with homology to ELKS/CAST, is required for structural integrity and function of synaptic active zones in *Drosophila*. Neuron 49(6):833-844.

Werren JH, Cohen LB, Gadau J, Ponce R, Baudry E, Lynch JA. 2016. Dissection of the complex genetic basis of craniofacial anomalies using haploid genetics and interspecies hybrids in *Nasonia* wasps. Dev Biol 415(2):391-405.

Werren JH, Loehlin DW. 2009. The parasitoid wasp *Nasonia*: an emerging model system with haploid male genetics. Cold Spring Harb Protoc 4(10):pdb emo134.

Werren JH, Richards S, Desjardins CA, Niehuis O, Gadau J, Colbourne JK, Group NGW. 2010. Functional and evolutionary insights from the genomes of three parasitoid *Nasonia* species. Science 327(5963):343-348.

Nasonia vitripennis

Chapter 5

No gains for bigger brains:

Functional and neuroanatomical consequences of artificial selection on relative brain size in a wasp

Emma van der Woude*,
Jitte Groothuis*,
Hans M. Smid
*These authors contributed equally to this publication

Submitted

Abstract

Cognitive constraints are shaped by ecological conditions, (1) by determining resources available for development and maintenance of brain tissue and (2) by requiring adaptive behavior to optimize an animal's fitness. As brain performance relates to relative brain size, there may be heritable genetic variation in relative brain size. Here, we used bidirectional artificial selection to study the consequences of genetic variation in relative brain size on brain morphology, cognition and longevity in *Nasonia vitripennis* Walker parasitoid wasps. Our results show a robust change in relative brain size after 26 generations of selection and 6 generations of relaxation, which indicates that there is heritable genetic variation in relative brain size. Total average neuropil volume of the brain was 16% larger in wasps selected for relatively large brains than in wasps selected for relatively small brains. This difference in brain volume differentially affected relative neuropil volumes, because the relative volume of the antennal lobes was larger in wasps with relatively large brains. We show that having a relatively small or large brain did not influence olfactory memory retention, whereas wasps with a larger relative brain size had a shorter longevity, which was even further reduced after a learning experience. These effects of genetic variation on neuropil composition and memory retention are different from previously described effects of phenotypic plasticity in absolute brain size. In conclusion, having relatively large brains is costly for *N. vitripennis*, whereas no cognitive benefits were recorded.

Introduction

Brain size is linked to brain performance through the number of neurons and their connectivity (Striedter, 2005; Chittka and Niven, 2009). Variation in brain size, both in absolute size and relative to body size, can therefore underlie differences in cognitive abilities (Dicke and Roth, 2016). Brain size variation can be caused by genetic variation, but also by phenotypic plasticity. Phenotypic plasticity can be regulated by genetically encoded developmental programs (e.g. Lanet and Maurange, 2014). These determine how a single genotype morphologically responds to different developmental conditions, such as differences in nutritional levels, caste differentiation and sex determination. Natural genetic variation in the plasticity genes that facilitate these differential development programs may predispose animals to optimize their development to match specific ecological circumstances, such as low food availability. Interestingly, animals that develop into differentially-sized individuals, for example due to differences in food availability during embryonic or larval development, do not scale their entire body size isometrically. One striking example of tissue-specific scaling is known for the brain, a phenomenon described by Haller's rule (Rensch, 1948; 1956). This rule states that small animals require relatively larger brains than large animals. The relationship between brain size and body size follows a power law function. In the case of a negative allometry that is described by Haller's rule, the scaling coefficient of this power law function is smaller than 1. Haller's rule holds both for interspecific (e.g. Pagel and Harvey, 1988; Harvey and Krebs, 1990; Wehner et al., 2007; Isler et al., 2008), and intraspecific (e.g. Wehner et al., 2007; Riveros and Gronenberg, 2010; Seid et al., 2011) comparisons.

Development and maintenance of relatively larger brains is more costly for smaller animals, because brain tissue has high metabolic costs (Aiello and Wheeler, 1995). This may present strong constraints on the evolution of extremely small animals. In this context, it is intriguing that one of the smallest animals on Earth, the parasitic wasp *Trichogramma evanescens*, shows a different brain scaling strategy than predicted by Haller's rule (van der Woude et al., 2013). These wasps are gregarious parasitic wasps that develop from egg to adult inside eggs of butterflies and moths. Body size depends on the level of scramble competition between larvae that develop inside the same host egg. This can lead to large phenotypic variation in absolute brain and body size, even between genetically identical individuals (van der Woude et al., 2013). Although body volume can vary with a factor 7 between sister wasps of the same inbred isofemale line, this does not affect their relative brain size; the wasps show isometric brain scaling.

This isometric brain scaling results in small wasps having brains that are smaller than predicted by Haller's rule. Interestingly, this does not affect their memory performance (Van der Woude and Smid, 2017a). Small and large *T. evanescens* show similar memory retention levels. Furthermore, the complexity of the olfactory pathway remains remarkably unaffected by its size: small wasps have the same number of antennal lobe glomeruli and most types of olfactory sensilla as large wasps (van der Woude and Smid, 2016). This indicates that *T. evanescens* is well adapted to develop as small adults.

The larger parasitoid wasp *Nasonia vitripennis* parasitizes and develops inside fly pupae, and body size depends on scramble competition in a similar way as in *T. evanescens*, scaling their dry body weight with a factor of 10. This parasitoid also deviates from Haller's rule, but applies a different brain scaling rule than *T. evanescens* (Groothuis and Smid, 2017). The wasps show diphasic brain scaling with isometry in small and negative allometry in large *N. vitripennis,* possibly because they switch to a different developmental program.

The isometric phase causes relatively smaller brains in small wasps than are predicted by Haller's rule. In contrast to *T. evanescens,* this does affect their memory performance: large *N. vitripennis* show higher levels of olfactory and visual memory retention than small *N. vitripennis* (Van der Woude and Smid, 2017a). This may be related to differences in relative neuropil volumes. Among other neuropils, the mushroom bodies (known to be important for memory formation in other insects) were relatively smaller in the smallest wasps; on the other hand, the relative volume of the lateral horn (known to be involved in naive responses to olfactory cues (Parnas et al., 2013; Strutz et al., 2014)) had not changed. This may indicate that, when challenged with restricted resources, isogenic *N. vitripennis* are able to utilize different developmental programs and develop differentially structured brains. In this example, the decrease in absolute and relative mushroom body volume may underlie their aforementioned lower memory performance. These studies indicate that *T. evanescens* and *N. vitripennis* are differentially adapted to dealing with the stringent dietary conditions that arise from larval scramble competition.

Ecological conditions may require adaptive behavior to optimize an animal's fitness. This may be realized by a relatively larger brain. However, higher developmental and operating costs of brain tissue, associated with a relatively larger brain, may incur negative effects on fitness and longevity (Aiello and Wheeler, 1995; Mery and Kawecki, 2005). Furthermore, populations that evolve under more stringent dietary conditions may experience different selection

pressures on genes that determine brain size than populations that evolve under more permissible dietary conditions. In the case of a parasitic wasp, such differences may exist by adapting to different host species. Different host species may require different cognitive abilities because host oviposition behavior may require different foraging strategies of the parasitic wasps (Smid et al., 2007; Kruidhof et al., 2012; Smid and Vet, 2016), while also requiring adaptations to differences in host quality or size.

To be able to adapt to such different ecological circumstances, heritable genetic variation in relative brain size must be present. For instance, our previous work on brain scaling in *T. evanescens* showed that the precise scaling coefficients differed for different isogenic lines, indicating genetic variation in the plasticity genes that determine brain size in this species (van der Woude et al., 2013). Recent studies show that relative brain size can be selected for in guppies (Kotrschal et al., 2013), and that this has correlated effects on learning abilities (Kotrschal et al., 2013; Kotrschal et al., 2015b), gut mass (Kotrschal et al., 2013), survival (Kotrschal et al., 2015a), proactiveness (Kotrschal et al., 2014), sexual traits (Kotrschal et al., 2015c), and the immune system (Kotrschal et al., 2016). The differences in relative brain size between large- and small-brained guppies are caused by differences in the expression of only a single gene: Angiopoietin-1 (Chen et al., 2015).

Our previous research showed that phenotypic differences in absolute brain and body size, induced by differences in scramble competition, affect neuropil composition and memory retention abilities in an isogenic strain of *N. vitripennis*. Here, we studied the consequences of genetic variation in relative brain size using constant, low levels of scramble competition to minimize such phenotypic effects of body size. This was done by means of a bidirectional artificial selection regime, using the ratio between head width and body length as proxy for relative brain size (Groothuis and Smid, 2017) in a population of *N. vitripennis* that was specifically collected and maintained to preserve natural genetic variation (Van de Zande et al., 2014). Furthermore, we studied the effects of this selection regime on brain structure, cognition and longevity. We expected that there is heritable variation in relative brain size under constant nutritional levels. We expected that (A) there is a positive correlation between relative brain size and memory performance, (B) relative neuropil volumes are affected by selection for relative brain size, and (C) there is a negative correlation between relative brain size and longevity.

Materials and methods

Insects

We used female *N. vitripennis* Walker (Hymenoptera: Pteromalidae) of strain HVRx, which was specifically collected and maintained to preserve natural genetic variation (Van de Zande et al., 2014). The wasps were reared on *Calliphora vomitoria* pupae (obtained as maggots from Kreikamp B.V., Hoevelaken, The Netherlands) and kept in a climate cabinet at 20±1 °C with a 16:8 L:D cycle. The generation time was ca. 3 weeks.

Selection regime

To initiate the selection lines, 200 mated female *N. vitripennis* were sedated with CO_2. Body length and head width of these wasps were measured using a dissection microscope with ocular micrometer. The ratio between head width and body length was calculated and used as proxy for relative head size. The 30 wasps with the largest ratio were randomly distributed over 3 rearing vials in groups of 10 wasps, to initiate 3 selection lines for large heads (defined as Large (L)). Similar procedures were used to initiate 3 selection lines for small heads (defined as Small (S)), using the 30 wasps with the smallest ratio.

Another set of 30 wasps were randomly selected from the starting population and used to initiate 3 control lines (defined as Control (C)) to control for the effect of selection on inbreeding. This resulted in three replicate lines per selection regime: large L1, L2, L3, small S1, S2, S3 and control C1, C2, C3. Each rearing vial contained 20 *C. vomitoria* pupae and a drop of honey.

In every subsequent generation, 50 mated female wasps per S and L line were sedated and measured as described above. The 10 wasps with the largest (for L) and smallest (for S) ratios between head width and body length were used to initiate the next generation. For the C lines, 10 randomly chosen females were used, without measurements. These selection procedures were repeated for 25 generations. After the 25th generation, selection was relaxed, with the exception of generations 30, 33 and 40.

Neuropil staining and relative neuropil measurements

Per replicate line, 12 randomly selected female wasps (108 in total) from generation 33 were sedated and their brains dissected. All incubations were

performed with brains grouped per replicate. We dissected, fixed, stained, and analyzed the brains as described in detail in the SI Methods. In brief, the neuropil was stained using the nc82 antibody against the presynaptic Bruchpilot protein (DSHB hybridoma product nc82) (Wagh et al., 2006) and the cell nuclei using propidium iodide. Volumetric neuropil analysis was performed on the 3 best-stained brains per replicate (9 per selection regime) by image segmentation and subsequent three-dimensional reconstruction using FIJI (Schindelin et al., 2012) and Amira 5.4.2 (Visage Imaging). Due to its tight connection with the eye, the optic lobe lamina is often damaged during dissection. Therefore, it was not included in this analysis. Relative neuropil volume was calculated as the percentage of the total neuropil volume.

Memory retention

Olfactory memory retention of the selection lines was tested in generation 33. We used single classical olfactory conditioning trials, as described before (Hoedjes et al., 2014b; Van der Woude and Smid, 2017a). Conditioning and memory testing procedures are described in full in the SI Methods. In short, groups of 60 wasps (1-2 days old) were provided with an oviposition experience (unconditioned stimulus, US) while experiencing an odor (conditioned stimulus, CS) during the CS+ phase. The rewarding unconditioned stimulus consisted of 40 *Calliphora vomitoria* pupae. The conditioned stimulus was either Royal Brand Bourbon Vanilla extract or Natural Chocolate extract (Nielsen-Massey Vanillas Intl., Leeuwarden, the Netherlands). This phase was followed by a CS- phase in which the wasps experienced the second of the two odors in the absence of hosts. The conditioning trials were performed in a reciprocal manner: one group of every line was conditioned using vanilla as CS+ and chocolate as CS-, another group was conditioned using chocolate as CS+ and vanilla as CS-. We conditioned four reciprocal groups per replicate line. Memory retention was tested in a T-maze containing vanilla and chocolate extract as described before (Hoedjes et al., 2014b). Wasps were inserted in the T-maze in groups of approximately 15 wasps, resulting in 3 assays per conditioned group. After 5 minutes, the number of wasps at the vanilla and chocolate sides was recorded. Memory of each reciprocal group was tested 1, 3 and 5 days after the conditioning trials.

Longevity

Longevity was studied in generation 40. Wasps of each replicate selection line were used either naively or after an olfactory conditioning trial (as described

above). Each replicate line was analyzed with 2 groups of naive and 2 groups of conditioned wasps, each group containing 30 wasps. These groups were placed in clean rearing tubes with unlimited access to water and honey and kept in a climate cabinet at 25 °C. The tubes were refreshed weekly. Every 2 days the number of dead wasps was counted.

Statistical analyses

Statistical procedures are described in full in the SI Methods. Response to selection was analyzed using a linear mixed model, with the ratio between head width and body length as dependent variable. Similar linear mixed models were used to test the effect of selection on body length and head width, using respectively the natural logarithm of body length or head width as dependent variable. Ordinary linear regression on head width and mean-centered body length was used to study if the difference in head-body size ratio between the selected lines can be explained by allometric brain scaling in combination with differences in body size. Body lengths were mean-centered by subtraction of the average body length of that generation, to reveal differences in head-body size ratio between selection regimes by differences in the intercept at mean body length.

Neuropil volumes were compared with a linear mixed model. We used the absolute total neuropil volume or relative volume per neuropil as dependent variables, with selection regime as fixed factor and line as random factor. As we compared multiple relative neuropil volumes, we corrected the p-values for multiple comparisons with the Holm-Bonferroni method ($m = 11$) (Holm, 1979). Neuropils with significant effects of selection regime on relative volume were further analyzed with χ^2 pairwise comparisons to test for differences between the selection regimes (43).

Memory retention was expressed as a performance index (PI), which is calculated as: 1st group(%CS+) − 2nd group(%CS−). Values of PIs were calculated from estimated response means obtained from generalized linear mixed models (GLMMs) with logit link function and binomial distribution. The dependent variable was the number of wasps that chose chocolate with the total number of wasps making a choice as denominator. Response rates of the memory retention tests were determined by a GLMM that used the fraction of wasps making a choice out of the total number of wasps inserted as dependent variable. Longevity was analyzed using a two-way ANOVA that tested for the effect of selection regime, conditioning and the interaction between these terms

on time till death, followed by TukeyHSD post-hoc tests. Statistical analyses were performed in R version 3.1.0 using packages lme4 (Bates et al., 2014), phia (De Rosario-Martinez, 2013), lsmeans (Lenth and Hervé, 2014).
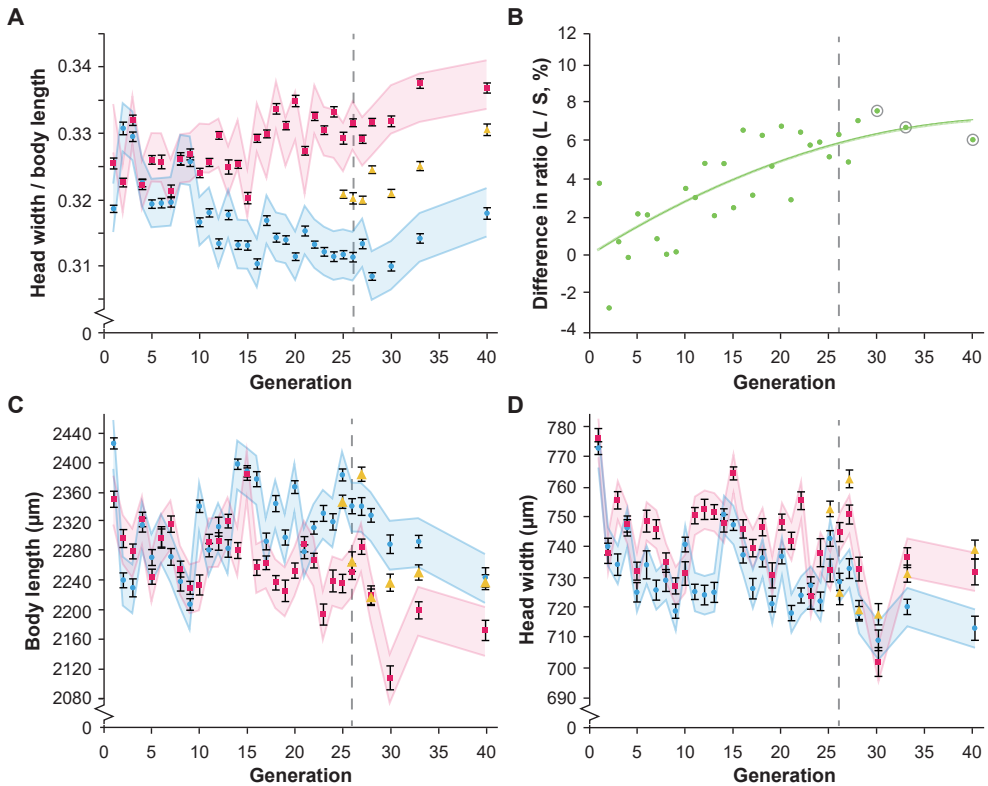

Figure 1. Relative brain size responds to bidirectional selection. Data points depict means over all individuals of all lines in a selection regime. Magenta squares: wasps selected for relatively large brains (L lines); blue circles: wasps selected for relatively small brains (S lines); yellow triangles: wasps of the control treatment (C lines). Dashed vertical lines in panels A-D show the start of relaxation of the selection regime, grey circles in panel B show generations used for additional selection. Linear mixed model predictions were used to calculate confidence intervals. **A.** Relative brain size is shown as the mean ± SE of the head-body size ratio for all wasps of a certain selection regime. **B.** Difference in the head-body size ratio between the L and S lines increases with each selected generation. Regression formula: $y = -0.0035x^2+0.317x$, $R^2 = 0.651$. **C.** Absolute body length (mean±SE), and **D.** Absolute head width (mean±SE) both respond to selection. Note that L wasps have shorter bodies than S (panel C), but wider heads (panel D).

Results

Selection regime

There was a significant effect of the selection regime on the head-body size ratio ($\chi^2_1 = 4496.16$, $p < 0.001$; Figure 1A). After generation 25 (the last generation undergoing selection), the difference between wasps of the large (L) and small (S) lines in head-body size ratio was 6.30% (Figure 1B). In generation 33 we assessed brain morphology and memory retention (discussed below); in this generation the difference in head-body size ratio was 6.67%. We assessed longevity in generation 40, here the difference in ratio was 6.03%. On average, the final differences in ratio were 6.41% in generations 26 to 40 (Figure 1B). Generation number significantly affected head-body size ratio ($\chi^2_{30} = 898.47$, $p < 0.001$), as did the interactions between selection regime and generation ($\chi^2_{30} = 1996.18$, $p < 0.001$). Realized heritability (h^2) of the ratio was 0.067 in generation 26.

Selection regime (for small versus large head-body size ratio) had a significant effect on body length (Figure 1C) ($\chi^2_1 = 322.437$, $p < 0.001$; Figure 1C). Body length was also affected by generation ($\chi^2_{30} = 888.169$, $p < 0.001$) and the interaction between selection and generation was significant ($\chi^2_{30} = 537.050$, $p < 0.001$). Selection regime also affected head width (Figure 1D) ($\chi^2_1 = 202.113$, $p < 0.001$; Figure 1D), as did generation ($\chi^2_{30} = 864.363$, $p < 0.001$) and the interaction between selection and generation was significant ($\chi^2_{30} = 191.226$, $p < 0.001$).

Figure 2 shows the relationship between head width and body length in wasps of the three lines in generation 33. Linear regression on head width and mean-centered body length revealed significant differences between the lines in generation 33 in intercept (L: 749.048, C: 730.396, S: 709.134; $F_{2,444} = 36.466$,
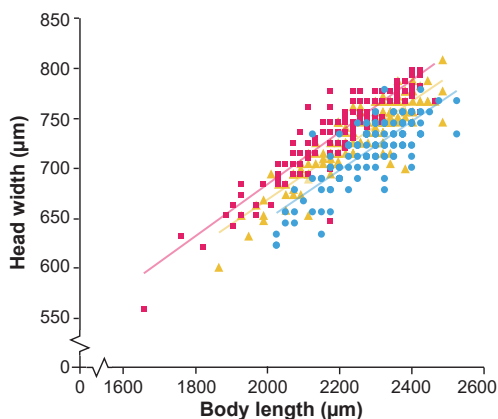
Figure 2. Head width and body length of individual wasps selected for relatively large (magenta squares) and small (blue circles) head-body ratio, and unselected control lines (yellow triangles). Data are shown for generation 33, which is the same generation used to study neuropil composition and memory performance. Regression analysis was performed on mean-centered body lengths, which ensured that differences in the intercept reflected differences in head-body ratio. This revealed differences in the intercepts, but not in the slopes. Similar results for generation 26 and 40 are shown in SI Figure S1.

$p < 0.001$), but not in slope (L: 0.260, C: 0.245, S: 0.244; $F_{2,444} = 0.670$, $p = 0.512$). Similar results were found for wasps of generations 26 and 40 (see SI Figure S1). This shows that wasps of the L, C and S lines differ in head width independent of the body size effects due to selection. The effect on head-body size ratio is, therefore, not caused by allometric brain scaling resulting from the difference in body size between the lines. Body lengths, head widths and ratios between head width and body length for all generations are shown in SI Table S1.
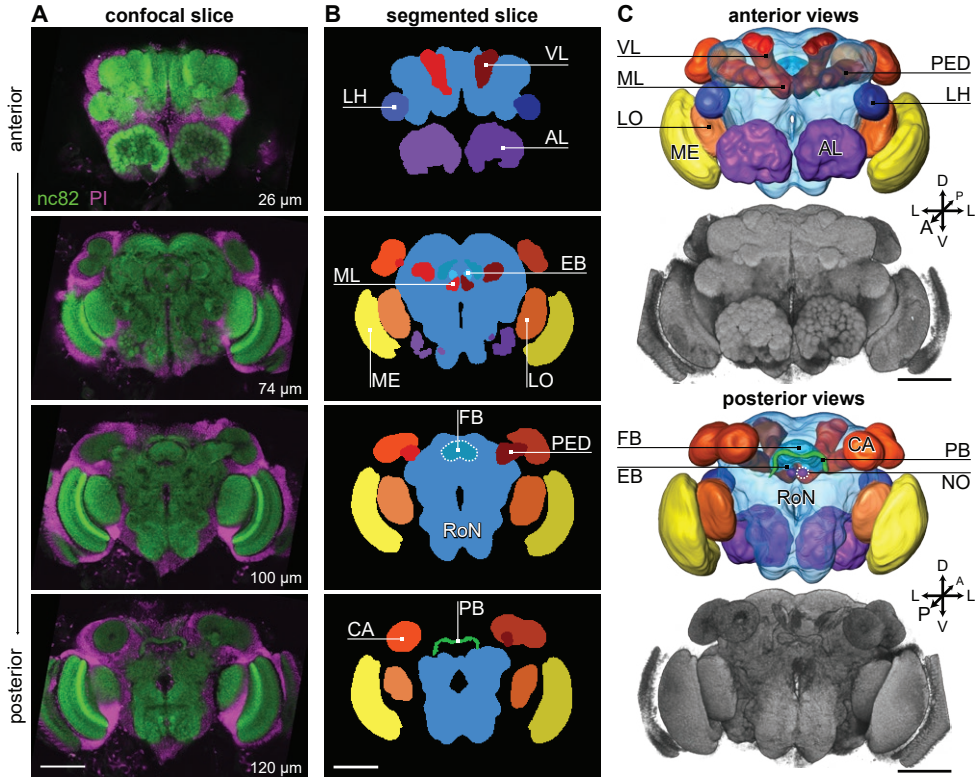

Figure 3. Overview of neuropils measured. Scale bars depict 100 µm in all panels. **A.** Selected slices through a single *N. vitripennis* brain from line L3, fluorescently labeled with nc82 (green) and PI (magenta). Bottom-right insets indicate slice depth in µm from the anterior direction. Image contrast was increased in FIJI. **B.** Schematic representation of segmented neuropils in the corresponding slices of panel A. Optic lobes (OL) consisting of lobula (LO) and medulla (ME); mushroom body (MB), consisting of the calyx (CA), pedunculus (PED), vertical lobe (VL), and medial lobe (ML). PED, VL, and ML were segmented as one label, the ventral mushroom body (MB-V); central complex (CX), consisting of fan-shaped body (FB), ellipsoid body (EB), protocerebral bridge (PB), and noduli (NO); lateral horn (LH); antennal lobe (AL) (the AL hub and glomeruli were segmented as a whole); and the remainder of the neuropil (RoN). The lamina, visible in panel A and the volume renderings of panel C, was not segmented. **C.** Anterior and posterior views of a surface model based on the segmentations shown in panel B, accompanied by a volume rendering of the nc82 channel shown in panel A (using the SurfaceGen and VolTex modules, respectively, of Amira). Orientation in panel C refers to the body axis (Haverkamp and Smid, 2014). Lettering as in panel B.

Brain morphology

In the analysis of neuropil composition, 3 out of 12 brains from each replicate line were analyzed, resulting in datasets for 9 brains per selection regime (Figure 3).
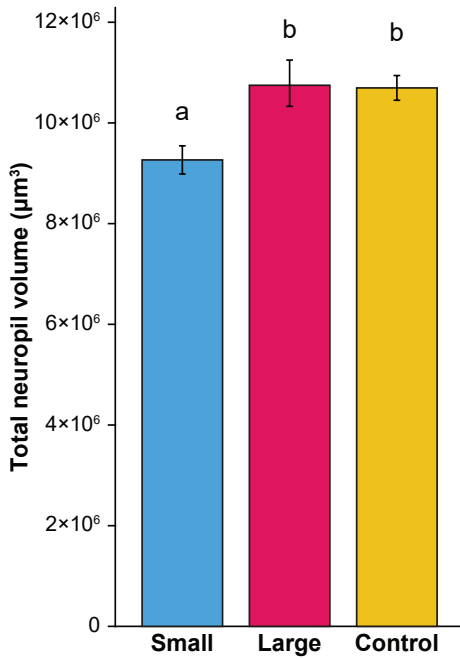

Figure 4. Absolute volumes of the total neuropil. Bars depict mean volume ± SE in μm³, *N* = 9 for each selection regime. Letters indicate significant differences between selection regimes based on post-hoc pairwise comparisons (α = 0.05).

First, we analyzed the absolute volume of the neuropil in the selected lines. Selection regime had a significant effect on total neuropil volume (Figure 4; $\chi^2_2 = 8.0793$, $p = 0.0176$). Post-hoc pairwise comparisons revealed that neuropil volume of wasps of the S lines was smaller ($9.27 \times 10^6 \pm 0.28 \times 10^6$ μm³, M ± SE) than wasps of the C lines ($10.70 \times 10^6 \pm 0.25 \times 10^6$ μm³, $\chi^2_1 = 5.8393$, $p = 0.016$) and the L lines ($10.75 \times 10^6 \pm 0.46 \times 10^6$ μm³, $\chi^2_1 = 6.2720$, $p = 0.012$). There was no difference between the C and L lines ($\chi^2_1 = 0.0077$, $p = 0.929$). On average, the total neuropil of the L lines was 16% larger than in the S lines.

We further analyzed the brains by comparing relative volumes of 11 neuropil regions, determined as percentages of the total neuropil volume (Figure 5). The only neuropil region that showed a significant effect of selection regime was the antennal lobe ($\chi^2_2 = 19.237$, Holm-Bonferroni corrected $p = 0.0007$). Post-hoc comparison revealed that the relative neuropil volume was higher in the L lines (12.08 ± 0.16 %, mean ± SE) compared to the C (11.29 ± 0.08 %, $\chi^2_1 = 14.0360$, $p = 0.00018$) and the S (11.27 ± 0.20 %, $\chi^2_1 = 14.8094$, $p = 0.00012$) lines. There were no differences between the control and small lines ($\chi^2_1 = 0.0104$, $p = 0.918$). Relative volumes and statistical comparisons of other neuropils are presented in SI Table S2.

Figure 5. Relative volumes (mean ± SE) of the neuropils defined in Figure 3, N = 9 for each selection regime. Y-axes have been split to better visualize differences between selection regimes for relatively smaller neuropils. Effects of selection regimes was first tested with a LMM, with Holm-Bonferroni correction for multiple comparisons (m = 11 neuropil regions). Letters indicate significant differences between selection lines based on post-hoc pairwise comparisons; unmarked bars indicate no significant effect was found for these neuropils.

Memory retention

Memory retention was analyzed in 2502 wasps of the L line, 2759 wasps of the S line and 2883 wasps of the C line. Memory retention 1 day after conditioning was analyzed in 12 reciprocal groups of each replicate line, resulting in 36 reciprocal groups per selection regime. Due to mortality this number decreased over the subsequent days, resulting in a final 23 reciprocal groups per selection regime at 3 days after conditioning, and 20 reciprocal groups at 5 days after conditioning.

Figure 6 shows memory retention (expressed as performance index, PI) levels for the different lines. There was significant memory retention (χ^2_1 = 62.238, $p < 0.001$), and this retention decreased over time (χ^2_2 = 20.349, $p < 0.001$). There was an overall difference in memory retention between the different selection regimes (χ^2_2 = 10.971, $p = 0.004$). Memory retention did not differ between S and L (χ^2_1 = 0.066, $p = 0.796$), but both lines differ in memory retention levels from C (L: χ^2_1 = 9.002, $p = 0.003$; S: χ^2_1 = 7.884, $p = 0.005$). The selected lines maintained memory up to 3 days after conditioning, and the C lines maintained memory up to 1 day after conditioning. However, there were no significant differences in decrease of memory retention level over time between the different lines (χ^2_4 = 2.794, $p = 0.593$). There was no difference in response rate between wasps of the different lines (χ^2_2 = 1.054, $p = 0.591$).
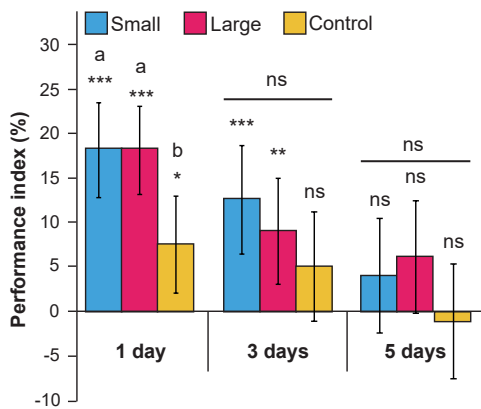
Figure 6. Memory retention over time for selection and control lines. Performance index (PI±SE) shows difference in percentage of preference between reciprocally trained groups. Asterisks indicate significant memory retention (χ^2 pairwise comparisons of GLMM response); *, $p < 0.05$; **, $p < 0.01$; ***, $p < 0.001$; ns, not significant; letters indicate significant differences between selection lines.

Longevity

Longevity (Figure 7) was affected by selection regime ($F_{2,1074} = 50.433$, $p < 0.001$), experience of a conditioning trial ($F_{1,1074} = 76.400$, $p < 0.001$) and the interaction between selection regime and conditioning was significant ($F_{2,1074} = 7.435$, $p < 0.001$). Longevity was lower in L than in S (TukeyHSD $p < 0.001$; SI Table S3) and C (TukeyHSD $p < 0.001$). There was no difference in longevity between S and C (TukeyHSD $p = 0.924$). Experience of a conditioning trial resulted in decreased longevity compared to naive wasps in L (TukeyHSD $p < 0.001$) and C (TukeyHSD $p < 0.001$), but not in S lines (TukeyHSD $p = 0.404$).
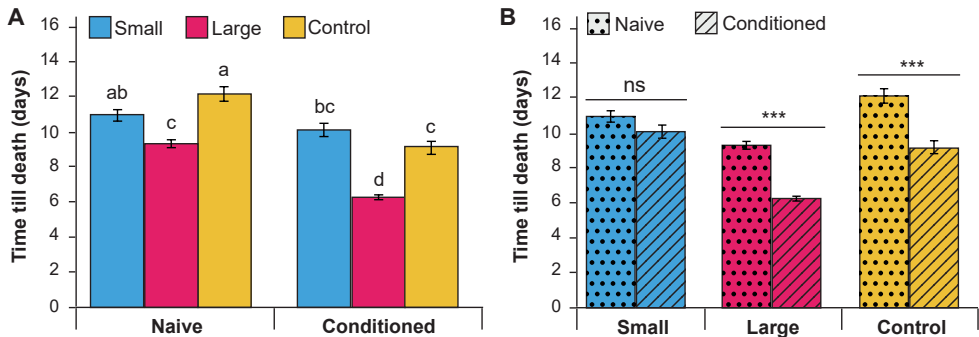
Figure 7. Survival of selection lines (mean ± SE), using a starting population of 180 wasps per group (60 per replicate line), with and without experiencing a single olfactory conditioning procedure. **A.** Wasps with a relatively large brain have lower longevity than wasps with relatively small brains. Longevity is not improved by having a relatively small brain compared to the control lines. **B.** A single olfactory conditioning experience affects longevity of wasps with a relatively large brain, but not of wasps with a relatively small brain. Asterisks and letters indicate significant differences between the groups based on Tukey HSD (see SI Table S3); ***, $p < 0.001$; ns, not significant.

Discussion

Our bidirectional selection regime on *N. vitripennis* wasps resulted in a robust response in relative brain size that was not sensitive to relaxation for several generations, with on average 6.4% difference in head-body size ratio between wasps of the L and S lines. Total neuropil volume was 16% larger in wasps of the L lines than in wasps of the S lines. The response to selection, expressed as realized heritability, was lower in our study than in previous artificial selection experiments in guppies (Kotrschal et al., 2013) (i.e. 0.07 in our study and 0.48 for guppies). The regulation of relative brain size may be more complex in *N. vitripennis* than in guppies, where a change in the expression of a single gene determines relative brain size (Chen et al., 2015). The slow, but substantial selection response indicates that there is heritable genetic variation in brain size in *N. vitripennis*, but that there are constraining factors that limit the response to artificial selection. These constraints may be particularly strong due to the small size of the wasps, which causes metabolic and cognitive trade-offs to have a large impact on the functioning of their miniaturized brains. The high metabolic costs of brain tissue (Aiello and Wheeler, 1995) may limit the development of relatively larger brains, while cognitive or behavioral costs may limit the formation of relatively smaller brains. Hence, relative brain size may be constrained by energetic costs on the upper limit and by functional requirements on the lower limit. Our study revealed such a cost of having large brains on longevity (Figure 7A), but no functional benefits for olfactory memory performance (Figure 6).

Deviation from Haller's rule

Our selection regime resulted in wasps of the S lines having on average larger body lengths than those of the L lines. Since Haller's rule predicts that larger wasps have relatively smaller brains, this could suggest that differences in head-body ratio reflect allometric brain scaling due to phenotypic plasticity in body size, such as we experimentally induced in a previous study (Groothuis and Smid, 2017). This could occur, for instance, if our selection regime resulted in wasps of the L lines laying more eggs in similar sized hosts than wasps of the S lines, resulting in smaller wasps. However, a brain-body size regression would then result in wasps of the S and L and C lines to be on the same regression line, with wasps of the S and L lines constituting the large and small individuals respectively. Figure 2 shows that this is not the case; the three lines differed in intercept, with L above C, and C above S. Moreover, wasps of the S lines, with larger body size, had not only relatively but also absolutely smaller brains than wasps of the L lines. Therefore, allometric brain scaling cannot explain the

difference in head-body size ratio and brain volume between the wasps of the S and L lines. Instead, grade shifts appear to have occurred. Such grade shifts are elevation displacements that illustrate a difference in the level of encephalization at similar body sizes between different groups (Striedter, 2005; Eberhard and Wcislo, 2011).

Our finding bears comparison with a recent analysis of brain scaling in 40 cichlid species (Tsuboi et al., 2016). Plotting both the inter- and intraspecific allometric brain-body size relationships, showed that the variation in intraspecific intercepts, rather than in the slopes, explained variation in relative brain size across species within a family (Tsuboi et al., 2016). Thus, the variation in relative brain size between these cichlid species was explained by overall differences in encephalization level, and not by species-specific variation in brain-body size scaling dynamics. Our results support this view, since our selection regime resulted in wasps of the L lines that had an absolutely larger brain size while having a smaller body size than wasps of the S lines. These differences in overall level of brain encephalization indicate that there was genetic variation in encephalization level in the starting (HVRx) population. This type of genetic variation may underlie evolution of differences in relative brain size.

Brain morphology

Our neuropil analysis (Figure 5) shows that our selection regime only affected the relative volume of the antennal lobe, which was larger in the L lines than in the S and C lines. These results are different from our previous work on body size effects on brain scaling and brain morphology in *N. vitripennis*, where we found differences in several neuropils, but not the AL (Groothuis and Smid, 2017). However, in that previous study we induced phenotypic plasticity in brain and body size, using varying degrees of scramble competition in an isogenic line. Genetic variation in brain size and phenotypic plasticity in brain size therefore appear to have different effects on neuropil composition, which implies that different mechanisms may be involved in regulating neuropil plasticity. Moreover, the difference in absolute neuropil volumes was much larger in our previous study addressing phenotypic plasticity: approximately 152% (Groothuis and Smid, 2017) in contrast to 16% in the present study (Figure 4).

These results suggest that the antennal lobe may have a fixed relative volume under scramble competition but a variable relative volume when genetic variation is present, whereas the opposite is the case for the other neuropils. For example, in both bumblebees and honeybees (which, in the same colony, have limited

genetic variation, but 2-3 fold variation in brain volume), relative AL volume does not vary over the size range of these species (Mares et al., 2005). Such constant scaling of AL volume was confirmed for honeybees in a later study (Gronenberg and Couvillon, 2010). By contrast, scramble competition in an isogenic strain of *T. evanescens* resulted in relatively smaller AL glomeruli in smaller brains (van der Woude and Smid, 2016). Thus, the relation between relative neuropil volume, body size and genetic background deserves further study.

Memory retention

Our study shows that relative brain size does not affect memory performance. Wasps of the L and S lines showed similar levels and duration of memory retention. In contrast, a positive effect of larger brains on memory retention levels was recorded in our previous study on phenotypic plasticity in absolute brain size in *N. vitripennis* (Van der Woude and Smid, 2017a). Furthermore, a study on guppies recorded higher memory retention levels in guppies that were selected for relatively larger brains (Kotrschal et al., 2013). Though other measures of brain size were used, thus hampering a comparison between guppies and wasps, the 16% difference in neuropil volume between *N. vitripennis* wasps of the L and S lines in our study exceeds the 9% difference in brain weight recorded in guppies. Hence, the similarity in olfactory memory performance of our selected *N. vitripennis* lines was surprising, but in line with our findings on relative neuropil volumes, as described below.

The mushroom bodies are important structures in the insect brain that are involved in learning and memory formation (Perry and Barron, 2012). Indeed, our previous study on phenotypic plasticity in body size shows that wasps with brains that are larger in absolute volume have higher memory retention levels (Van der Woude and Smid, 2017a), and relatively larger mushroom bodies (Groothuis and Smid, 2017). In the current study, there was no difference in relative volumes of the mushroom bodies between the S, C and L lines (Figure 5), which is in line with the observed similarity in olfactory memory performance between wasps of the S and L lines. The combined results of the memory performance tests and neuropil analyses suggest that the costs and benefits of genetic changes in relative brain size may not be related to memory but to olfaction.

Our study also revealed a significantly higher level of memory retention abilities in the selected (S and L) than in the unselected C lines. Memory in the unselected C lines is, however, similar as in the original starting population HVRx (SI Figure S2). This indicates that our bidirectional selection regime resulted in increased

memory retention abilities, whereas memory retention abilities remained unchanged in the C lines. Our neuropil analysis suggests that this observed increase in both S and L lines does not have a basis in mushroom body volume, but potentially in other aspects of brain morphology not recorded in the present study.

Longevity

Our findings show that wasps with relatively larger brains live shorter than wasps with relatively small brains (Figure 7A). This illustrates the constitutive, global costs of brain tissue, in line with the theory that brain tissue is metabolically expensive (Aiello and Wheeler, 1995; Snell-Rood et al., 2009). Our results also show that C and L lines, but not the S lines, had lower longevity after an olfactory conditioning experience with a host as a reward, which is known to induce long-term, protein synthesis-dependent memory (Hoedjes et al., 2014a). (Figure 7B). Memory formation can affect neuropil size and relative neuropil distribution. For instance, the relative volume of the mushroom bodies was found to increase with host-finding experience in the butterfly *Pieris rapae* (Snell-Rood et al., 2009). Such experience-dependent plasticity, in combination with the associated changes in metabolic costs, constitute the induced costs of learning (Snell-Rood et al., 2009). This could also underlie the learning-induced costs that were found in *Drosophila*, which live shorter after forming long-term memory (Mery and Kawecki, 2005) or when selected for improved aversion learning (Burger et al., 2008). It should be noted that *N. vitripennis* wasps do not actually oviposit within the single hour of the conditioning experience, but feed on their host after drilling (Hoedjes et al., 2014a), and this host feeding induces egg maturation (Whiting, 1967). Thus, the costs that underlie the decreased longevity after a conditioning experience in the L wasps may be caused by the host encounter, the host feeding-induced egg maturation and long-term memory formation, but not oviposition. That a conditioning experience did affect longevity of wasps of the L lines but not the S lines in our study, suggests stronger energetic constraints in wasps with relatively large brains, because of reallocation of resources from general somatic and reproductive processes towards processes involved in operating and maintaining the larger brain.

Conclusion

Our study shows for the first time the effects of artificial bidirectional selection on relative brain size in insects. Due to its small size, *N. vitripennis* experiences

particularly strong energetic and cognitive constraints that limit the variation in relative brain size. The variation in relative brain size is further limited by the unique brain-body size scaling relationship of *N. vitripennis*, with allometry in large individuals and isometry in the smallest individuals, which indicates that there is little phenotypic plasticity in relative brain size. The limited selection response in our study indeed shows that the genetic variation in brain size is strongly constrained in this species. We have shown that small differences in relative brain size have large effects on longevity, indicating that strong energetic constraints act on relative brain size. The effect of relative brain size on relative antennal lobe volume indicates a specific adaptation in terms of olfaction. In the ongoing investigation of the question whether and how bigger brains are better (Chittka and Niven, 2009) we have provided a comprehensive and important dataset from the perspective of the smallest animal species studied in this regard, showing that bigger brains are not necessarily better, but certainly more costly.

Acknowledgements

References

Aiello LC, Wheeler P. 1995. The expensive-tissue hypothesis - the brain and the digestive-dystem in human and primate evolution. Curr Anthropol 36(2):199-221.

Bates D, Maechler M, Bolker B, Walker S. 2014. lme4: Linear mixed-effects models using Eigen and S4. Version R package version 1.1-7.

Burger JMS, Kolss M, Pont J, Kawecki TJ. 2008. Learning ability and longevity: a symmetrical evolutionary trade-off in *Drosophila*. Evolution 62(6):1294-1304.

Chen Y-C, Harrison PW, Kotrschal A, Kolm N, Mank JE, Panula P. 2015. Expression change in Angiopoietin-1 underlies change in relative brain size in fish. Proc R Soc B 282(1810):20150872.

Chittka L, Niven J. 2009. Are bigger brains better? Curr Biol 19(21):R995-R1008.

De Rosario-Martinez H. 2013. Phia: post-hoc interaction analysis. Version R package version 0.1-3.

Dicke U, Roth G. 2016. Neuronal factors determining high intelligence. Philos Trans R Soc B 371(1685):20150180.

Eberhard WG, Wcislo WT. 2011. Grade changes in brain-body allometry: morphological and

behavioural correlates of brain size in miniature spiders, insects and other invertebrates. In: Casas J, ed. Advances in Insect Physiology. Vol 40: Elsevier Limited. p 155-214.

Gronenberg W, Couvillon MJ. 2010. Brain composition and olfactory learning in honey bees. Neurobiol Learn Mem 93(3):435-443.

Groothuis J, Smid HM. 2017. *Nasonia* parasitic wasps escape from Haller's rule by diphasic, partially isometric brain-body size scaling and selective neuropil adaptations. Brain Behav Evol 90(3):243-254.

Harvey PH, Krebs JR. 1990. Comparing brains. Science 249(4965):140-146.

Haverkamp A, Smid HM. 2014. Octopamine-like immunoreactive neurons in the brain and subesophageal ganglion of the parasitic wasps *Nasonia vitripennis* and *N. giraulti*. Cell Tissue Res 358(2):313-329.

Hoedjes KM, Kralemann LEM, van Vugt JJFA, Vet LEM, Smid HM. 2014a. Unravelling reward value: the effect of host value on memory retention in *Nasonia* parasitic wasps. Anim Behav 96:1-7.

Hoedjes KM, Smid HM, Vet LEM, Werren JH. 2014b. Introgression study reveals two quantitative trait loci involved in interspecific variation in memory retention among *Nasonia* wasp species. Heredity 113(6):542-550.

Holm S. 1979. A simple sequentially rejective multiple test procedure. Scand J Stat 6(2):65-70.

Isler K, Christopher Kirk E, Miller JM, Albrecht GA, Gelvin BR, Martin RD. 2008. Endocranial volumes of primate species: scaling analyses using a comprehensive and reliable data set. J Hum Evol 55(6):967-978.

Kotrschal A, Buechel SD, Zala SM, Corral-Lopez A, Penn DJ, Kolm N. 2015a. Brain size affects female but not male survival under predation threat. Ecol Lett 18(7):646-652.

Kotrschal A, Corral-Lopez A, Amcoff M, Kolm N. 2015b. A larger brain confers a benefit in a spatial mate search learning task in male guppies. Behav Ecol 26(2):527-532.

Kotrschal A, Corral-Lopez A, Zajitschek S, Immler S, Maklakov AA, Kolm N. 2015c. Positive genetic correlation between brain size and sexual traits in male guppies artificially selected for brain size. J Evol Biol 28(4):841-850.

Kotrschal A, Kolm N, Penn DJ. 2016. Selection for brain size impairs innate, but not adaptive immune responses. Proc R Soc B 283(1826):20152857.

Kotrschal A, Lievens EJP, Dahlbom J, Bundsen A, Semenova S, Sundvik M, Maklakov AA, Winberg S, Panula P, Kolm N. 2014. Artificial selection on relative brain size reveals a positive genetic correlation between brain size and proactive personality in the guppy. Evolution 68(4):1139-1149.

Kotrschal A, Rogell B, Bundsen A, Svensson B, Zajitschek S, Brannstrom I, Immler S, Maklakov AA, Kolm N. 2013. Artificial selection on relative brain size in the guppy reveals costs and benefits of evolving a larger brain. Curr Biol 23(2):168-171.

Kruidhof HM, Pashalidou FG, Fatouros NE, Figueroa IA, Vet LEM, Smid HM, Huigens ME. 2012. Reward value determines memory consolidation in parasitic wasps. PLoS One 7(8):e39615.

Lanet E, Maurange C. 2014. Building a brain under nutritional restriction: insights on sparing and plasticity from *Drosophila* studies. Front Physiol 5:117.

Lenth RV, Hervé M. 2014. lsmeans: least-squares means. Version R package version 2.11.

Mares S, Ash L, Gronenberg W. 2005. Brain allometry in bumblebee and honey bee workers. Brain Behav Evol 66(1):50-61.

Mery F, Kawecki TJ. 2005. A cost of long-term memory in *Drosophila*. Science 308(5725):1148-1148.

Pagel MD, Harvey PH. 1988. The taxon-level problem in the evolution of mammalian brain size

- facts and artifacts. Am Nat 132(3):344-359.

Parnas M, Lin AC, Huetteroth W, Miesenbock G. 2013. Odor discrimination in *Drosophila*: from neural population codes to behavior. Neuron 79(5):932-944.

Perry CJ, Barron AB. 2012. Neural mechanisms of reward in insects. Annu Rev Entomol.

Rensch B. 1948. Histological changes correlated with evolutionary changes of body size. Evolution 2(3):218-230.

Rensch B. 1956. Increase of learning capability with increase of brain-size. Am Nat 90(851):81-95.

Riveros AJ, Gronenberg W. 2010. Brain allometry and neural plasticity in the bumblebee *Bombus occidentalis*. Brain Behav Evol 75(2):138-148.

Schindelin J, Arganda-Carreras I, Frise E, Kaynig V, Longair M, Pietzsch T, Preibisch S, Rueden C, Saalfeld S, Schmid B, Tinevez JY, White DJ, Hartenstein V, Eliceiri K, Tomancak P, Cardona A. 2012. Fiji: an open-source platform for biological-image analysis. Nat Methods 9(7):676-682.

Seid MA, Castillo A, Wcislo WT. 2011. The allometry of brain miniaturization in ants. Brain Behav Evol 77(1):5-13.

Smid HM, Vet LEM. 2016. The complexity of learning, memory and neural processes in an evolutionary ecological context. Curr Opin Insect Sci 15:61-69.

Smid HM, Wang G, Bukovinszky T, Steidle JL, Bleeker MA, van Loon JJA, Vet LEM. 2007. Species-specific acquisition and consolidation of long-term memory in parasitic wasps. Proc R Soc B 274(1617):1539-1546.

Snell-Rood EC, Papaj DR, Gronenberg W. 2009. Brain size: a global or induced cost of learning? Brain Behav Evol 73(2):111-128.

Striedter GF. 2005. Principles of brain evolution. Sunderland, MA: Sinauer.

Strutz A, Soelter J, Baschwitz A, Farhan A, Grabe V, Rybak J, Knaden M, Schmuker M, Hansson BS, Sachse S. 2014. Decoding odor quality and intensity in the *Drosophila* brain. eLife 3.

Tsuboi M, Kotrschal A, Hayward A, Buechel SD, Zidar J, Lovlie H, Kolm N. 2016. Evolution of brain-body allometry in Lake Tanganyika cichlids. Evolution 70(7):1559-1568.

Van de Zande L, Ferber S, De Haan A, Beukeboom LW, Van Heerwaarden J, Pannebakker BA. 2014. Development of a *Nasonia vitripennis* outbred laboratory population for genetic analysis. Mol Ecol Res 14(3):578-587.

van der Woude E, Smid HM. 2016. How to escape from Haller's rule: olfactory system complexity in small and large *Trichogramma evanescens* parasitic wasps. J Comp Neurol 524(9):1876-1891.

Van der Woude E, Smid HM. 2017a. Differential effects of brain scaling on memory performance in parasitic wasps. In prep.

van der Woude E, Smid HM, Chittka L, Huigens ME. 2013. Breaking Haller's rule: brain-body size isometry in a minute parasitic wasp. Brain Behav Evol 81(2):86-92.

Wagh DA, Rasse TM, Asan E, Hofbauer A, Schwenkert I, Durrbeck H, Buchner S, Dabauvalle MC, Schmidt M, Olin G, Wichmann C, Kittel R, Sigrist SJ, Buchner E. 2006. Bruchpilot, a protein with homology to ELKS/CAST, is required for structural integrity and function of synaptic active zones in *Drosophila*. Neuron 49(6):833-844.

Wehner R, Fukushi T, Isler K. 2007. On being small: brain allometry in ants. Brain Behav Evol 69(3):220-228.

Whiting AR. 1967. The biology of the parasitic wasp *Mormoniella vitripennis* [=*Nasonia brevicornis*] (Walker). Q Rev Biol 42(3):333-406.

SUPPLEMENT

Supplementary Methods

Neuropil staining

Randomly selected female wasps were sedated on ice, after which they were decapitated in ice-cold phosphate buffered saline (PBS, Oxoid, Dulbecco 'A' tablets). The brains were removed using sharpened tweezers (Dumont #5, Sigma), placed in phosphate buffered (0.1M) 4% formaldehyde solution (pH 7.2) and fixed for 2.5 h at room temperature. After fixation, the brains were rinsed in PBS 6 times for 5 mins and treated with 5 mg/ml collagenase (Sigma) in PBS for 1 h at RT. Following rinsing in PBS containing 0.5% Triton-X-100 (PBS-T) 4 times for 5 mins, brains were incubated for 1 h in blocking buffer, PBS-T containing 10% normal goat serum (PBS-T-NGS, Dako, Glostrup, Denmark). Incubation in primary antibody, 1:250 nc82 (mouse-anti-Bruchpilot concentrate, NC82-c, Developmental Studies Hybridoma Bank, University of Iowa, Iowa City, IA; Cat. no. nc82, RRID:AB_528108) in PBS-T-NGS was overnight at RT, followed by 6 times 20 mins rinsing in PBS-T and 4 h incubation at RT in secondary antibody, 1:100 rabbit-anti-mouse (Dako) in PBS-T-NGS. After another 6 times 20 mins rinse in PBS-T the brains were incubated overnight at 4 °C in tertiary antibody, 1:200 Alexa Fluor® 488-conjugated goat-anti-rabbit (Invitrogen) and 1:250 propidium iodide (Sigma-Aldrich) in PBS-T-NGS. Subsequent steps were performed in the dark as much as possible. Brains were dehydrated through a series of increasing EtOH dilutions (30%, 50%, 70%, 80%, 90%, 96%, 2×100%), degreased via a 50/50 EtOH/xylene step, and kept in xylene until mounting. Brains were mounted in DPX (Sigma) between a glass microscope slide, fitted with two stacked strips of double-sided adhesive tape (Henzo, Roermond, The Netherland) as spacer, and a 18 mm x 18 mm #1 cover slip.

Whole mount Z-stacks were acquired using a Zeiss LSM 510 confocal microscope equipped with a Plan-Neofluar 25×/0.8 oil immersion objective. Alexa Fluor® 488 and PI were excited using the Ar-488 nm line and captured with 505-550 nm BP and 560 nm LP filters, respectively. Images were obtained at 512×512 px with a 0.7× digital zoom and a step size of 2 μm, resulting in a final voxel calibration of 1.018×1.018×2 μm. As the refractive indices of immersion and mounting medium match, no z-correction was required. Depending on the size and orientation of a scanned brain, 1 to 3 stacks were acquired and later

combined with the Stitching plugin (Preibisch et al., 2009) in FIJI (Schindelin et al., 2012). Due to the fragile nature of *Nasonia* brains (Haverkamp and Smid, 2014), we inspected the obtained stacks for integrity of all neuropils and selected 3 out of 12 brains of every line for analysis (resulting in 9 brains per treatment, and 27 brains for the entire experiment).

Neuropil segmentation was performed in Amira 5.4.2 (Visage Imaging). The nc82 channel was used to assign 11 unique labels to the neuropil in the Segmentation Editor, see Figure 3 in the main text. Each neuropil was manually labeled each 1-3 slices, after which the Interpolate option was used. Manual correction was performed to ensure correct labeling of each slice. Neuropil volumes were calculated by the MaterialStatistics module and saved as .csv file for collection and calculation of relative volume in an MS Excel spreadsheet. In one case, a brain turned out to have previously unnoticed damage to one of the calyces. For this brain, the duplicated volume of the undamaged calyx was used to calculate the total calyx volume. Relative neuropil volume was calculated as the percentage of the total neuropil volume.

Memory retention

Olfactory memory retention of the selection lines was tested in generation 33. We used single classical olfactory conditioning trials, as described before (Hoedjes and Smid, 2014; Van der Woude and Smid, 2017a). The wasps were 1 - 2 days old and kept on water and honey until use in the conditioning trials. Groups of approximately 60 wasps were distributed over a Petri dish (8.5 cm diameter). Here, the wasps obtained an oviposition experience (unconditioned stimulus, US) while experiencing an odor (conditioned stimulus, CS): the CS+ phase. The rewarding unconditioned stimulus consisted of 40 *C. vomitoria* pupae. The conditioned stimulus was 5 μl of either Royal Brand Bourbon Vanilla extract or Natural Chocolate extract (Nielsen-Massey Vanillas Intl., Leeuwarden, the Netherlands), pipetted on small squares of filter paper. The wasps were allowed to drill and oviposit inside the pupae for 1 hour, while experiencing the odor of the CS+. Wasps that were not drilling in the pupae were removed after 15 minutes. After 1 hour, the wasps were removed from the pupae with an aspirator and placed in a clean petri dish for a neutral resting phase of 15 minutes. Next, the wasps experienced 5 μl of the second of the two odors in absence of hosts: the CS- phase. This phase lasted for another 15 minutes. After this phase, the wasps were collected in clean vials and stored with water and honey until use in the memory retention tests.

The conditioning trials were performed in a reciprocal manner: one group of every line was conditioned using vanilla as CS+ and chocolate as CS-, another group was conditioned using chocolate as CS+ and vanilla as CS-. Four groups per replicate line were conditioned on chocolate and four groups per replicate line were conditioned on vanilla.

Memory retention was tested in the T-maze as described before (Hoedjes et al., 2014b). One side of the T-maze contained a glass capillary (ID 1.3 mm, Stuart SMP1/4, Bibby Scientific, Staffordshire, UK) filled with vanilla extract, and the other side contained chocolate extract. Charcoal filtered, moisturized air (60–70% relative humidity) flowed past the odor capillaries at 100 ml/min per side. Wasps were inserted in the T-maze in groups of approximately 15 wasps, resulting in 3 measurements per conditioned group. Memory of each wasp was tested 1, 3 and 5 days after the conditioning trials. After 5 minutes the number of wasps on the vanilla and chocolate side was recorded.

Statistical analyses

Response to selection was analyzed using a linear mixed model with the ratio between head width and body length as dependent variable. Selection regime (L or S), generation and the interaction between these two were used as fixed factors. Replicate number was used as a random factor. Deviance of model terms was analyzed using type II Wald χ^2 tests. Similar linear mixed models were used to test the selection's effect on body length and head width, using body length or head width as dependent variable respectively.

Ordinary linear regression on head width and body length was used to study if the difference in head-body size ratio between the selected lines within a generation is a side-effect of the brain scaling mechanism described by Haller's rule. Head width was used as dependent variable, and body length and selection regime (L, C or S) as fixed factors. Body lengths were mean-centered by subtraction of the average body length of all wasps in that generation. This ensured that differences in the intercept reflect differences in head-body ratio between the selected lines, as head width is compared at mean-centered body length (Egset et al., 2011; Tsuboi et al., 2016). If there are still differences in head-body ratio at mean-centered body length, these are not caused by allometric brain scaling resulting from the difference in body size between the lines. ANOVA comparisons were used to test for differences in slope and intercept between the lines. We used this method to analyze wasps separately for generation 26, 33 and 40.

We calculated realized heritability after 25 generations of selection. We used the ratio between the cumulative selection response and the cumulative selection differential, following the method for divergent selection described by Walsh & Lynch (Walsh and Lynch, 2009). The cumulative selection response was defined as the difference in mean head-body ratio between L and S in generation 26. The cumulative selection differential was defined as the cumulative difference in selection differentials (mean head-body ratio of the selected group subtracted from the mean of that whole population) between L and S of 25 generations. The value for realized heritability was duplicated to correct for selection on only females, instead of on both parents. Differences in neuropil volumes were analyzed in generation 33.

Neuropil volumes were compared with a linear mixed model. We used the absolute total neuropil volume or relative volume per neuropil as dependent variables, with selection regime as fixed factor and line as random factor. As we compared multiple relative neuropil volumes, we corrected the *p*-values for multiple comparisons with the Holm-Bonferroni method (*m = 11)* (Holm, 1979) in MS Excel. Neuropils with significant effects of selection regime on relative volume were further analyzed with χ2 pairwise comparisons to test for significant differences between the selection regimes.

Differences in memory retention abilities were analyzed in generation 33. Memory retention was expressed as a performance index (PI): the difference in preference between reciprocally trained groups. This PI is calculated by subtracting the fraction of wasps that chose the odor of their CS- from the fraction of wasps in the reciprocal group, which chose that same odor but received it as their CS+. Values of PIs were calculated from estimated response means that were obtained from generalized linear mixed models (GLMMs) with logit link function and binomial distribution. The dependent variable was the number of wasps that chose chocolate with the total number of wasps making a choice as denominator. Fixed effects included the odor of CS+, time after conditioning, selection line and the interactions between these effects. Random effects were included to correct for date of conditioning, selection line repeat and reciprocal conditioning pair. Presence of memory was tested with χ2 pairwise comparisons, which test for the effect of CS+ on the preference for the conditioned stimuli. Similar tests were used to analyze differences in memory retention between the different lines. Response rates of the memory retention tests were determined by a GLMM that used the fraction of wasps making a choice out of the total number of wasps inserted as dependent variable, and selection regime and time after conditioning as fixed factors. Differences in response rate between the lines

and times were determined with χ^2 pairwise comparisons.

Longevity was analyzed in generation 40. We used a two-way ANOVA that tested for the effect of selection regime, conditioning and the interaction between these terms using time till death as dependent variable. This was followed by TukeyHSD post-hoc tests to analyze differences in longevity between selected lines and to test for an effect of conditioning on longevity within selected lines.

Statistical analyses were performed in R version 3.1.0 in combination with packages lme4 (Bates et al., 2014), phia (De Rosario-Martinez, 2013), lsmeans (Lenth and Hervé, 2014).

Supplementary Results

Response to selection

Table S1. Measured head and body size parameters for wasps of selected lines. Average body length in μm (±SE), head width in μm (±SE) and ratio between head width and body length (±SE) per generation in the selected lines. Final column shows the difference in average head-body ratio between the L and S lines (L-S) in percentages. $N = 150$ for each cell except generation 0, in which $N = 300$.

Gen.	Body length			Head width			Head - body ratio			Difference ratio L-S (%)
	Small	Large	Control	Small	Large	Control	Small	Large	Control	
0	1967 ± 10.2	1967 ± 10.2		668 ± 3.3	668 ± 3.3		0.3403 ± 0.0011	0.3403 ± 0.0011		
1	2426 ± 7.5	2350 ± 11.0		773 ± 2.1	776 ± 3.1		0.3186 ± 0.0005	0.3306 ± 0.0008		3.75
2	2240 ± 10.1	2297 ± 12.2		740 ± 2.6	738 ± 3.4		0.3307 ± 0.0010	0.3215 ± 0.0007		-2.78
3	2230 ± 10.2	2280 ± 10.1		734 ± 3.5	756 ± 2.9		0.3295 ± 0.0007	0.3317 ± 0.0008		0.68
4	2315 ± 9.6	2323 ± 9.8		746 ± 2.7	748 ± 2.7		0.3225 ± 0.0006	0.3221 ± 0.0007		-0.14
5	2271 ± 10.9	2245 ± 10.3		725 ± 3.2	732 ± 3.0		0.3194 ± 0.0006	0.3262 ± 0.0006		2.15
6	2299 ± 14.6	2298 ± 12.3		734 ± 4.7	749 ± 3.6		0.3195 ± 0.0007	0.3262 ± 0.0010		2.1
7	2272 ± 11.3	2317 ± 11.1		726 ± 3.3	746 ± 3.2		0.3196 ± 0.0007	0.3223 ± 0.0009		0.84
8	2239 ± 12.6	2256 ± 10.7		729 ± 3.6	735 ± 3.2		0.3259 ± 0.0007	0.3260 ± 0.0009		0.04
9	2208 ± 7.8	2230 ± 8.8		719 ± 2.4	727 ± 2.7		0.3257 ± 0.0007	0.3262 ± 0.0008		0.16
10	2341 ± 8.4	2234 ± 13.6		741 ± 2.4	731 ± 3.9		0.3166 ± 0.0007	0.3276 ± 0.0007		3.47
11	2281 ± 9.0	2293 ± 10.0		725 ± 2.5	750 ± 2.7		0.3180 ± 0.0006	0.3276 ± 0.0006		2.99
12	2313 ± 12.9	2293 ± 12.0		724 ± 3.3	752 ± 3.4		0.3134 ± 0.0007	0.3284 ± 0.0006		4.79
13	2284 ± 11.8	2321 ± 9.2		725 ± 3.3	752 ± 2.4		0.3177 ± 0.0007	0.3242 ± 0.0011		2.06
14	2398 ± 6.9	2281 ± 10.8		751 ± 2.0	748 ± 2.9		0.3132 ± 0.0007	0.3282 ± 0.0006		4.78
15	2388 ± 7.7	2385 ± 8.4		747 ± 1.8	764 ± 2.1		0.3131 ± 0.0007	0.3209 ± 0.0009		2.47
16	2378 ± 10.1	2258 ± 10.6		737 ± 2.6	746 ± 3.0		0.3104 ± 0.0008	0.3307 ± 0.0006		6.54
17	2293 ± 11.4	2264 ± 9.2		727 ± 3.4	740 ± 2.9		0.3169 ± 0.0007	0.3268 ± 0.0006		3.12
18	2345 ± 10.9	2237 ± 9.7		736 ± 2.9	747 ± 2.9		0.3143 ± 0.0007	0.3340 ± 0.0008		6.26
19	2299 ± 10.2	2226 ± 14.5		721 ± 2.6	731 ± 4.2		0.3140 ± 0.0006	0.3286 ± 0.0006		4.65
20	2367 ± 8.7	2253 ± 10.3		737 ± 2.4	749 ± 2.6		0.3115 ± 0.0006	0.3324 ± 0.0009		6.74
21	2279 ± 9.5	2289 ± 10.4		719 ± 2.5	742 ± 2.9		0.3153 ± 0.0007	0.3244 ± 0.0007		2.88
22	2312 ± 8.6	2267 ± 9.9		724 ± 2.5	755 ± 2.9		0.3133 ± 0.0005	0.3334 ± 0.0006		6.42
23	2331 ± 10.8	2194 ± 14.3		727 ± 2.9	724 ± 4.3		0.3122 ± 0.0007	0.3301 ± 0.0006		5.75
24	2320 ± 11.0	2240 ± 14.9		722 ± 3.1	738 ± 4.6		0.3115 ± 0.0007	0.3298 ± 0.0008		5.9
25	2383 ± 8.2	2236 ± 12.5	2347 ± 9.1	743 ± 2.6	732 ± 3.8	753 ± 2.6	0.3118 ± 0.0006	0.3278 ± 0.0009	0.3208 ± 0.0006	5.14
26	2341 ± 10.2	2252 ± 10.6	2266 ± 13.3	728 ± 2.9	745 ± 3.1	725 ± 4.1	0.3114 ± 0.0007	0.3310 ± 0.0006	0.3202 ± 0.0008	6.3
27	2341 ± 12.0	2286 ± 10.4	2384 ± 9.7	733 ± 3.3	751 ± 3.2	763 ± 3.0	0.3134 ± 0.0007	0.3286 ± 0.0006	0.3199 ± 0.0006	4.86
28	2329 ± 9.2	2220 ± 12.6	2218 ± 11.2	718 ± 2.4	733 ± 4.0	719 ± 3.2	0.3085 ± 0.0006	0.3302 ± 0.0006	0.3245 ± 0.0006	7.02
30	2289 ± 12.7	2108 ± 16.2	2237 ± 11.6	709 ± 3.4	702 ± 4.8	718 ± 3.5	0.3100 ± 0.0007	0.3334 ± 0.0008	0.3209 ± 0.0006	7.55
33	2293 ± 8.3	2200 ± 11.7	2251 ± 10.3	720 ± 2.5	737 ± 3.3	731 ± 2.9	0.3142 ± 0.0007	0.3352 ± 0.0007	0.3251 ± 0.0007	6.67
40	2244 ± 13.1	2172 ± 13.8	2238 ± 10.0	713 ± 4.0	732 ± 4.3	739 ± 3.1	0.3180 ± 0.0009	0.3371 ± 0.0008	0.3305 ± 0.0009	6.03

Deviation from Haller's rule

Statistical analysis was performed on mean-centered body lengths (subtraction of mean body length of whole generation), whereas Figure S1 shows uncorrected body lengths and head widths. Using mean-centered body lengths for analysis ensured that differences in head-body ratio between the selected lines are reflected by differences in the intercept.

Regression with mean-centered body length in generation 26: significant differences in intercept ($F_{2,444} = 48.523$, $p < 0.001$), but not in slope ($F_{2,444} = 2.844$, $p = 0.059$). $R^2 = 0.805$.

Large: HW = 0.273 × sBL + 757.123
Small: HW = 0.238 × sBL + 717.817
Control: HW = 0.273 × sBL + 733.394

Regression with mean-centered body length in generation 33: significant differences in intercept ($F_{2,444} = 36.466$, $p < 0.001$), but not in slope ($F_{2,444} = 0.670$, $p = 0.512$). $R^2 = 0.784$.

Large: HW = 0.260 × sBL + 749.048
Small: HW = 0.244 × sBL + 709.134
Control: HW = 0.245 × sBL + 730.396

Regression with mean-centered body length in generation 40: significant differences in intercept ($F_{2,444} = 60.432$, $p < 0.001$), but not in slope ($F_{2,444} = 2.042$, $p = 0.131$). $R^2 = 0.809$.

Large: HW = 0.292 × sBL + 745.181
Small: HW = 0.271 × sBL + 705.932
Control: HW = 0.258 × sBL + 734.108
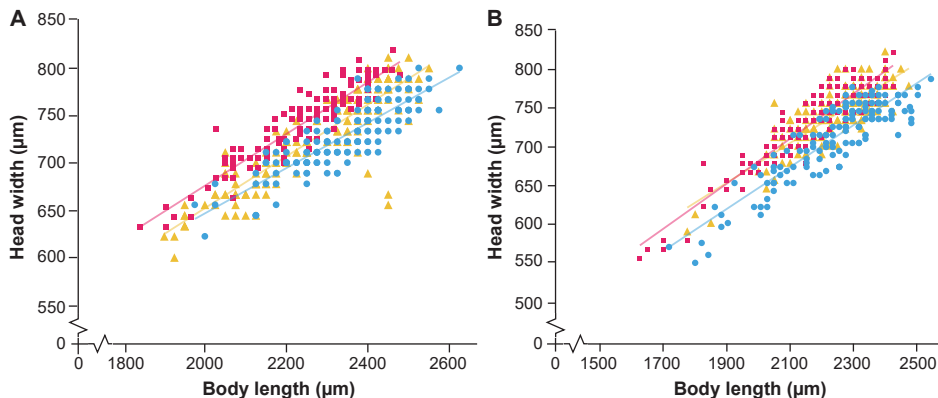
**Figure S1.** Head width and body length of wasps selected for relatively large (magenta squares) and small (blue circles) head-body ratio, and unselected control lines (yellow triangles). Measurements are shown for generation 26 (**A**) and generation 40 (**B**). Regression analysis was performed on mean-centered body lengths, because differences in head-body ratio can then be revealed by differences in the intercepts.

Brain morphology data

Table S2. Relative and absolute volumetric data on several neuropil regions in Small (S), Large (L), and Control (C) lines of selected *Nasonia vitripennis* wasps. Descriptives for all measurements are reported with $N = 9$ per selection regime.

	Line	Relative volume [1]		Absolute volume [2]	
		Statistics	Mean (%) ± SE	Statistics	Mean (μm^3) ± SE
Total neuropil	S		100		a $9.27\times10^5 \pm 2.80\times10^5$
	L	N.S.	100	$\chi^2_2 = 8.0793$ $p = 0.0176$	b $1.07\times10^7 \pm 4.60\times10^5$
	C		100		b $1.07\times10^7 \pm 2.46\times10^5$
Lobula (Optic Lobe)	S		8.55 ± 0.231		$7.97\times10^5 \pm 4.35\times10^4$
	L	N.S.	8.79 ± 0.285		$9.47\times10^5 \pm 5.41\times10^4$
	C		8.59 ± 0.214		$9.23\times10^5 \pm 4.27\times10^4$
Medulla (Optic Lobe)	S		18.37 ± 0.411		$1.71\times10^6 \pm 8.57\times10^4$
	L	N.S.	18.68 ± 0.263		$2.01\times10^6 \pm 9.49\times10^4$
	C		18.5 ± 0.346		$1.99\times10^6 \pm 8.29\times10^4$
Antennal Lobe	S	$\chi^2_2 = 19.237$ $p = 0.0007$	a 11.27 ± 0.205		$1.04\times10^6 \pm 2.18\times10^4$
	L		b 12.08 ± 0.161		$1.30\times10^6 \pm 6.49\times10^4$
	C		a 11.29 ± 0.082		$1.21\times10^6 \pm 2.48\times10^4$
Lateral Horn	S		2.53 ± 0.092		$2.35\times10^5 \pm 1.17\times10^4$
	L	N.S.	2.66 ± 0.067		$2.86\times10^5 \pm 1.50\times10^4$
	C		2.76 ± 0.128		$2.94\times10^5 \pm 1.44\times10^4$
Calyx (Mushroom Body)	S		4.9 ± 0.105		$4.53\times10^5 \pm 1.35\times10^4$
	L	N.S.	4.78 ± 0.121		$5.12\times10^5 \pm 2.10\times10^4$
	C		5.04 ± 0.118		$5.37\times10^5 \pm 1.12\times10^4$
Lobes & Pedunculus (Mushroom Body)	S		7.13 ± 0.18		$6.59\times10^5 \pm 2.12\times10^4$
	L	N.S.	6.98 ± 0.231		$7.49\times10^5 \pm 3.64\times10^4$
	C		7.45 ± 0.212		$7.95\times10^5 \pm 1.97\times10^4$
Fan-shaped Body (Central Complex)	S		1.02 ± 0.043		$9.35\times10^4 \pm 3.06\times10^3$
	L	N.S.	0.92 ± 0.031		$9.94\times10^4 \pm 6.60\times10^3$
	C		0.99 ± 0.054		$1.06\times10^5 \pm 4.70\times10^3$
Ellipsoid Body (Central Complex)	S		0.16 ± 0.01		$1.48\times10^4 \pm 7.78\times10^2$
	L	N.S.	0.15 ± 0.011		$1.67\times10^4 \pm 1.57\times10^3$
	C		0.16 ± 0.009		$1.70\times10^4 \pm 7.46\times10^2$
Noduli (Central Complex)	S		0.09 ± 0.005		$7.86\times10^3 \pm 4.34\times10^2$
	L	N.S.	0.08 ± 0.005		$8.67\times10^3 \pm 6.33\times10^2$
	C		0.08 ± 0.006		$8.37\times10^3 \pm 5.61\times10^2$
Protocerebral Bridge (Central Complex)	S		0.24 ± 0.017		$2.27\times10^4 \pm 1.87\times10^3$
	L	N.S.	0.23 ± 0.013		$2.48\times10^4 \pm 1.74\times10^3$
	C		0.26 ± 0.021		$2.77\times10^4 \pm 2.15\times10^3$
Rest of neuropil	S		45.73 ± 0.376		$4.23\times10^6 \pm 1.08\times10^5$
	L	N.S.	44.65 ± 0.446		$4.79\times10^6 \pm 1.97\times10^5$
	C		44.87 ± 0.319		$4.80\times10^6 \pm 9.06\times10^4$

[1]) Relative neuropil volumes were analyzed with linear mixed model in R, followed by Holm-Bonferroni correction for multiple comparisons $m = 11$ (LO,ME,AL,LH,MB-V,CA,FB,EB,NO,PB,RoN). A post-hoc comparison (using the phia package) showed that the L line was different from S & C, with no difference between those. S↔L $p = 0.00012$, C↔L $p = 0.000179$, S↔C N.S. $p = 0.9188$.

[2]) Absolute neuropil volumes were only statistically analyzed for the total neuropil volume. Selection regime had a significant effect on total neuropil volume, $\chi^2_2 = 8.0793$, $p = 0.0176$. Post-hoc pairwise comparisons revealed that S was different from L&C, with no difference between those. S↔C $p = 0.016$, S↔L $p = 0.012$, C↔L N.S. $p = 0.929$.

Memory retention levels

One day after conditioning, wasps from the S lines showed a mean PI (± SE) of 18.37 ± 5.39%, L of 18.36 ± 5.01% and C of 7.62 ± 5.51%. This memory retention was significant in all lines (S: χ^2_1 = 28.878, p < 0.001; L: χ^2_1 = 34.082, p < 0.001; C: χ^2_1 = 5.096, p = 0.024). There was a significant difference in the level of memory retention between the selected and C lines 1 day after conditioning (S vs. C: χ^2_1 = 5.26, p = 0.022; L vs. C: χ^2_1 = 7.84, p = 0.005), but not between the S and L lines (χ^2_1 = 0.33, p = 0.567). Three days after conditioning, wasps from the S lines showed a PI of 12.73 ± 6.17%, L of 9.14 ± 6.03% and C of 5.14 ± 6.22%. This memory retention was significant in the S and L lines (S: χ^2_1 = 13.935, p < 0.001; L: χ^2_1 = 7.429, p = 0.006), but not in C (χ^2_1 = 2.363, p = 0.124). There were no significant differences in the level of memory retention between the lines 3 days after conditioning (S vs. C: χ^2_1 = 2.57, p = 0.109; L vs. C: χ^2_1 = 0.82, p = 0.365; S vs. L: χ^2_1 = 0.46, p = 0.498). Five days after conditioning, S showed a PI of 4.10 ± 6.52%, L of 6.23 ± 6.40% and C of -1.09 ± 6.52%. None of this was significant memory retention (S: χ^2_1 = 1.20, p = 0.273; L: χ^2_1 = 2.783, p = 0.095; C: χ^2_1 = 0.084, p = 0.772), and there were no differences in memory retention levels between the lines (S vs. C: χ^2_1 = 0.95, p = 0.329; L vs. C: χ^2_1 = 1.96, p = 0.161; S vs. L: χ^2_1 = 0.21, p = 0.649).

Response rate was defined as the percentage of wasps that made a choice, out of the total amount of wasps that were inserted into the T-maze. There was no difference in response rate between wasps of the different lines (χ^2_2 = 1.054, p = 0.591). Time after conditioning did affect response rate (χ^2_2 = 33.296, p < 0.001), with higher response rates longer after conditioning (day 1 – 3: χ^2_1 = 11.363, p < 0.001; day 3 – 5: χ^2_1 = 5.742, p = 0.017; day 1 – 5: χ^2_1 = 31.834, p < 0.001). The average response rate (±SE) was 72.53 ± 0.24 % on day 1, 77.79 ± 0.19 % on day 3 and 81.21 ± 0.27 % on day 5. There was no significant effect of the interaction between the lines and time after conditioning (χ^2_4 = 1.302, p = 0.861) on response rate.

Memory comparison with HVRx and AsymCx strains

We performed additional controls to compare memory performance of our selection and control lines to memory performance of the HVRx starting population and the AsymCx strain that we used in our previous study (Van der Woude and Smid, 2017a). We therefore analyzed memory retention of 2470 HVRx and 2179 AsymCx wasps following the same methodology as for our selection and control lines (Figure S2). There was significant memory retention

(GLMM: conditioning $\chi^2_1 = 157.37$, $p < 0.001$), and this retention decreased over time (GLMM: conditioning*time $\chi^2_2 = 32.59$, $p < 0.001$). There was an overall difference in memory retention between the different lines (GLMM: conditioning*line $\chi^2_4 = 67.64$, $p < 0.001$). Memory retention did not differ between S and L ($\chi^2_1 = 0.090$, $p = 0.767$), nor between C and HVRx. ($\chi^2_1 = 0.840$, $p = 0.359$). All other pairwise comparisons did yield significant differences (AsymCx – L: $\chi^2_1 = 18.46$, $p < 0.001$; AsymCx – C: $\chi^2_1 = 61.04$, $p < 0.001$; AsymCx – S: $\chi^2_1 = 44.81$, $p < 0.001$; AsymCx – HVRx: $\chi^2_1 = 22.23$, $p < 0.001$; L – C: $\chi^2_1 = 11.88$, $p < 0.001$; L – HVRx: $\chi^2_1 = 5.97$, $p = 0.015$; C – S: $\chi^2_1 = 10.64$, $p = 0.001$; HVRx – S: $\chi^2_1 = 4.95$, $p = 0.026$). Memory was maintained up to 3 days after conditioning in HVRx, and up to 5 days in AsymCx.
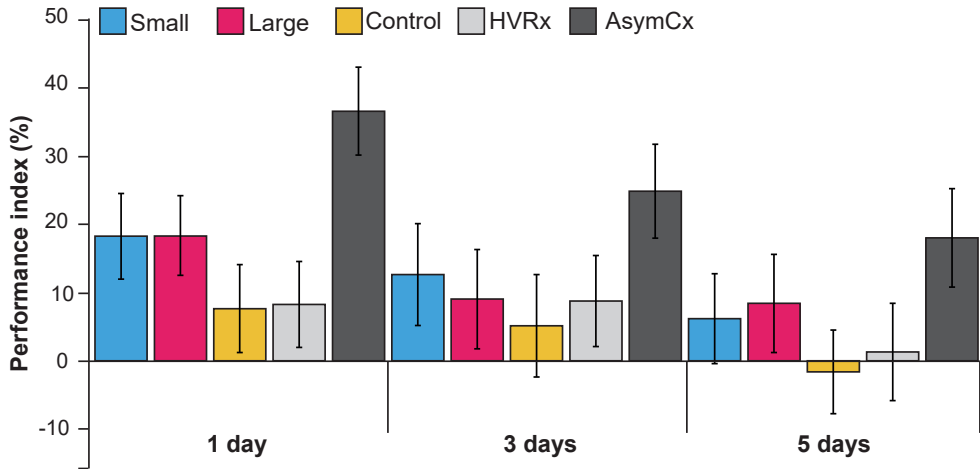
Figure S2. Memory retention over time for selection and control lines, and additional controls with the HVRx starting population and isogenic AsymCx line. Performance index (mean ± SE) shows difference in percentage of preference between reciprocally trained groups.

Longevity

Within the wasps that received a conditioning trial, mean longevity (± SE) was 10.11 ± 0.38 days in S, 6.28 ± 0.13 days in L and 9.17 ± 0.37 days in C. Within naive wasps, mean longevity was 10.98 ± 0.32 days in S, 9.32 ± 0.22 days in L and 12.17 ± 0.42 days in C.

**Table S3.** All TukeyHSD comparisons of longevity in naive and conditioned wasps of the three lines. These values were used for Figure 7A.

|		Naive			Conditioned		
		Small	Large	Control	Small	Large	Control
Naive	Small	-	-	-	-	-	-
	Large	$p = 0.004$	-	-	-	-	-
	Control	$p = 0.097$	$p < 0.001$	-	-	-	-
Conditioned	Small	$p = 0.404$	$p = 0.513$	$p < 0.001$	-	-	-
	Large	$p < 0.001$	$p < 0.001$	$p < 0.001$	$p < 0.001$	-	-
	Control	$p = 0.001$	$p = 0.999$	$p < 0.001$	$p = 0.304$	$p < 0.001$	-

Supplementary References

Bates D, Maechler M, Bolker B, Walker S. 2014. lme4: Linear mixed-effects models using Eigen and S4. Version R package version 1.1-7.

De Rosario-Martinez H. 2013. Phia: post-hoc interaction analysis. Version R package version 0.1-3.

Egset CK, Bolstad GH, Rosenqvist G, Endler JA, Pelabon C. 2011. Geographical variation in allometry in the guppy (*Poecilia reticulata*). J Evol Biol 24(12):2631-2638.

Haverkamp A, Smid HM. 2014. Octopamine-like immunoreactive neurons in the brain and subesophageal ganglion of the parasitic wasps *Nasonia vitripennis* and *N. giraulti*. Cell Tissue Res 358(2):313-329.

Hoedjes KM, Smid HM. 2014. Natural variation in long-term memory formation among *Nasonia* parasitic wasp species. Behav Processes 105:40-45.

Hoedjes KM, Smid HM, Vet LEM, Werren JH. 2014b. Introgression study reveals two quantitative trait loci involved in interspecific variation in memory retention among *Nasonia* wasp species. Heredity 113(6):542-550.

Holm S. 1979. A simple sequentially rejective multiple test procedure. Scand J Stat 6(2):65-70.

Lenth RV, Hervé M. 2014. lsmeans: least-squares means. Version R package version 2.11.

Preibisch S, Saalfeld S, Tomancak P. 2009. Globally optimal stitching of tiled 3D microscopic image acquisitions. Bioinformatics 25(11):1463-1465.

Schindelin J, Arganda-Carreras I, Frise E, Kaynig V, Longair M, Pietzsch T, Preibisch S, Rueden C, Saalfeld S, Schmid B, Tinevez JY, White DJ, Hartenstein V, Eliceiri K, Tomancak P, Cardona A. 2012. Fiji: an open-source platform for biological-image analysis. Nat Methods 9(7):676-682.

Tsuboi M, Kotrschal A, Hayward A, Buechel SD, Zidar J, Lovlie H, Kolm N. 2016. Evolution of brain-body allometry in Lake Tanganyika cichlids. Evolution 70(7):1559-1568.

Van der Woude E, Smid HM. 2017a. Differential effects of brain scaling on memory performance in parasitic wasps. In prep.

Walsh B, Lynch M. 2009. Least squares analysis of short-term selection experiments. Evolution and Selection of Quantitative Traits: In press. p 241.

5
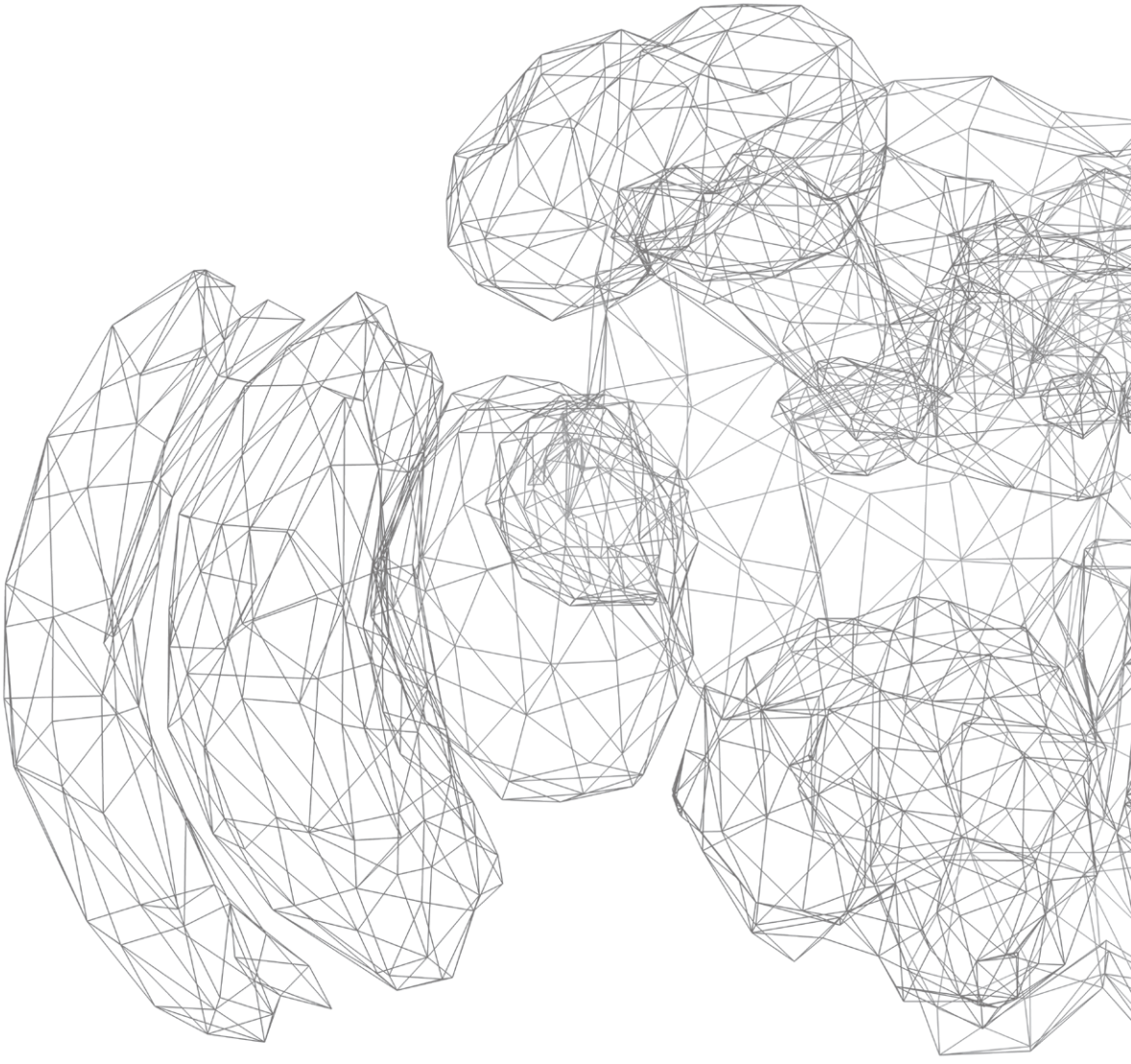
Chapter 6

General discussion
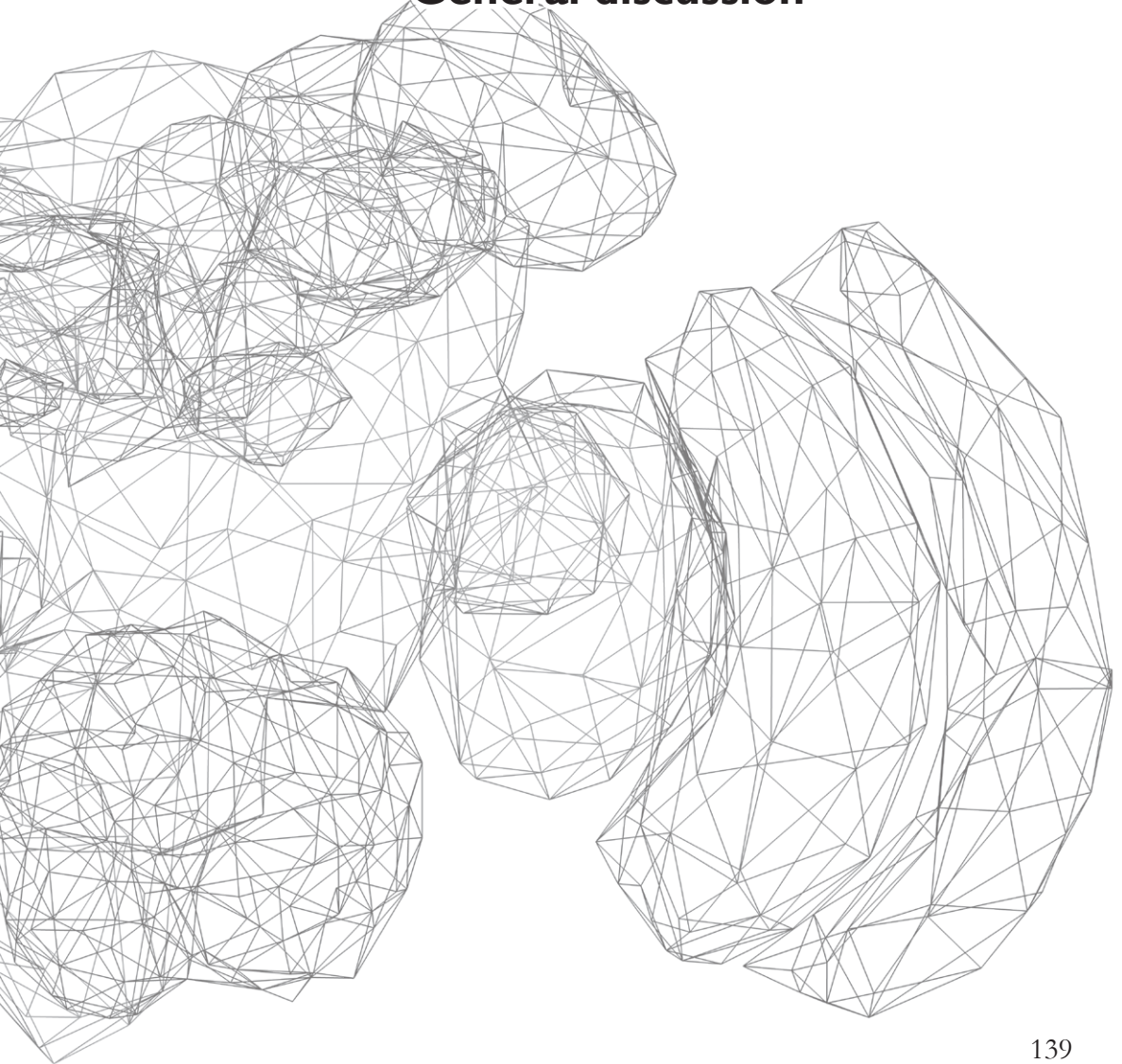
Introduction

Isometric brain scaling was first observed in the tiny egg parasitoid *Trichogramma evanescens* (van der Woude et al., 2013). The brain of this parasitic wasp has the same relative size over a body size range varying seven-fold. As Haller's rule (Rensch, 1948) predicts allometric scaling (relatively larger brains at smaller body sizes), this novel finding raised many new questions:

Is isometric brain scaling unique for *T. evanescens*, unique to the Hymenoptera, or perhaps linked to the small body size of this species? What is the role of brain scaling in miniaturization of body size, and does this give clues towards the evolution of miniaturization? Are there specific adaptations or sacrifices in isometrically scaled brains?

The parasitoid *Nasonia vitripennis* is slightly larger than *T. evanescens*, but varies even more in body size, attaining over ten-fold variation in body weight (40-438 µg). Due to this variation, as well as its status as a hymenopteran model species, this parasitoid is well suited to address some of these questions. In this thesis I therefore focused on the neurobiology of *N. vitripennis* to address the following research topics:

- How does the brain of *N. vitripennis* scale over its large body size range, and does this influence the modular layout of its neuropils?
- Are there adaptations to the dopaminergic cells in brains of different sizes, and does this relate to cognition?
- Is relative brain size a trait that can be selected for, and what are the effects of such a selection?

As there were no descriptions of the *N. vitripennis* nervous system available, I first needed to address the following question:

- What is the general morphology of the *N. vitripennis* brain, and how does it compare to the brain of other insects?

In Chapter 2, which serves as a basis for answering my other research questions, I showed that the brain of *N. vitripennis* shares many similarities with other Hymenoptera. A comparison with other insect brains revealed several interesting insights into the interaction between animal ecology and neurobiology, which I will discuss in context of brain scaling below. In addition to addressing the main research question of this chapter, I was able to use the data obtained here to develop the Jewel Wasp Standard Brain (JWSB). The JWSB is a reference brain based on the iterative shape averaging of 10 individual female *N. vitripennis* wasps which can be used for the consolidation and

visualization of multidisciplinary data. I will discuss several promising uses of the JWSB in further detail below. This tool will greatly benefit future studies of *Nasonia* neurobiology and will be available for use at the Insect Brain Database (insectbraindb.org) and integrated in WaspAtlas (Davies and Tauber, 2015).

Having established a neurobiological foundation, I used the large variation in body size of *N. vitripennis* to address the intraspecific brain scaling of this parasitoid and compare it with that of *T. evanescens* (van der Woude et al., 2013) and of the ant *Atta colombica* (Seid et al., 2011), which also has a large body size range. In Chapter 3, I used a combination of bleaching and confocal laser scanning microscopy (a novel technique) to measure head capsule volume, a proxy for brain size, through which I obtained the surprising result that *N. vitripennis* shows diphasic scaling, i.e. two scaling modes. Though larger wasps showed allometric scaling (following Haller's rule), smaller wasps scaled their brains isometrically, like *T. evanescens*. This finding answers the question whether isometric brain scaling is unique in *T. evanescens*, and implies that intraspecific isometry might be a function of body size due to restricted energy availability, as was hypothesized by Van der Woude et al. (2013).

Combining volumetric data from Chapter 2 with new measurements of the smallest *N. vitripennis* brains, I then addressed the questions of whether such extreme variation in brain and body size is accompanied by specific adaptations in the modular layout of the brain neuropils (Chapter 3) and the dopaminergic neurotransmitter system (Chapter 4). In both these cases I found large differences between *N. vitripennis* of different sizes, which provides novel insights into the link between the brain and behavioral ecology, especially considering the effect of size on the learning ability of these wasps (Van der Woude and Smid, 2017a). I will discuss the specific findings in the context of other insect species in a section below.

As the memory dynamics of *Nasonia giraulti*, a closely-related species, differ from *N. vitripennis* as well, I also compared the dopaminergic clusters of *N. vitripennis* with those of *N. giraulti* in Chapter 4. In contrast to a previous study that found no differences in the octopaminergic system (Haverkamp and Smid, 2014), I did find species-specific differences for dopaminergic clusters. Like in differently-sized *N. vitripennis*, these findings may be associated with behavioral differences between these two species.

Lastly, I sought to find out if relative brain size is a selectable trait in *N. vitripennis*. My results in Chapter 5, obtained using a genetically diverse strain, show that it is indeed possible to select for both small-brained and large-brained wasps.

As selective pressures can indeed shape the relative brain size, this may give clues towards how animals with different relative brain sizes, and perhaps miniaturization in general, evolve.

Below, I will discuss the results I obtained in relation to my research questions (and new questions brought up by them) in a larger context. My focus will be on three main topics:

- The relationship between 'relative brain size' and 'brain scaling'.
- Brain scaling in extreme size ranges, and what this says about the link between brain and behavior in general.
- What the finding of isometric scaling in both *T. evanescens* and *N. vitripennis* means for Haller's rule.

Finally, I discuss how the Jewel Wasp Standard Brain that I developed opens several promising new avenues for neurobiological research in *Nasonia* parasitoids.

Relative brain size versus brain scaling

Although the terms 'relative brain size' and 'brain scaling' seem redundant (does one not follow from the other?), let us explore it in further detail. With '*relative brain size*' I mean the relative size of the brain to the body, or the average for a group (or strain, or species) of animals. With '*brain scaling*' I refer to (relative or absolute) brain size as a function of body size, which relates to developmental plasticity. So, 'relative brain size' is a data point, or an average of data points; whereas 'brain scaling' is the relation between such points, which can be described by the coefficients in the power law of scaling:

$$[\text{Brain size}] = a \times [\text{Body size}]^b$$

or

$$\text{Log}([\text{Brain size}]) = \text{Log}(a) + b \times \text{Log}([\text{Body size}])$$

A difference in relative brain size may follow from actual changes in brain scaling, but may just as well stem from a simple difference in body size range. Take, for example, a comparison between two members from a fictional species that, like most species, follows Haller's rule. With an increase in body size range, the larger individual will have a smaller relative brain. Both follow the same brain scaling rule, with different relative brain sizes as a result. If we would compare individuals from different species, we do not know if a difference in relative

brain size is because both follow the same rules, or, if this is not the case, to what extent these are divergent.

Note that even in the first example its conclusion could only be drawn if enough data is available on that fictional species to *know* its brain scaling rules. Although it has only been shown in one species of ants (Seid et al., 2011) and in *N. vitripennis* (Chapter 3), brain scaling rules may vary even within a species: scaling in multiple phases.

If one was to ask how 'relative brain size' and/or 'brain scaling' evolve, we now see that, to answer this question using interspecific comparisons, we need more data than just an average relative brain size per species. Although informative, we cannot draw conclusions about relative brain size (let alone brain scaling) in different species when data points are represented by a very few specimens, as was done in recent comparisons within the Hymenoptera (Seid et al., 2011; Polilov, 2015; Polilov, 2016). While some species show little variation in body size, other species may have a large body size range. Using low numbers or averages of relative brain size effectively ignores the intricacies that may be present within a single species, such as the aforementioned diphasic scaling.

Using artificial selection in an outbred *N. vitripennis* population, I tried to answer part of this question in Chapter 5. Here I showed that it is possible to select for relative brain size, which suggests that it is possible for this trait to evolve. The selection regime affected both the average brain size and body size over 25 generations, but I needed to look at individuals within a generation to know its actual effect on brain scaling. At first glance, the results indicate that the observed differences in relative brain size are due to a *grade shift*, a similar scaling relationship (slope) but at a different offset. How, and, if the full potential for brain scaling over the entire size range (as seen in Chapter 3) is affected in the resulting lines will be an exciting follow-up opportunity.

As brain tissue has been thought to be energetically costly (Aiello and Wheeler, 1995), does this imply that brain size is a limiting force in the developmental plasticity of the *N. vitripennis* brain? Are these selection lines more, or less, limited in their body size range? Lines with relatively large brains, for example, would have costlier brains and may therefore not be able to develop into very small-sized adults as I observed in Chapter 3. Large-brained lines may thus have a smaller size range. One alternative could be that the diphasic brain scaling of *N. vitripennis* allows large-brained lines to change their scaling coefficient to an extent that would negate their relatively larger brains at a smaller body size—and the costs associated with these—allowing these lines to use the entire size range

that I observed for *N. vitripennis* previously. Another alternative is that the switch between isometric and allometric scaling is shifted to another breaking point in the selection lines, which may also affect their body size range.

Are large- or small-brained lines further affected at body sizes smaller than those studied in Chapter 5? Would the effects on longevity that I observed similar, or perhaps enhanced in small-sized large-brained wasps? Small *N. vitripennis* have shorter longevity in general (unpublished observations), so I expect that the increased costs for large-brained wasps would result in an even shorter longevity.

A parallel study to Chapter 3 revealed a decrease in memory retention in *N. vitripennis* of smaller body size (Van der Woude and Smid, 2017a). Although I saw no apparent gains for being large-brained, could these lines benefit from their larger brain by enhanced cognitive abilities at smaller body sizes? The smallest *N. vitripennis* studied in Chapter 3 showed significant changes in the modular makeup of their brain; for wasps from the large-brained selection lines, these modular changes may be less severe.

Although these questions were out of the scope of my original chapter, they might prove interesting entry points for follow-up studies. The (as of yet unpublished) development of an isofemale line panel from the outbred HVRx line (Van de Zande et al., 2014), in particular, may provide an excellent opportunity to zoom in on the genetic basis of brain scaling in insects. A similar approach in *Drosophila*, using the Drosophila Genetics Reference Panel, yielded interesting results about the genes involved with mushroom body development (Zwarts et al., 2015). Moreover, it may also provide clues to a genetic basis for the large potential variation in body size in *Nasonia* and the effect of this variation on the extreme adaptation in brain mosaicism.

Extreme brain adaptation and its relation with neuroethology

In this thesis I have discussed the link between the relative volume of specific neuropils and behavior several times. Some striking examples are the link between optic lobe volume (and optic/antennal lobe ratio) in ants in relation to their visual ecology (Gronenberg and Hölldobler, 1999), and differences in cue preferences for moths that differ in the volumes of their optic and antennal lobes (Stöckl et al., 2016).

Within species, differences in neuropil volumes are often studied (a) in relation to caste or caste-related behavioral differences, such as between worker and

queen paper wasps (O'Donnell et al., 2014), or minor and major workers in ants (Muscedere and Traniello, 2012); or (b) as a function of plasticity during adult life, such as the decline in optic lobe volume in ant queens after mating (presumable due to a lower need for visual cues) (Julian and Gronenberg, 2002), or changes in mushroom body volume as a result of sociality (Seid and Junge, 2016) or colony growth and task specialization (Amador-Vargas et al., 2015).

Of particular interest is the finding that variation in relative neuropil volume within a species can predict behavior (Snell-Rood et al., 2009). This, to my knowledge, showed for the first time that it is possible to not reason back from ethology to the brain, but use differences in the brain to predict differences in ethology.

Summarizing, the relative size of neuropils is related to the ecological importance of its function. On this knowledge I based the assumption that *developmental plasticity* of a neuropil also reflects this importance. Neuropils that grow to a smaller relative volume under restricting circumstances are expected to be less important than neuropils that are not as variable or that show larger relative volumes. This seems to be confirmed by what I found in Chapter 3. Increased scramble competition of the developing larvae caused extreme brain-body size scaling (made even more extreme by the isometric scaling at the lower end of their size range). The smallest N. vitripennis wasps resulting from this scramble competition had a changed modular layout of their brain when compared to larger, normal-sized wasps. One of the most obvious changes was the lower relative volume of the optic lobes (which are already small in normal-sized individuals, compared to several other flying Hymenoptera). Experiments in 1939 had already shown that N. vitripennis females do not need visual cues for host finding (Jacobi, 1939), arguably the most important behavior for this parasitic wasp. It stands to reason that, if visual information is not crucial for this behavior and the optic lobe is scaled down under pressure, these matters are related.

One might ask why the optic lobes are not smaller in normal-sized individuals, if vision is so seemingly unimportant. In Chapter 3 I observed that the anterior optic tubercle (a secondary visual neuropil) maintains its relative volume at small body size. Although knowledge on this neuropil is not complete, it is clear that the anterior optic tubercle is involved in chromatic discrimination (Mota et al., 2013), processing of light polarization (Pfeiffer et al., 2005; Homberg et al., 2011), and it is, through those functions, relevant for the sky compass (e.g. el Jundi et al. (2014); Held et al. (2016)). Different aspects of vision are therefore

likely to be important for *N. vitripennis*, and uncovering these in future research may be of great aid to the "sky compass"-field, particularly due to the additional tools that the *Nasonia* model system provides.

These insights in brain adaptations—different neuropil scaling for different brain sizes—may provide new ways to assess the behavior of insects. If one were to try to train an insect to perform a task, one would need to know the best cues to do so (e.g. vision or olfaction). If size variation is present (or inducible) in that insect, developmental plasticity of its neuropils would provide clues towards the right cue to use (or confounding cues to avoid) in the training.

Furthermore, a study of neuropil scaling in the *N. vitripennis* isofemale panel mentioned above, linked to behavioral data of these lines, could provide answers to the question "what makes a good parasitic wasp for biocontrol?". If behavioral studies would show that learning ability is an important trait for biological control, or if wasps would need to be trained before release, researchers could take lines with relatively large mushroom bodies to start as an initial selection of biocontrol candidates.

Care must be taken to properly control and analyze differences in relative neuropil volumes. Certain types of mosaicism (Montgomery et al., 2016) may cause other neuropils to scale in similar ways as a neuropil of interest. It could be, for example, that the smaller calyx observed in Chapter 3 is solely due to less visual input from the optic lobes, because those were smaller too.
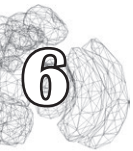
Other factors besides adaptations in neuropil volume play a role when parasitoids are faced with extreme variation in body and brain size. The neuropil, after all, is the place in the insect brain where synapses are formed; its volume therefore reflects connectivity between cells. A smaller neuropil volume may mean fewer connections, but also that there are fewer or smaller cells to make connections. In Chapter 4, I showed that specific clusters of dopaminergic cells did indeed contain fewer cells in smaller brains. Interestingly, size variation in the even smaller *T. evanescens* did not cause variation in cell number for dopaminergic clusters, nor for octopaminergic and serotonergic cells, but did lead to a smaller cell body size in small individuals for several of these clusters (van der Woude and Smid, 2017b).

What underlies this difference in "cluster scaling" between *T. evanescens* and *N. vitripennis*? *T. evanescens* may have reached the limits of miniaturization already at its larger body sizes. The number of cells present in its bioaminergic clusters is already very low, with numbers of 2-4 cells per cluster for dopaminergic

cells. A decrease in cell number may therefore constitute a (too great a) loss of function, leaving only a decrease in cell size as a possibility to accommodate the smaller available volume and increase in energetic constraints. The larger *N. vitripennis* does not reach these constraints at smaller body sizes and has larger dopaminergic clusters (i.e. clusters containing more cells), so this species copes by developing a smaller brain by having fewer cells in specific clusters (and other structural changes discussed above).

How unique is isometric brain scaling?

As mentioned above, interspecific comparisons of miniaturized insects imply that the negative brain-body size allometry described by Haller's rule still applies to even the tiniest of insects (Polilov, 2016). However, our recent intraspecific findings on isometric brain scaling in *T. evanescens* (van der Woude et al., 2013) and, here, *N. vitripennis* (Chapter 3) cast doubt on Haller's rule being true at small body sizes. For animals of larger size, allometry is typically stronger in intra- than in interspecific comparisons: intraspecific allometric coefficient (slope) values are lower than those found for interspecific relationships (Pagel and Harvey, 1988). So, if this is true for small insects as well, the interspecific studies on miniaturized insects should find isometry, and studies in *T. evanescens* and *N. vitripennis* should have found allometry. How, then, to explain the finding of isometry in *T. evanescens* and my observation of isometric brain scaling in *N. vitripennis*, a species that, even at its smallest, is larger than *T. evanescens* wasps?

T. evanescens and *N. vitripennis* may be the only small insects that have been thoroughly studied (assuming no negative results are left unreported due to publication bias): the smallest beetles (Makarova and Polilov, 2013a), Hymenoptera (Makarova and Polilov, 2013b), barklice (Makarova and Polilov, 2017a), and thrips (Makarova and Polilov, 2017b) have only been studied in interspecific studies and in too low numbers for an intraspecific comparison. These low numbers may also have confounded the measurement of an average relative brain size for the studied species. Other small Hymenoptera such as ants have also been part of interspecific comparisons (Wehner et al., 2007; Seid et al., 2011), but these studies may suffer from an additional problem: small ants may lack, due to their monomorphic nature, the variation in body size required to assess brain-body size scaling in their respective species.

At the small end of the ant size spectrum (for questions regarding miniaturization the most interesting group of ants), small *Brachymyrmex* spp. may measure only

39 to 49 µg in body weight (Seid et al., 2011), the same order of magnitude as the smallest *N. vitripennis*. Though knowledge on *Brachymyrmex* brain scaling would be extremely valuable to this field, a mere 20% of variation in body size may not be enough to reveal patterns in the brain-body size relationship (considering the seven- and tenfold variation in body size for *T. evanescens* and *N. vitripennis*, respectively).

Yet, large variation in body size is present in many other genera. Parasitoid species are ideal candidates for future studies, as the amount of food available for developing larvae is easily restricted by the choice of hosts used for rearing. In the case of gregariously developing animals, such as *Nasonia*, levels of scramble competition can be used to influence the size of adults. In the supplement of Chapter 3 I have already shown that this is possible for species and strains other than the *N. vitripennis* AsymCx strain (for *N. giraulti* and the outbred HVRx *N. vitripennis* strain). Many of these species, Trichogrammatidae and other small Chalcidae in particular, are readily reared (some are available as biocontrol agents) and obtained in similar size ranges as discussed above.

The question should therefore not be "how unique is isometric brain scaling?" but "when will we start looking for it properly?".
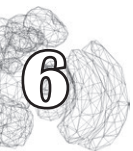
The future of *Nasonia* neurobiology

In addition to novel insights on brain scaling and adaptation in small insects, a major contribution put forth in this thesis is the development of the Jewel Wasp Standard Brain in Chapter 2. Based on an average of ten female *N. vitripennis* brains, the JWSB will serve as a reference framework for future studies on *Nasonia* neurobiology, with potential expansions to the male brain and those of related *Nasonia* species.

The *Nasonia* system is poised to make large impacts in the field of insect neurobiology. Points in its favor are access to the known genome of three different *Nasonia* species (Werren et al., 2010; Rago et al., 2016), the ability to introgress traits by hybridization (e.g. Hoedjes et al. (2014b); Werren et al. (2016)), influence development by means of, for example, RNAi (e.g. Mukai and Goto (2016)), and the use of ecologically relevant rewards in the study of learning and memory (Hoedjes et al., 2011; Hoedjes et al., 2012). Now, with the introduction of the JWSB and the morphological description of its neuropils, the field can take off.

The functionality of the Jewel Wasp Standard Brain will only increase, as new methods are developed to drive or alter genes and gene expression in *Nasonia* wasps. With new transformation methods or the CRISPR-Cas9 system (Li et al., 2017), it will become possible to target and visualize (by expression of fluorescent markers) specific cell types. The next hurdle will be the finding of cell type-specific promotors to drive such systems, but with the availability of *Nasonia* genomes this hurdle does not have to be taken in a vacuum. Of particular interest would be the use of "Brainbow"-like fluorescence labeling techniques (reviewed by Lichtman et al. (2008)). Brainbow uses recombinases to randomly express a combination of fluorescent proteins in genetically targeted cells. The combination of fluorophores yields unique staining patterns for individual cells, which would enable the tracing of multiple cells for registering into the JWSB. A similar approach has already proved to be possible in *Drosophila* (Hadjieconomou et al., 2011; Hampel et al., 2011).

Although the difficulties in the development of these techniques are certainly non-trivial, *Nasonia* neurobiologists can profit from the wealth of information and expertise available from previous developments in other model systems (such as *Drosophila*).

In addition, the availability of the JWSB may breathe new life into classical neurobiological techniques such as electrophysiological recordings and the injection of anterograde or retrograde fluorescent tracer dyes, which will benefit greatly from the common reference provided by this standard brain.

One of the main benefits of using genetic or dye-injection techniques is that these methods do not rely on specific methodologies such as the use of immunohistochemistry, or simply the choice of fixative. This means that stainings of interest can always be accompanied by standardized morphological background immunofluorescence. This will greatly ease the registration of interesting results onto the JWSB.

The Jewel Wasp Standard Brain, in conclusion, will enable many exciting and promising new possibilities for neurobiological research.

Conclusion

In this thesis I have shown that *N. vitripennis* wasps break Haller's rule by diphasic brain-body size scaling over its extreme body size range. Though normal-sized wasps scale their brain allometrically, strong scramble competition during development makes the smallest *N. vitripennis* have an isometrically scaled brain.

Subsequently, I carried out analyses of the adaptations made in the complexity of the brains to allow such strong scaling. In these studies I found that, unlike the brain of the tiny *T. evanescens*, *N. vitripennis* brains show differences in the relative size of several neuropils, as well specific changes in the modulatory dopaminergic network. Both these kinds of differences seem to be associated with size-related behavioral changes. Additionally, I showed that relative brain size can be selected for, but that this is costly. Yet, there are no apparent gains for having relatively larger brains.

These findings may provide clues for new research on the neuroethology of parasitic wasps: the links between brain structure and their behavior and ecology. I predict that these findings and the development of the Jewel Wasp Standard Brain will greatly aid future research into fundamental and applied questions about the development of the insect nervous system.

References

Aiello LC, Wheeler P. 1995. The expensive-tissue hypothesis - the brain and the digestive-dystem in human and primate evolution. Curr Anthropol 36(2):199-221.

Amador-Vargas S, Gronenberg W, Wcislo WT, Mueller U. 2015. Specialization and group size: brain and behavioural correlates of colony size in ants lacking morphological castes. Proc R Soc B 282(1801).

Davies NJ, Tauber E. 2015. WaspAtlas: A *Nasonia vitripennis* gene database and analysis platform. Database 2015(1).

el Jundi B, Pfeiffer K, Heinze S, Homberg U. 2014. Integration of polarization and chromatic cues in the insect sky compass. J Comp Physiol A 200(6):575-589.

Gronenberg W, Hölldobler B. 1999. Morphologic representation of visual and antennal information in the ant brain. J Comp Neurol 412(2):229-240.

Hadjieconomou D, Rotkopf S, Alexandre C, Bell DM, Dickson BJ, Salecker I. 2011. Flybow: genetic multicolor cell labeling for neural circuit analysis in *Drosophila melanogaster*. Nat Methods 8(3):260-U111.

Hampel S, Chung P, McKellar CE, Hall D, Looger LL, Simpson JH. 2011. *Drosophila* Brainbow: a recombinase-based fluorescence labeling technique to subdivide neural expression patterns. Nat Methods 8(3):253-U102.

Haverkamp A, Smid HM. 2014. Octopamine-like immunoreactive neurons in the brain and subesophageal ganglion of the parasitic wasps *Nasonia vitripennis* and *N. giraulti*. Cell Tissue Res 358(2):313-329.

Held M, Berz A, Hensgen R, Muenz TS, Scholl C, Rossler W, Homberg U, Pfeiffer K. 2016. Microglomerular synaptic complexes in the sky-compass network of the honeybee connect parallel pathways from the anterior optic tubercle to the central complex. Front Behav Neurosci 10.

Hoedjes KM, Kruidhof HM, Huigens ME, Dicke M, Vet LEM, Smid HM. 2011. Natural variation in learning rate and memory dynamics in parasitoid wasps: opportunities for converging ecology and neuroscience. Proc R Soc B 278(1707):889-897.

Hoedjes KM, Smid HM, Vet LEM, Werren JH. 2014b. Introgression study reveals two quantitative trait loci involved in interspecific variation in memory retention among *Nasonia* wasp species. Heredity 113(6):542-550.

Hoedjes KM, Steidle JLM, Werren JH, Vet LEM, Smid HM. 2012. High-throughput olfactory conditioning and memory retention test show variation in *Nasonia* parasitic wasps. Genes Brain Behav 11(7):879-887.

Homberg U, Heinze S, Pfeiffer K, Kinoshita M, El Jundi B. 2011. Central neural coding of sky polarization in insects. Philos T R Soc B 366(1565):680-687.

Jacobi EF. 1939. Über Lebensweise, Auffinden des Wirtes und Regulierung der Individuenzahl von *Mormoniella vitripennis* Walker. Arch Neer Zool 3(2):139-282.

Julian GE, Gronenberg W. 2002. Reduction of brain volume correlates with behavioral changes in queen ants. Brain Behav Evol 60(3):152-164.

Li M, Au LYC, Douglah D, Chong A, White BJ, Ferree PM, Akbari OS. 2017. Generation of heritable germline mutations in the jewel wasp *Nasonia vitripennis* using CRISPR/Cas9. Sci Rep 7(1):901.

Lichtman JW, Livet J, Sanes JR. 2008. A technicolour approach to the connectome. Nat Rev Neurosci 9(6):417-422.

Makarova AA, Polilov AA. 2013a. Peculiarities of the brain organization and fine structure in small insects related to miniaturization. 1. The smallest Coleoptera (Ptiliidae). Entomological review 93(6):703-713.

Makarova AA, Polilov AA. 2013b. Peculiarities of the brain organization and fine structure in small insects related to miniaturization. 2. The smallest Hymenoptera (Mymaridae, Trichogrammatidae). Entomological review 93(6):714-724.

Makarova AA, Polilov AA. 2017a. Peculiarities of the brain organization and fine structure in small insects related to miniaturization. 3. Barklice (Psocoptera, Liposcelididae). Entomological Review 97(3):288-301.

Makarova AA, Polilov AA. 2017b. Peculiarities of the brain organization and fine structure in small insects related to miniaturization. 4. Thrips (Thysanoptera, Thripidae). Entomological Review 97(3):302-309.

Montgomery SH, Mundy NI, Barton RA. 2016. Brain evolution and development: adaptation, allometry and constraint. Proc R Soc B 283(1838).

Mota T, Gronenberg W, Giurfa M, Sandoz JC. 2013. Chromatic processing in the anterior optic tubercle of the honey bee brain. J Neurosci 33(1):4-U411.

Mukai A, Goto SG. 2016. The clock gene period is essential for the photoperiodic response in the jewel wasp *Nasonia vitripennis* (Hymenoptera: Pteromalidae). Appl Entomol Zool 51(2):185-194.

Muscedere ML, Traniello JF. 2012. Division of labor in the hyperdiverse ant genus *Pheidole* is associated with distinct subcaste- and age-related patterns of worker brain organization. PLoS One 7(2):e31618.

O'Donnell S, Clifford MR, Bulova SJ, DeLeon S, Papa C, Zahedi N. 2014. A test of neuroecological predictions using paperwasp caste differences in brain structure (Hymenoptera: Vespidae). Behav Ecol Sociobiol 68(4):529-536.

Pagel MD, Harvey PH. 1988. The taxon-level problem in the evolution of mammalian brain size - facts and artifacts. Am Nat 132(3):344-359.

Pfeiffer K, Kinoshita M, Homberg U. 2005. Polarization-sensitive and light-sensitive neurons in two parallel pathways passing through the anterior optic tubercle in the locust brain. Journal of Neurophysiology 94(6):3903-3915.

Polilov AA. 2015. Consequences of miniaturization in insect morphology. Moscow University Biological Sciences Bulletin 70(3):136-142.

Pollilov AA. 2016. At the size limit: Effects of miniaturization in insects: Springer.

Rago A, Gilbert DG, Choi JH, Sackton TB, Wang X, Kelkar YD, Werren JH, Colbourne JK. 2016. OGS2: genome re-annotation of the jewel wasp Nasonia vitripennis. BMC Genomics 17:678.

Rensch B. 1948. Histological changes correlated with evolutionary changes of body size. Evolution 2(3):218-230.

Seid MA, Castillo A, Wcislo WT. 2011. The allometry of brain miniaturization in ants. Brain Behav Evol 77(1):5-13.

Seid MA, Junge E. 2016. Social isolation and brain development in the ant *Camponotus floridanus*. Sci Nat 103(5):1-6.

Snell-Rood EC, Papaj DR, Gronenberg W. 2009. Brain size: a global or induced cost of learning? Brain Behav Evol 73(2):111-128.

Stöckl A, Heinze S, Charalabidis A, el Jundi B, Warrant E, Kelber A. 2016. Differential investment in visual and olfactory brain areas reflects behavioural choices in hawk moths. Sci Rep 6:26041.

Van de Zande L, Ferber S, De Haan A, Beukeboom LW, Van Heerwaarden J, Pannebakker BA. 2014. Development of a *Nasonia vitripennis* outbred laboratory population for genetic analysis. Mol Ecol Res 14(3):578-587.

Van der Woude E, Smid HM. 2017a. Differential effects of brain scaling on memory performance in parasitic wasps. In prep.

van der Woude E, Smid HM. 2017b. Effects of isometric brain-body size scaling on the complexity of monoaminergic neurons in a minute parasitic wasp. Brain Behav Evol 89(3):185-194.

van der Woude E, Smid HM, Chittka L, Huigens ME. 2013. Breaking Haller's rule: brain-body size isometry in a minute parasitic wasp. Brain Behav Evol 81(2):86-92.

Wehner R, Fukushi T, Isler K. 2007. On being small: brain allometry in ants. Brain Behav Evol 69(3):220-228.

Werren JH, Cohen LB, Gadau J, Ponce R, Baudry E, Lynch JA. 2016. Dissection of the complex genetic basis of craniofacial anomalies using haploid genetics and interspecies hybrids in *Nasonia* wasps. Dev Biol 415(2):391-405.

Werren JH, Richards S, Desjardins CA, Niehuis O, Gadau J, Colbourne JK, Group NGW. 2010. Functional and evolutionary insights from the genomes of three parasitoid *Nasonia* species. Science 327(5963):343-348.

Zwarts L, Vanden Broeck L, Cappuyns E, Ayroles JF, Magwire MM, Vulsteke V, Clements J, Mackay TF, Callaerts P. 2015. The genetic basis of natural variation in mushroom body size in *Drosophila melanogaster*. Nat Commun 6:10115.

Nasonia vitripennis and *Trichogramma evanescens*

Summary

The parasitic wasp *Nasonia vitripennis* is a small insect that can vary over ten times in adult body weight, ranging from 40 to 438 μg. Due to this interesting characteristic and due to its overall small size (1.5-2.5 mm in length), *N. vitripennis* is an ideal candidate for the study of brain scaling and its relation with the miniaturization of insects in general. The peculiar adaptations by which insects and other arthropods manage to miniaturize their body but still maintain behavioral complexity have long fascinated many researchers. In addition, *N. vitripennis* and related *Nasonia* species provide a novel hymenopteran model system poised to be the "new *Drosophila*", which allows for the placing of such knowledge in a wider theoretical context.

In this thesis, I aimed to gain further understanding of brain scaling at the limits of miniaturization, as well as to provide the research community with fundamental knowledge of the brain of *N. vitripennis*.

Chapter 2 provides an answer to the question "What is the general morphology of the *N. vitripennis* brain, and how does it relate to the brain of other insects?" Here, I describe 14 regions of interest, or **neuropils**, of the *N. vitripennis* brain: the optic lobes (comprised of the lobula, medulla, and lamina), the anterior optic tubercle, the antennal lobe, the lateral horn, the mushroom body (comprised of the calyces and the lobes), and the central complex (comprised of the fan-shaped body, the ellipsoid body, the noduli, and the protocerebral bridge). I compare the shape and (relative) volumes of these neuropils with the other model organisms the honey bee *Apis mellifera* and the fruit fly *Drosophila melanogaster*, as well as a diverse group of paper wasps. Furthermore, this chapter introduces the **Jewel Wasp Standard Brain** (JWSB), an average brain obtained by iterative shape averaging of 10 brains from recently eclosed female *N. vitripennis* (AsymCx strain). Standard brains such as the JWSB can be used as reference frameworks for integration of **multidisciplinary results**, such as protein expression data, single neuron recordings, and tracer injections. In contrast to most other standard brains, the JWSB is not based on dehydrated and shrunken tissue, thereby representing a brain closer to the *in vivo* shape and size, which may aid future stereological studies. Volumetric descriptions and an interactive 3D model of the Jewel Wasp Standard Brain have been deposited in the online **Insect Brain Database** (insectbraindb.org), which will serve as a resource for comparative studies, as well as an excellent tool for demonstrations and education.

In **Chapter 3** I expand on this basic knowledge of the *N. vitripennis* brain by seeking answers to the question "How does the brain of *N. vitripennis* scale over

its large body size range, and are there specific adaptations to accommodate this range?" Due to its large variation in body size, *N. vitripennis* is an ideal candidate for the study of **Haller's rule**, which states that larger animals have a relatively smaller brain (*allometric* scaling). Until now, the "breaking" of this rule has only been observed in the miniscule egg parasitoid *Trichogramma evanescens*, which had the same relative brain size regardless of its body size (*isometric* scaling). Unexpectedly, my data show that the slightly larger *N. vitripennis* wasps had **diphasic**, or bimodal, brain scaling: the larger individuals did adhere to Haller's rule, but under a body weight of 183 µg these wasps showed isometric brain scaling as in *T. evanescens*. This may indicate that isometric brain scaling might be a scaling "mode" that is related to very small absolute body sizes. Regardless of its cause, the basic knowledge I describe in Chapter 2 allows me to see how the brain of *N. vitripennis* is affected by brain scaling. Is the brain of a small individual a one-to-one copy of that of a large individual, although of smaller size), or do specific neuropils scale at different rates (a notion best described as brain mosaicism)? I show that the brains of the smallest individuals had large differences in the relative neuropil distribution when compared to the larger wasps. The smallest wasps had relatively smaller optic lobes, indicating that *N. vitripennis*, which can easily find hosts without using sight, can easily sacrifice visual tissues to maintain other neuropils such as the antennal lobes, which had the same relative size. The mushroom bodies, which are often described as memory centers in insect brains, also were relatively smaller in the smallest wasps. A parallel study by colleagues showed that small *N. vitripennis* performed worse in memory tests, which may be explained by this difference in neuropil volume. Finally, the relative volume of the central complex was larger in the smallest wasps, indicating that this neuropil is probably of large importance. A possible reason for this remains unknown, as the functions of the central complex are very diverse.

The neuropil is only one part of the insect brain, what about the outer layer of cell bodies? In **Chapter 4**, I explore the question "Are there cell type-specific adaptations in brains of different sizes, and does this relate to behavior?" Specifically, I describe investigations of the **dopaminergic** network in *N. vitripennis* of different sizes, because of the role of this neurotransmitter in learning (and the changes therein that were observed in these wasps). In addition, I expanded on a previous study that compared the octopaminergic network of *N. vitripennis* with *Nasonia giraulti*, a related species that shows different memory dynamics than *N. vitripennis*. Although a measurement of the total number of all neurons in the *N. vitripennis* brain proved to be unattainable, I do show variation in the dopaminergic network. First, I provide a description of the location and average number of cells for

nine different dopaminergic clusters located in the cell body rind of the *Nasonia* brain. Most of these clusters could be compared, based on their location, with the clusters in the honey bee, the fruit fly, and the egg parasitoid *Trichogramma evanescens*. Based on this comparison, I identified clusters **D2**, **D3**, and **D5** as clusters that are likely innervate the mushroom body, thereby influencing the memory dynamics of *Nasonia*. Comparing *N. vitripennis* of different size, I found fewer dopaminergic cells in clusters D5 and D7 in small *N. vitripennis*; comparing *N. vitripennis* with *N. giraulti* showed that *N. giraulti* had fewer cells in clusters D2 and D4a, but more in D4b. More analyses are needed to confirm that differences in cluster D2 and D5 play a causal role in the different memory dynamics of the studied wasps, but these results are a good indication that dopamine is important in the memory dynamics of *N. vitripennis*.

Finally, I sought to answer the question "Is relative brain size a trait that can be selected for, and what are the effects of such a selection?" in **Chapter 5**. In the previous chapters, I specifically address brain scaling in an isogenic line (AsymCx), meaning that all wasps were genetically identical. Any variance in brain structure would be due to plasticity, not due to some wasps simply having a genetic propensity for a specific larger or smaller neuropil. To investigate a potential genetic basis of relative brain size I started with a population of **genetically diverse** *N. vitripennis* wasps (the HVRx strain). Every generation, I measured and selected wasps with the largest or smallest relative brain size to proceed to the next generation. After 25 generations of 3 weeks, I found a robust difference in relative brain size between the resulting selection lines. In absolute terms, large-brained lines had 16% larger brains, despite being smaller on average. Although Haller's rule predicts a relative larger brain for smaller individuals, I showed (in a limited size range) that the brain scaling relationship is grade shifted. In this size range, large-brained lines always had a larger brain than a small-brained wasp of equal size. I expected to find cognitive benefits for the large-brained wasps, but they performed as well as the small-brained lines in a **memory performance** test. An analysis of the neuropil distribution showed that all lines had equal relative mushroom body volumes, which might be related to the lack of differences in memory performance. In contrast to my study on neuropil differences between extremely different size groups in Chapter 3 (230% difference in total neuropil volume), the only neuropil that was affected in this study was the **antennal lobe**, which was relatively larger in the large-brained wasps. As the antennal lobe is apparently important enough to maintain its relative volume at the small end of an extreme size range (Chapter 3), it could make sense if the antennal lobe would grow larger when brains are selected to grow beyond their normal relative size. A larger antennal lobe may improve the
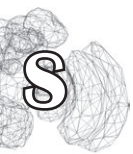
wasps' ability to discriminate odors, or increase its olfactory sensitivity, but this was not tested. Despite this lack of visible benefits for large-brained lines, they were worse off. On average, they had a shorter **longevity** to start with (which may be explained by their overall smaller body size), but the large-brained wasps also died sooner after a conditioning experience. The small-brained lines did not suffer from this effect. As the title of this chapter already mentions: there appear to be no gains for bigger brains.

In conclusion, this thesis provides a wealth of information on the genotypic and phenotypic aspects of brain scaling, as well as many new questions and reference points for further studies. With the development of the Jewel Wasp Standard Brain a new tool is available for the overall neuroscience community and the *Nasonia* community in particular, which will likely benefit from its use as a framework to consolidate results from past and future studies, but also as an interactive tool for educational purposes.

Curriculum vitae
and
list of publications

Publications

Jitte Groothuis, Nick F. Ramsey, Geert M. J. Ramakers, Geoffrey van der Plasse. 2014. Physiological challenges for intracortical electrodes. Brain Stimulation 7(1):1-6.

Jitte Groothuis, Hans M. Smid. 2017. *Nasonia* parasitic wasps escape from Haller's rule by diphasic, partially isometric brain-body size scaling and selective neuropil adaptations. Brain, Behavior & Evolution 90(3):243-254.

Emma van der Woude*, **Jitte Groothuis***, Hans M. Smid. No gains for bigger brains: functional and neuroanatomical consequences of artificial selection on relative brain size in a wasp. *Submitted.*

* These authors contributed equally to this work.

Jitte Groothuis, Keram Pfeiffer, Hans M. Smid. The Jewel Wasp Standard Brain: Average shape atlas and morphology of the female *Nasonia vitripennis* brain. *Submitted.*

About the Author

Jitte Groothuis, from the village of Noordeloos, the Netherlands, is an inquisitive being, born May 11th, 1986, with an avid love for curiosity-driven and fundamental research. He obtained his Bachelor of Science degree in Biomedical Sciences from Utrecht University. His BSc thesis was on the subject of axon guidance molecules and their role in the pathogenesis of epilepsy.

Becoming increasingly interested in all matters pertaining to the brain, he proceeded the pursuit of a Master of Science degree at the Rudolf Magnus Institute of Utrecht University by enrolling in the Experimental and Clinical Neuroscience track of the Neuroscience & Cognition programme. At the RMI, in the group of Prof. dr. Jeroen Pasterkamp, he was first involved in a Major Research Project regarding the axon guidance of dopaminergic neurons in the developing midbrain. Later, he studied the role of the proteasome and microglia cells in Alzheimer's Disease in a Minor Research Project at the Netherlands Institute for Neuroscience in the group of Prof. dr. Elly Hol. Finally, his MSc thesis consisted of a literature review on the response of brain tissue to implantable electrodes for use in e.g. Brain-Computer Interfaces.

During his studies, Jitte started keeping ants as pets and exploring macro photography of insects. When the opportunity arose to combine these hobbies and his previous enthusiasm for Neuroscience, the switch to the Laboratory of Entomology at Wageningen University & Research was easily made. Under daily supervision of Dr. Hans Smid, Jitte worked on the PhD thesis you are reading now, which pertains to the study of the brains of small insects: the lovely parasitic wasp *Nasonia vitripennis*.

Lured in with the false promise to "maybe also study ant brains", Jitte proceeded to be fascinated by these insects. As a result, he has given talks about ant brains for: the Dutch 'Hersenstichting', a 'Vroege Vogels' radio segment, the 'WURtalks', (celebrating the WUR centennial), foundation 'Burenhulp en Wijkbelangen Wageningen-Hoog', and the 'Mierenwerkgroep' of the Netherlands Entomological Society.

Continuing to mix Neuroscience and Entomology, Jitte is currently studying viral manipulation of behavior in caterpillars in a Post-Doctoral research project at the Laboratory of Virology (Wageningen University & Research).

PE&RC Training and Education Statement

With the training and education activities listed below the PhD candidate has complied with the requirements set by the C.T. de Wit Graduate School for Production Ecology and Resource Conservation (PE&RC) which comprises of a minimum total of 32 ECTS (= 22 weeks of activities)

Review of literature (4.5 ECTS)
- Miniature master minds: a standard brain for *Nasonia vitripennis*

Post-graduate courses (3.1 ECTS)
- PhD excursion to 3 Swiss Universities: Neuchâtel, Lausanne and Basel (2013)
- Iterative shape averaging for standard brains; University Philipps-Universitaet Marburg, University of Würzburg (2015- 2017)
- Introduction to R; PE&RC (2017)

Invited review of (unpublished) journal manuscript (1 ECTS)
- Proc Roy Soc B: evolution of brain size and brain morphology (2014)

Competence strengthening / skills courses (2.2 ECTS)
- Jouw idee in 3D: 3D printen en tekenen; ProtoSpace (2013)
- Vervolgworkshop 3D printen; ProtoSpace (2013)
- Communication with the media and the general public; WGS (2014)
- Adobe InDesign; WUR Library (2017)

PE&RC Annual meetings, seminars and PE&RC weekend (1.8 ECTS)
- PE&RC Day (2014, 2015, 2016)
- PE&RC Midterm weekend (2016)
- Workshop carousel (2017)

Discussion groups, local seminars, other scientific meetings (12.2 ECTS)
- Brains and Behavior discussion group with WUR, VU, NIOO (2013-2016)
- Wageningen Evolution and Ecology Seminars (2013-2017)
- NEV Entomologendag; poster presentation (2014)
- NEV Entomologendag; oral presentation (2016)
- Hersenstichting afscheidsymposium; oral presentation (2016)
- WURtalks; oral presentation (2016)
- Wageningen PhD symposium; oral presentation (2017)

International symposia, workshops and conferences (8.2 ECTS)
- Netherlands-Japan parasitoid meeting; poster presentation
- 12th International Congress of Neuroethology; poster presentation; Montevideo, Uruguay
- Dutch neuroscience meeting; poster presentation
- International *Nasonia* meeting; oral presentation

Lecturing / supervision of practicals / tutorials (7.65 ECTS)
- Molecular and evolutionary ecology (2014)
- Behavioural ecology (2014, 2015)
- Ecophysiology (2014, 2015, 2016)

Supervision of MSc students (6 ECTS)
- Variation in morphology of dopaminergic neurons in 6 parasitic wasps
- The morphology of dopaminergic neurons in *Nasonia* parasitic wasps

Acknowledgements

I would like to start by thanking **Hans**. Hans, thank you for welcoming me in your group, your supervision, all your support and understanding, the inspiration you give me to push forward with my macro photography, all the nerdy chats we had about said photography, your technical expertise, the bicycle repairs, the trip to Uruguay, but most of all: always being there when I needed you.

Then **Marcel**, who let this ignorant-about-insects neuroscientist feel at place at Entomology: thank you for this opportunity that has changed my perspective about a great many things, your inspiring talks, thoughtful comments on my chapters, and motivating me to look at the broader context of my work.

On to my great paranymphs: **Emma**! Thank you for everything! Teaching me how to work with tiny insects, being a shining example for *pretty much everything* (grr!), assisting in (maybe a few too many) hilarious photo shoots, traveling to Uruguay, having fun in the lab, the pet-sitting, and many more things that I'm probably forgetting. **Jeroen**! It seems as if you only just joined the Ento crew, but time "flies" and you've embedded yourself in the group. Thanks for all the good talks, games, moving help, also pet-sitting, and the beers!

I could not be here without **Ties**. It feels a bit weird, but I'm happy you decided that you needed a change. If not for you, I would not have had this opportunity to turn your Post-Doc into my PhD! Thank you for staying involved with the project, I've always valued your perspective and input.

My thanks go out to members of the "Brain lab" and the overarching "Brains & Behavior" group: **Katja**, **Joke**, **Maartje**, **Louise**, **Michel**, **Sara**, **Jessica**, and I might be forgetting some people. Thanks for all the discussions and post-B&B-beers.

Of course my students: **Mark**, **Krista**, and **Lorenzo**. I had fun being your supervisor and am happy with your results; I hope you also enjoyed your time in our lab and your struggles with those tricky dissections. I wish you all the best in your future careers.

A shout out to my Ento ant buddies: **Fernando**, it was great to have you around for a while and nerd out about ants. It's a shame we never managed to get your cool animals over here, but who knows what the future will bring! **Tim**, I'm glad there's someone who is at least, if not more, as crazy as me about our little six-legged ladies. I always enjoy our chats about ant

keeping, and of course our big WURtalk!

I cannot forget to thank my desk mates: **Enric** and **Janneke**. Thank you for sticking with me, tolerating my dirty desk, smelly peanut butter sandwiches, incessant finger drumming, foot tapping, speed cubing, and all the other annoying habits I probably have.

There are too many **entomologists** to name personally, so please allow me to thank you all this way. Thank you for all the good times, all the break-time chats, cakes, and nice events. The 'Labuitjes', 'YELREMs', and 'Entomologendagen'. I'm also grateful for all of you who were patient enough to let me sate my photography hunger on your precious study subjects, and for you actually using my photos (I'm especially looking at you, **Cindy**!). Being around you all and listening to all your talks has taught me so much more than I had expected and has changed me a lot. They may have taken the Jitte out of Entomology, but you can't take Entomology out of the Jitte. You have not seen the last of me...

My thanks go out to my sole external co-author: **Keram**. Keram, thank you for your patience, expertise, and perseverance when we worked on the Jewel Wasp Standard Brain. I wish you all the best with your new position in Würzburg. Of course I now also want to thank **Basil** for introducing me to Keram, giving me a home for all my standardization woes. Meeting you in Uruguay was a fun and unexpected highlight to that trip. Related to these Standard Brain matters are my thanks to **Stanley**: thank you for organizing the InsectBrainDB and your help in hosting the Nasonia brain there.

Family and **friends**, thank you all for your support and kind smiles and nods when I tried to explain what I was doing (and why), or went off on a rant about how cool insect brains are. Extra thanks to my Magic buddies (**Niels**, **Joris**, and the Gorinchem crew) for some much needed distractions (or was it the research that distracted me from playing??).

Further thanks go out to the **Ingress** community. You may not realize it, but you have been with this from the start: I received my Beta invite just after landing this PhD position. There are too many of you to name, my thanks go out to all the **SmurfEaters** and past and current members of our local **West-Veluwe** gang. Thank you for all the distractions, sense of community, providing an additional social life, and all the fun we had at events and XM Anomalies. To new friendships!

Last, but definitely not least, my darling wife-to-be **Yessica**. Thank you so much for finding me after all those years and not giving up. You got me in the end, and now I got you. If people need an example of tolerance, they only need to look at you. Thank you for suffering through all my hobbies and the mess they/I create, I know that is not an easy thing to do! Moreover, thank you for your support and motivating presence during this final year. I'm not sure I could have managed without you to come home to. Thank you.